DETERMINATION OF THERAPEUTIC POTENTIAL OF APIGENIN ON ACUTE LYMPHOBLASTIC LEUKEMIA CELLS

A Thesis Submitted to
the Graduate School of Engineering and Sciences of
İzmir Institute of Technology
in Partial Fulfillment of the Requirements for the Degree of

MASTER OF SCIENCE

in Molecular Biology and Genetics

by
Erez UZUNER

December 2019
İZMİR

ACKNOWLEDGMENTS

I wish to my deepest thank my supervisor, Prof. Dr. Yusuf BARAN for his endless support, encouragement, confidence and priceless guidance for both my studies and my life. He has always been a role model to me with his personality, perspective and success. He has become not only a supervisor but also a family member for us and will always enlighten my way with his everlasting energy. I am so lucky to work with him and his lovely team.

I would like to thank my committee members Prof. Dr. Bünyamin Akgül and Assoc. Prof. Dr. Duygu SAĞ for their valuable critics, contributions, suggestions, and support.

I also would like to deepest thank my friends and colleagues, Sevim Beyza GÜRLER, Yağmur KİRAZ, Gizem Tuğçe ULU, Nusaiba ALDOSARY, Melisa ÇETİNKAYA, Polen YUNUS, Muharrem Şevki PAZARÇEVİREN, Mustafa ÖZTÜRK for their valuable help and support in not only our laboratory but also life.

I really appreciate to have my lovely friends, Resul AKDUMAN, Cihan Civan CİVAŞ, Hasan Ozan OTAŞ and Aylin ALKAN and they have always been a family to me, for their endless love, motivation, support and for our unforgettable memories.

I am also lucky to have my friends, Nihan AKTAŞ PEPE, Mina KÜÇÜKTAŞ, Esra BİLGİÇ, Seren KEÇİLİ, İsmail TAHMAZ, Büşra ACAR, Sefayi Merve ÖZDEMİR, and Berkay Berkant ULU to their love, motivation, support and for our unforgettable memories.

I am so grateful to have my parents Hatice UZUNER and Nazif UZUNER, my brother Orçun UZUNER and my whole family to their endless love, trust, motivation, support, understanding and encouragement during my whole life.

I want to thank IZTECH Molecular Biology and Genetics Department, especially. Prof. Dr. Bünyamin AKGÜL and his laboratory members and Assoc. Prof. Dr. Gülistan Meşe ÖZÇİVİCİ and her laboratory members to their help, suggestions and contributions.

I also want to thank IZTECH Biotechnology and Bioengineering Research and Application Center specialists for their valuable help, support and knowledge for my study.

ABSTRACT

DETERMINATION OF THERAPEUTIC POTENTIAL OF APIGENIN ON ACUTE LYMPHOBLASTIC LEUKEMIA CELLS

Acute lymphoblastic leukemia (ALL) is a hematological disorder initiating from blood-forming cells of bone marrow. ALL is characterized by the Philadelphia chromosome (Ph) arisen from a translocation between chromosome 9 and 22. This chromosome encodes BCR-ABL oncogene that is a driver regulator. BCR-ABL based studies improved tyrosine kinase inhibitors (TKI) including imatinib, dasatinib, nilotinib, and ponatinib to eliminate this disease. However, the studies on Ph+ ALL patients showed that bioactive sphingolipids have crucial roles in the elimination of the positive effects of these drugs by activating the proliferation-associated pathways, inhibition of apoptosis and increasing drug resistance of the cells treated with these drugs.

In this study, therapeutic potential of apigenin, which is a natural flavonoid obtained from celery, parsley and chamomile was investigated on Ph+ ALL cell line, SD-1, and non-cancerous lung cell line Beas-2B. The cytotoxic effects of apigenin on SD-1 and Beas-2B cells were determined by MTT cell proliferation assay. The cell viability analyses on SD-1 cells were conducted by Trypan blue dye exclusion assay following apigenin treatment. Cell cycle and apoptosis analyses including Annexin V/PI-dual staining and JC-1 dye-based mitochondrial membrane potential were examined by flow cytometry. Expression levels of bioactive sphingolipids were determined by RT-PCR and western blot.

The cytotoxic analyses indicated that apigenin selectively inhibits the expression of SD-1 cells whereas the IC50 value of apigenin for SD-1 cells has the anti-apoptotic roles in Beas-2B cells. SD-1 cells experience cell death via apoptosis-related pathways and apigenin might arrest the cells at G2/M phases. Indeed, the changes in the expression levels of bioactive sphingolipids genes indicated their roles in apigenin-induced apoptosis in SD-1 cells. This study investigated the cytotoxic and apoptotic effects of apigenin on SD-1 cells and the roles of apigenin in bioactive sphingolipid metabolism for the first time.

ÖZET

APİGENİN'İN AKUT LENFOBLASTİK LÖSEMİ HÜCRELERİ İÇİN TERAPÖTİK POTANSİYELİNİN BELİRLENMESİ

Akut lenfoblastik lösemi (ALL), kemik iliği kan hücrelerini oluşturan hücrelerden oluşan hematolojik bir hastalıktır ve kromozom 9 ve 22 arasındaki karşılıklı parça değişimi sonucu ortaya çıkan Philadelphia kromozomu (Ph) ile karakterize edilir. Bu kromozom, birincil düzenleyici onkogen BCR-ABL'i kodlar. BCR-ABL temelli çalışmalar bu hastalığı ortadan kaldırmak için imatinib, dasatinib, nilotinib ve ponatinib gibi tirozin kinaz inhibitörleri (TKI) geliştirilmiştir. Ph+ ALL hastaları üzerinde yapılan çalışmalar, biyoaktif sfingolipidlerin hücre çoğalması ile ilişkili yolakları aktive ederek bu ilaçların olumlu etkilerinin ortadan kaldırılmasında, apoptozun inhibisyonunda ve ilaçlarla tedavi edilen hücrelerin direnci artırılmasında önemli rol oynadıklarının göstermiştir.

Bu çalışmada kereviz, maydanoz ve papatyadan elde edilen doğal flavonoid apigeninin terapötik potansiyeli Ph+ ALL hücre hattı SD-1 ve kanser olmayan akciğer hücre hattı Beas-2B üzerinde araştırıldı. Apigeninin bu hücreler üzerindeki sitotoksik etkileri MTT hücre çoğalması deneyi ile belirlendi. SD-1 hücreleri üzerindeki hücre canlılığı analizleri apigenin uygulamasının ardından Trypan mavisi deneyi ile yapılmıştır. Aneksin V/PI çift boyaması ve mitokondriyal membran potansiyelini belirlemek için kullanılan JC-1 boyası ile hücre döngüsü ve apoptoz analizleri akış sitometrisi ile incelendi. Biyoaktif sfingolipidlerin ekspresyon düzeyleri RT-PCR ve western blotlama ile belirlendi.

Sitotoksik analizler apigenin SD-1 hücrelerinin ekspresyonunu seçici olarak inhibe ettiğini, SD-1 hücreleri için apigenin IC50 değerinin ise Beas-2B hücrelerinde anti-apoptotik rollere sahip olduğunu göstermiştir. SD-1 hücrelerinin apoptosis ile ilgili yollar aracılığıyla hücre ölümünü deneyimlediğini ve apigenin G2/M evresinde hücreleri durdurabileceğini belirlemiştir. Gerçekten de, biyoaktif sfingolipid gen ekspresyon düzeylerindeki değişiklikler apigenin uygulanan SD-1 hücrelerinin apoptozdaki rollerini göstermiştir. Bu çalışmada ilk kez SD-1 hücreleri üzerinde apigeninin sitotoksik ve apoptotik etkileri ve sfingolipid metabolizmasındaki rolleri araştırılmıştır.

TABLE OF CONTENTS

LIST OF TABLES

LIST OF FIGURES

LIST OF ABBREVIATIONS

ABL1, Abelson tyrosine kinase 1

ADC, Antibody-Drug Conjugates

ADCC, Antibody-Dependent Cytotoxicity

ALL, Acute Lymphoblastic Leukemia

AML, Acute Myeloid Leukemia

ATCC, American Type of Culture Collection

ABCC1 or ABCC2, ATP-Binding Cassette sub-family C member 1 or 2

B-ALL, B cell lineage Acute Lymphoblastic Leukemia

BCR, Breakpoint Cluster Region

BiTE, Bispecific T cell Engaging

BRMS1, Breast cancer Metastasis-Suppressor 1

BSA, Bovine Serum Albumin

CAR, Chimeric Antigen Receptor

C1PP, Ceramide-1-Phosphate

CDase, Ceramidase

CDC, Complement-Dependent Cytotoxicity

Cer, Ceramide

CERS (LASS), Ceramide Synthase

CERT, Ceramide Transporter Protein

CK, Cer Kinase

CML, Chronic Myeloid Leukemia

CR, Complete Remission

CRC, Colorectal Cancer

DAG, Diacylglycerol

DH, Dbl Homology

DMSO, Dimethyl sulfoxide

EMT, Epithelial-Mesenchymal Transition

ERK-1/2, Extracellular Signal-regulated Kinase-1/2

ER, Endoplasmic Reticulum

EsR, Estrogen Receptor

FADD, Fas-Associated protein with Death Domain

FDA, Food and Drug Administration, US

FGF, Fibroblast Growth Factor

FLT3, FMS-like tyrosine kinase 3

GAB2, GRB-Associated Binding protein 2

Gal-Cer, Galactosylceramide

GAP, GTPase-Activating Protein

GCase, Glucosyl CDase.

GCS, Glucosylceramide synthase

GEF, Guanine nucleotide Exchange Factor

GluCer, Glycosylceramide

GLUT1, Glucose transporter 1

GPCRs, G-Protein-Coupled Receptors

GRB2, Growth Factor Receptor-Bound Protein 2

HCC, Hepatocellular Carcinoma

HDACs, Histone Deacetylases

HLB, HMG-like boxes

HNSCC, Head and Neck Squamous Cell Carcinoma

hTERT, human Telomerase Reverse Transcriptase

JAK, Janus Kinase

MAPK, Mitogen-Activated Protein Kinase

mTOR, Mammalian Target of Rapamycin

NEDD9, Neural precursor cell Expressed Developmentally Down-regulated 9

NES, Nuclear Export Signal

NLS, Nuclear Localization Signal

NSCLC, Non-Small-Cell Lung Cancer

OS, Overall Survival

PAGE, Polyacrylamide Gel Electrophoresis

PC, Phosphatidylcholine

PDGF, Platelet-Derived Growth Factor

PH, Pleckstrin Homology

Ph, Philadelphia Chromosome

Ph+ ALL, Philadelphia Chromosome Positive Acute Lymphoblastic Leukemia

Ph- ALL, Philadelphia Chromosome Negative Acute Lymphoblastic Leukemia

PI, Propidium Iodide

PI3K, Phosphatidylinositol 3-Kinase

PP2A, serine/threonine-Protein Phosphatase 2A

Rho/GEF, Ras Homolog Gene Family/Guanine Nucleotide Exchange Factors

R/R, Relapsed and Refractory

PxxPs, Proline-Rich Sequences

S1P, Sphingosine-1-phosphate

SDS, Sodium Dodesil Sulphate

SH, Src Homology

SK 1/2 or SPHK 1/2, Sphingosine Kinase 1/2

SM, Sphingomyelin

SMase, Sphingomyelinase

SMS, SM Synthase

SOCS2, Suppressor of Cytokine Signalling 2

SPNS2, Protein Spinster Homologue 2

SPT, Serine Palmitoyl Transferase

STAT, Signal Transducers and Activation of Transcription

TAE, Tris- Acetate- EDTA

TKI, Tyrosine Kinase Inhibitor

TRAF2, TNF Receptor-Associated Factor 2

TRAIL, Tumor necrosis factor (TNF)-related apoptosis-inducing ligand

VEGF, Vascular Endothelial Growth Factor

XPB, Xeroderma Pigmentosum group

To My Lovely Family…

To Leukemia Patients who Continue to Fight…

CHAPTER 1

INTRODUCTION

1.1. Acute Lymphoblastic Leukemia

Acute Lymphoblastic Leukemia (ALL) is a hematological disorder initiating from blood-forming cells of bone marrow and characterized by the growing number of immature white blood cells[1]. The word "acute" declares the rapid progression of this leukemia type resulting in death if it is not treated. The word "lymphoblastic or lymphocytic" clarifies that the cells of this disease originate from immature B lymphocytes or T lymphocytes, which are not able to eliminate the infection effectively[2].

GLOBOCAN 2018 database has revealed that 18.1 million new cancer cases were diagnosed worldwide and 9.6 million cancer patients will be died because of cancer in 2018. 437,033 patients of new cancer cases with 2.4 percentage of all cases belong to Leukemia disease. It is estimated that 3.2% of all sites or 309,006 leukemia patients will die according to the same database. When male and female patient cases are compared in this worldwide database, the incidence and mortality cases of male patients are much higher than female patients' cases[3].

Leukemia between various cancer types comprises a 3.5 percentage of all cancer cases in the United States. National Cancer Institute estimates that 22,840 patients of 61,780 new patients will die because of leukemia in 2019 [4]. GLOBOCAN 2018 database revised in March 2019 reveals cancer cases of Turkey and death numbers or percentages of cancer types. Leukemia represents 3.09% (6,029 new cases) of all cancer cases and 4.31% of all deaths of this disease[3, 5]. American Cancer Society reveals statistical information about ALL for 2019 in the United States. It is stated that there will be 5,930 new cases and about 1,500 patients will die because of ALL. The main risk group for this ALL is children who are younger than 5 years of age. However, 4 of 10 ALL patients are adults and 4 of 5 deaths occur in adult ALL patients[6].

ALL is a well-documented leukemia type and many patients face poor prognosis and relapse. The patients especially children who are younger than five years of age need the most effective treatment way[6]. However, although there are many treatment ways

such as chemotherapeutic drugs, specific inhibitors, tyrosine kinase inhibitors (TKIs), monoclonal antibodies, chimeric antigen receptor (CAR) T cells and hematopoietic stem cell transplantation for ALL patients, there is no highly effective cure for ALL patients[7]. Thus, the discovery of natural products, which selectively eliminate the cancer cells of patients or have the synergetic effects with current widely used drugs on the cancer cells, is needed to treat the patients especially children suffering from hematological disorders.

1.1.1. Molecular Biology of Philadelphia Positive (Ph+) ALL

ALL is an aggressive kind of leukemia containing various mutation types such as deletions of some parts in chromosomes, small DNA rearrangements within the chromosome and translocations that are the rearrangements of chromosome breaks from one chromosome to other for becoming active chromosome regions[8-9].

One of the most widespread translocations in ALL is Philadelphia chromosome (Ph) which arises from a reciprocal translocation of ABL proto-oncogene (Abelson leukemia virus oncogene) on chromosome 9 to BCR (breakpoint cluster region) gene on chromosome 22, abbreviated as t(9;22)[10]. Ph is found in only 2% to 5% of childhood and 25% of adult ALL[8]. Therefore, this type of ALL is classified as adult hematological disorder disparately whereas childhood ALL with 25 percent of all childhood cancers has a higher incidence rate in childhood cancers[11]. The resultant BCR-ABL1 fused gene in Philadelphia chromosome-positive acute lymphoblastic leukemia (Ph+ ALL) patients, codes for BCR-ABL1 oncoprotein with a constitutive tyrosine kinase activity that leads to negatively control of cell growth and increases cellular proliferation[12].

Molecular analyses of BCR-ABL oncoprotein indicates that BCR-ABL takes action by binding of ATP and transfers a phosphate from ATP to tyrosine residues in the cytoplasm of cancerous cells thereby resulting in the activation of multiple signaling pathways. These activated pathways influence the excessive cellular survival and proliferation of Ph+ ALL cells, increase the resistance ability of the cells to the current drugs and alter the adhesion properties of these cells for escaping of well-organized control mechanisms. Besides, BCR-ABL is affiliated with aggressive disease in the patients especially children younger than five years old and has been shown as the main cause of death in adult ALL patients. Thus, BCR-ABL is a driver protein in the Ph+ ALL progression and is a potential switch for molecular-targeted therapies of Ph+ ALL.

1.1.1.1. Molecular Anatomy of the BCR-ABL Translocation

Philadelphia chromosome, a fusion chromosome arisen from reciprocal translocation was first identified in a patient with Chronic Myeloid Leukemia (CML) in 1960[13]. Molecular analysis of Ph revealed that BCR-ABL1 translocation arises on chromosome 22 from the head to tail recombination between 3' end of *ABL1* gene on the long arm of chromosome 9 (9q34) and 5' end of BCR gene on the long arm of chromosome 22 (22q11)[12, 14]. Although the positions of genomic breakpoints in this fusion gene are excessively variable in leukemia types, this translocation usually occurs within intron 1, intron 13/14 or exon 19 of BCR gene and 140 kb ABL1 gene region between exon 1b and 2[12].

The breakpoints of BCR gene determine three frequent types of BCR-ABL fusion genes[12, 15]. The most frequent type is consisted of the truncation in 5.8-kb BCR gene sequence[16]. This region is named as the major breakpoint cluster region (M-BCR) which includes five exons identified as b1-b5 but currently classified as exons 12-16 or e12-e16 of BCR gene[15, 17]. The great majority of BCR breakpoints in the 5.8-kb gene sequence occur in the introns located after either exon 13 (e13 or b2) or exon 14 (e14 or b3)[15]. The head to tail joining of ABL exon a2 to either e13 or e14 of BCR gene comprises of either e13a2 (b2a2) or e14a2 (b3a2) BCR-ABL mRNA which is 8.5 kb transcript and encodes chimeric 210-kD fusion protein also referred as $p210^{BCR\text{-}ABL}$ [12, 15]. Moreover, clinical cases clearly indicated that almost all CML patients transcribe $p210^{BCR\text{-}ABL}$ or M-BCR mRNA with b3a2 and b2a2 breakpoint cluster-Abelson variants[18].

In addition to Ph-positive CML patients, the breakpoint in BCR sequence which occurs in two alternative second exons e2' and e2 of BCR gene arises from a region upstream of M-BCR and this point named as the minor breakpoint cluster region (m-bcr). The merging of m-bcr with another breakpoint within introns 1 or 2 of the ABL gene results in e1a2 mRNA of the BCR-ABL fusion gene. This hybrid 7.0-kb in length mRNA encodes a 190-kD fusion protein or $p190^{Bcr\text{-}Abl}$. This BCR-ABL translocation is found in mostly Ph+ ALL patients and rarely CML patients[18].

The third identified breakpoint cluster region in the BCR gene was classified as the "micro" breakpoint cluster region (μ-bcr)[19]. The breakpoints arise within BCR gene sequence between exon 19 and 20 and these breakpoints can merge with others in introns 1 or 2 of ABL gene. This fusion BCR-ABL gene transcribes e19a2 fusion mRNA and translated into 230-kD hybrid protein or $p230^{BCR\text{-}ABL}$ [15].

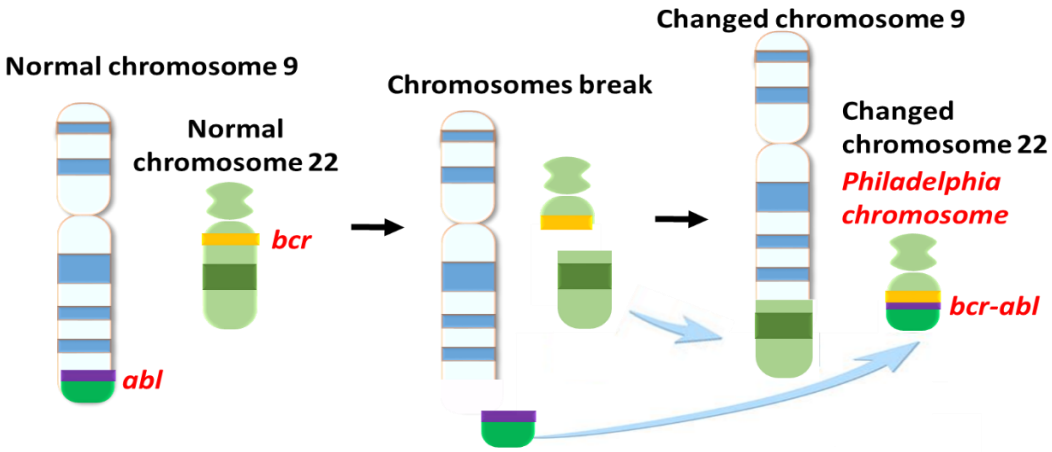

Figure 1. 1. Bcr-Abl translocations

BCR-ABL is a fusion protein in which several breakpoints within BCR gene merge with the breakpoints in intron 1 and 2 of ABL gene.

1.1.1.2. The Physiological Functions of the Translocation Partners

The BCR gene is found in chromosome 22q11 and its entire size is 130 kb in the genome. The ubiquitously expressed gene with 23 exons results in a 160-kD cytoplasmic protein with various functional domains and plays a role in the regulation of intracellular signaling[20]. The first exon located in the N-terminus of BCR gene comprises of 426 amino acids found in all isoforms of BCR-ABL hybrid proteins: p190, p210 and p230. This region includes the serine-threonine kinase domain and two Src Homology 2 (SH2) domains, which are located within its inside. This kinase domain is auto-phosphorylated itself and activates Bcr-associated protein-1, Bap-1 a member of 14-3-3 acidic protein families recruited by binding its own SH2 domain for cell-cycle control, growth regulation and development[21]. Furthermore, the phosphorylation on Tyrosine 177 within this kinase domain influences the binding of an adaptor protein, Grb-2 through its SH2 domain in order to activate the Ras pathway for cellular proliferation. Additionally, a coiled-coil oligomerisation domain that includes a repeated seven-amino acid pattern to be allowed for the feasible tetramerization is located in the N-terminus of BCR and enables the activation of BCR-ABL fusion protein via the ABL tyrosine kinase domain. Moreover, this oligomerisation domain of BCR helps BCR-ABL localization in the cytoplasm by rising its ability to bind F-actin in the membrane[22].

The central domain of BCR protein occurs within 501-870 amino acids and has several interaction regions with other proteins. Firstly, BCR central region has domains: Dbl Homology (DH) and Pleckstrin Homology (PH), which share the highly similar domains with the members of GEF (Guanine nucleotide Exchange Factor) family[23-24]. BCR-ABL p210 has these DH-PH tandem domains whereas BCR-ABL p190 lacks these tandem domains because of the different translocation points in BCR gene. Although there is contradiction information about the DH domain[25], this domain is functional to catalyze the conversion of GDP to GTP on the members of small GTPases: RhoA, Rac1 and Cdc42[23]. The PH domain is functional to bind the phosphoinositide lipids in order to localize the BCR-ABL p210 protein in the plasma membrane[25]. Due to a lack of PH domain, the $p190^{BCR-ABL}$ protein becomes free to associate with the cytoskeleton[26]. Secondly, xeroderma pigmentosum group B (XPB) is classified as an ATP-dependent helicase, a member of the TFIIH transcription factor. Binding of XBP to BCR or p210 BCR-ABL regulates the phosphorylation of XBP to prevent the correction of defects in the DNA repair process unlike $p190^{BCR-ABL}$ does not have this type of interaction[27].

The C-terminus domain of BCR contains the shared sequences with GAP homology regulating the conversion of GTP to GDP unlike the GEF domain in the central region of BCR. This regulation is well-studied in the $p21^{Ras}$ oncoprotein and is illustrated that BCR-GAP (GTPase-activating protein) region binds Rac which is found in the Ras superfamily[15]. This binding stimulates the GTP hydrolysis of Rac and thereby resulting in the downregulation of membrane ruffling[20, 28]. The studies indicated above demonstrate that BCR-ABL can regulate the intracellular signaling pathway by accelerating or decelerating the GTP hydrolysis of the G (guanine nucleotide-binding) proteins.

The ABL gene is located on chromosome 9q34 with more than 230kb in gene size. This gene shares the human homology of v-abl identified as an oncogene of the Abelson murine leukemia virus[29]. The ubiquitously expressed ABL gene containing 11 exons with 2 alternative first exons results in a 145-kD non-receptor tyrosine kinase with two alternative ABL proteins: Abl type 1a and type 1b[15, 20]. Due to the alternative splicing at the N-terminus of ABL, the ABL type 1b protein containing a myristoylation (myr) site is able to localize in the plasma membrane with several functions[15].

There are three Src homology (SH) domains proximal to the NH_2-terminus domain of ABL protein: SH1, SH2 and SH3. SH1 domain carries the kinase features of ABL whereas SH2and SH3 domains function in the interaction with other proteins[15]. The SH1 domain functions as a switch between active and inactive kinase conformation

following the auto-phosphorylation of its activation loop by ATP[12, 30]. SH2 domain of ABL protein is able to bind the regions containing phosphotyrosine such as the sites in BCR[31] and this domain stimulates the activation of ABL1 by interacting with SH1 domain in the "open" ABL conformation[32]. Besides, SH3 domain might regulate the SH1 domain kinase activity of ABL protein and a mutation in its myristate-binding site causes a decline in the tyrosine kinase activity of ABL protein[12, 33]. Moreover, PxxPs that are proline-rich sequences are found in the central region of ABL protein in order to interact with SH3 region of other functional proteins for the phosphorylation[34].

The COOH terminus of mammalian ABL protein contains nuclear localization signals (NLS), DNA- and actin-binding domains. NLS including the three unlinked motifs plays a crucial role in the driving of nuclear entry of ABL[15, 35]. The ABL protein in the nucleus decelerates the growth of cells by stimulating cell cycle arrest in the G_1 phase[36]. Conversely, mammalian ABL can be transported outside of the nucleus because of its unwilling roles in the nucleus. This nucleocytoplasmic shuttle of ABL requires the binding of NES namely Nuclear Export Signal to exportin-1 protein[37]. NES motif located within the actin-binding domain allows cytoplasmic ABL for the transduction of integrin-based signals[37]. The acting-binding domain is responsible for the localization of ABL protein by interacting F-actin while the DNA-binding domain includes three HMG-like boxes (HLB) that regulate ABL interaction with A/T-rich sequences in the genome[35, 38]. A mutation in the F-actin domain can cause a reduction in the oncogenic activity of BCR-ABL protein due to the lack of interactions with other signaling molecules[39]. Overall, ABL plays crucial roles in a cell lifetime by processing intracellular or extracellular signals and influencing the decisions regarding survival, cell cycle and apoptosis.

1.1.1.3. BCR-ABL1 Signaling Mechanisms

The aberrant tyrosine kinase activity of BCR-ABL fusion protein brings about the variation in the signaling pathways and thus, the activity of a pathway induced by BCR-ABL might influence the internal and external signal transductions directly as well. The presence of BCR-ABL1 implicates leukemogenesis in the primary signaling pathways.

The MAPK/ERK (RAS/RAF/MEK/ERK) pathway is major signal transduction pathway connecting signals from outside of a cell to nuclear transcription factors, which are responsible for activation/deactivation of cytoplasmic proteins and expressions of cell

survival, motility, division and differentiation-related genes as well. BCR-ABL1 bearing cells experience aberrant proliferation due to over-activation of the MAPK/ERK pathway[40]. The auto-phosphorylation of Tyr177 on the BCR region of BCR-ABL reveals a binding site for an adaptor protein, Grb-2 and following its binding to BCR-ABL, Grb-2 interacts with SOS that is a guanine nucleotide exchanger of RAS to activate Ras by promoting the binding of GTP[41]. Additionally, Ras is activated by BCR-ABL substrate proteins Shc1 and Dok1 and in the comparison of BCR-ABL isoforms, Shc1 is highly active to interact with $p210^{BCR-ABL}$ while Dok1 is another adaptor protein, which prefers to bind $p190^{BCR-ABL}$ to activate Ras and its connected pathway for cellular proliferation[26, 42]. The activated Ras can induce Raf-1 namely a serine-threonine kinase and thereby resulting in the activation of the mitogen-activated protein kinase (MAPK) signaling pathway including three inter-connected kinases. One of these kinases, MEK is stimulated to activate extracellular signal-related kinases (ERK)-1/2 proteins to promote the activation of gene expression[40]. Furthermore, BCR-ABL positive cells undergo the over-activation of osteopontin (OPN) recruiting for the stem cell niche of $p210^{BCR-ABL}$ expressing stem cells via the RAS/RAF/MEK/ERK pathway[43].

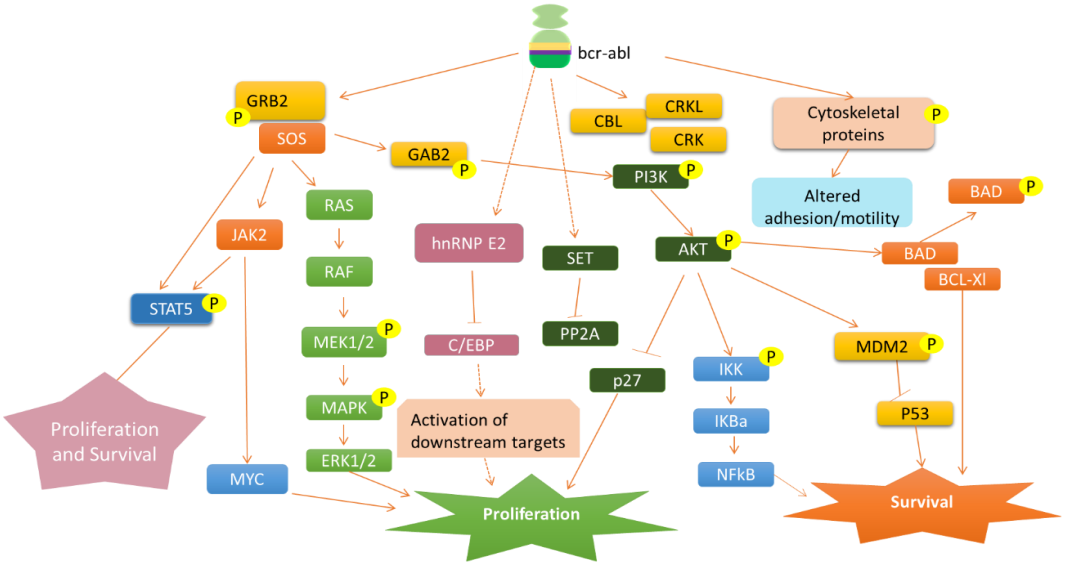

Figure 1. 2. Bcr-Abl Signalling

Both BCR-ABL variants can regulate the activation of Janus Kinase (JAK) and signal transducers and activators of transcription (STAT) proteins directly for stimulating cell survival and growth[44]. One of three JAK proteins, JAK 2 is able to phosphorylate the BCR-ABL fusion protein on tyrosine 177 directly in order to promote the BCR-ABL

signaling[12]. Conversely, $p210^{BCR-ABL}$ can activate JAK2 protein and thereby promoting BCL-XL activation in the nucleus for cell survival through the activation of STAT5 protein[45-46]. When comparing the interactions of BCR-ABL1 variants with STAT proteins, STAT1 and STAT6 prefer to bind $p190^{BCR-ABL}$ whereas STAT3 and STAT5 are involved in $p210^{BCR-ABL}$ regulated signaling pathway[26]. Moreover, $p210^{BCR-ABL}$ positive patients who experience the imatinib resistance have higher activation of phosphorylated STAT3 protein to maintain the survival of CML cells following the imatinib treatment[47]. Besides, the studies revealed that Src kinase family members are differentially activated in two BCR-ABL variants. The members of this SRC family: Hck, Lyn, and Fgr are phosphorylated by $p190^{BCR-ABL1}$ [48] and Lyn kinase is over-activated in p190 positive cells for cell survival. Thus, the usage of kinase inhibitor induces the survival of Ph+ B-ALL diagnosed mice but not in CML[48].

Phosphatidylinositol-3 (PI3) kinase activity contributes to the proliferation of BCR-ABL positive leukemia cells. BCR-ABL fusion protein variants activate the PI3 kinase with the help of Crk and Crkl adaptor proteins. Additionally, BCR-ABL protein can activate PI3 kinase through the binding of GAB2 (GRB-associated binding protein 2) to GRB2 adaptor protein in $p210^{BCR-ABL}$ positive cells[49]. Then, this activated kinase promotes Akt, a serine-threonine kinase and then, Akt suppresses $p27^{Kip1}$, a cell cycle inhibitor and thereby resulting in the acceleration of entering S-phase of the cell cycle[50]. Akt functions in the downregulation of the apoptotic signaling pathway by phosphorylating a pro-apoptotic protein Bad, which stimulates the inactivation of anti-apoptotic proteins: BCL-2 and BCL-XL[15]. Furthermore, the combined deletion of PI3 kinase causes its binding activity to Akt and thereby preventing the $p190^{BCR-ABL}$-based leukemogenesis in mice. The usage of PI3K/ mammalian target of rapamycin (mTOR) inhibitor (PI-103) inhibits the proliferation of mouse p190-positive ALL cells. The obtained results indicated that the combination of imatinib and PI-103 has a higher inhibitory effect on the proliferation of Ph+ ALL cells comparing the rapamycin and PI-103 combination results[51]. A similar result was obtained in the treatment of Ph+ ALL cells with both PI3K and mTOR inhibitors as well as in the ALL cells resistant to TKIs[52].

BCR-ABL1 variants are strong regulators in CML and Ph+ ALL cells and thus, there are various pathways influenced by BCR-ABL1 directly or indirectly. Although the signaling pathways mentioned above indicate the primary functions of the BCR-ABL1, the interactions of both variants in several pathways such as TRAIL-induced apoptosis, autophagy, genomic instability and adhesion should be revealed [12].

1.1.2. Current Targeted Treatment Strategies for Ph+ ALL

The history of BCR-ABL-positive leukemia cells was started in the 19th century by using arsenic for CML patients. In spite of serious toxicity on the patients, arsenic was used for a treatment option of CML patients until the usage of radiotherapy at the beginning of the twentieth century[53]. In the starting of the second half of the twentieth century, the effective drugs were developed to treat CML patients and then, the allogeneic stem cell transplantation was introduced to the patients who have the similar tissue properties in order to improve the survival of CML patients[54]. Besides, although there is no clear information about the treatment of Ph+ ALL patients in history, the outcomes of chemotherapy-treated patients have highly negative results in the overall survival of the patients. The patients who had the ability to live during the first five years after treatment is almost 12 percent of Ph+ ALL patients[55]. Therefore, there is a necessity to develop targeted agents to kill not only Ph+ ALL cells but also other cancerous cells effectively.

1.1.2.1. Tyrosine Kinase Inhibitors

The lightning of the functions of BCR-ABL fusion proteins in Ph+ leukemia is bound to discover agents that are able to deactivate BCR-ABL oncoprotein and thereby resulting in the elimination of cancerous cells in the patient's blood. The pioneer developed agent, imatinib mesylate (STI571, Gleevec, Novartis) is the first-generation tyrosine kinase inhibitor (TKI) approved by U.S. Food and Drug Administration (FDA) in 2001[56]. Imatinib mesylate has been designed to block the ATP binding site of BCR-ABL and thereby resulting in the inhibition of downstream signaling pathways related to Ph+ ALL cell survival and proliferation[57]. The combination of imatinib with chemotherapy leads to an increase in the overall survival of both younger and older patients in contrast to the single application of either chemotherapy or imatinib[58].

The molecular interaction related studies revealed that imatinib interacts with the ABL kinase domain of BCR-ABL1 by binding its catalytically inactive structure[59]. CML-based studies indicate that imatinib can also lead to inhibition of several receptors such as platelet-derived growth factor (PDGF) receptor, Kit receptor, and MAPK activation. [60]. The analysis of BCR-ABL1 fusion protein in which patients have resistance to imatinib treatment revealed that point mutations in the ABL region can result in the reduction

between imatinib and ABL complex[59]. Although imatinib is the first inspiring agent for both Ph+ ALL and CML treatments, most patients may not give positive respond because of the drug resistance. This phenomenon leads to the development of second-generation TKIs, dasatinib and nilotinib for those patients who fail to respond to imatinib treatment.

Dasatinib (BMS-354825, Sprycel, Bristol-Myers Squibb) is the second generation TKI that inhibits the activities of both Src and ABL kinases[61]. Dasatinib also suppresses the activity of PDGFR-α and β, c-KIT and ephrin receptor kinases[61-62]. Their inhibition leads to binding to their ATP-binding site in both active and inactive states with higher efficiencies compared to imatinib regardless of protein structure[62]. It was declared that dasatinib is functional to arrest the cells in the transition from G1 to S phase and thereby inhibiting the cell growth in CML patients[63]. Despite the lack of clear information about the feasible dose for dasatinib treatment for Ph+ leukemia, FDA approved the dasatinib application as 70 mg twice per day for CML patients in 2006. Besides, 100 mg dose of single application per day to the patients has similar efficacy with the approval method[64-65]. The application to imatinib-resistant patients with various BCR-ABL mutations is highly effective to overcome but, the cells carrying T315I mutation (threonine to isoleucine mutation at codon 315) might prevent the dasatinib activity in the patients[66].

Nilotinib (AMN107, Tasigna, Novartis) is a second-generation TKI approved by FDA in 2007 in order to treat CML patients with resistance to imatinib[65]. This TKI was synthesized followed by properties of the molecular basis and crystal structures of both wild and mutant ABL kinase domains in imatinib sensitive and resistant CML patients[67]. Therefore, nilotinib is able to bind the inactive form of ABL kinase due to the topologically better fitting to the hydrophobic domain and thereby resulting in the higher potency to inhibit its activity[68]. At the molecular level, nilotinib causes the inhibition of BCR-ABL autophosphorylation on Tyr177 in not only wild type but also many mutant BCR-ABL positive cells. However, there is no clear evidence that this TKI can overcome the imatinib resistance of the cells carrying T315I mutation[69]. Additionally, nilotinib can inhibit the activities of PDGF and c-Kit receptors[70]. A phase 2 clinical study in Korea revealed that the combination of nilotinib with chemotherapy provides the increase in 2-year OS of newly diagnosed Ph+ ALL to 72% while complete remission (CR) rate in these 90 patients was 91% [71]. Collectively, there is a distinct role of nilotinib on not only CML patients but also Ph+ ALL patients by clearly inhibiting BCR-ABL protein.

It has become obligatory to find an agent that can overcome T315I mutation for the patients who relapse after imatinib treatment. Ponatinib is a third-generation TKI,

which specifically inhibits the BCR-ABL carrying kinase domain mutation, especially T315I mutation[72]. The discovery of this TKI has revolutionized the treatment ways of a patient because it is revealed that kinase domain mutations were present in 40% of Ph+ ALL patients who newly diagnosed and were not treated by any agent[73]. The pan-BCR-ABL inhibitor ponatinib is more than five hundred times effective than imatinib for inhibition of ABL kinase and this inhibitor can suppress activities of several proteins such as vascular endothelial growth factor (VEGF) and fibroblast growth factor (FGF) receptors, KIT, FLT3 and SRC[74]. The ponatinib combination with chemotherapy regime has illustrated the best anti-leukemic activity within the developed agents for Ph+ ALL patients. The application of this combination to 37 patients had resulted in a good 2-year survival rate as 81% while 4 patients died because of the treatment-irrelevant reasons[75].

The development of TKIs for CML and Ph+ ALL patients has offered highly feasible treatment ways for the patients who experience the different levels of the diseases. Since BCR-ABL positive cancer cells seek the best way to overcome the killing activity of these drugs, it is a necessity to develop safe and highly effective agents.

1.1.2.2. Immunotherapeutic Approaches

The discovery of genes and proteins in death-causing disease revealed that cancer cells could express some proteins on their surfaces and these lead to the developments in immunotherapy for many cancers including ALL. The developed treatment ways mainly target the cell surface antigens of B lymphoblast that are CD19, CD20 and CD22. These options can be divided into two classes: antibody-based and cell-based immunotherapies. While antibody-based therapy is classified based on antibody properties into bare monoclonal antibodies, bispecific T cell engaging (BiTE) antibodies, and antibody-drug conjugates (ADC), cell-based treatment includes CAR-T cells for ALL[11, 76].

1.1.2.2.1. Monoclonal Antibodies

Antibodies are significant members of the immune system, which have higher specificity and binding affinity to an antigenic epitope. Therefore, they are potent candidates to eliminate the unwanted cells or molecules by targeting the surface receptors

such as CD22, CD20 and CD19 [77] [7]. The developed monoclonal antibodies can effectively promote the complement-dependent cytotoxicity (CDC), antibody-dependent cytotoxicity (ADCC), and direct induction of apoptosis by binding surface receptors[76].

CD22 surface receptor recruited in the differentiation of B-lineage is internalized following the binding of an antibody[7]. CD22 directed therapy includes inotuzumab ozogamicin (InO), moxetumomab pasudodotox, Combotox and epratuzumab, which are linked with toxin molecules to increase the treatment efficiency of relapsed and refractory (R/R) ALL. InO has linked calicheamicin, which promotes the apoptosis by binding to DNA and increasing the cytotoxicity. The obtained impressive results from these ALL patients pave the way for that FDA approved this agent in 2017 as a treatment option for these patients[76]. However, the studies including Ph+ ALL patients revealed that although a single application of InO to Ph+ ALL patients needs still development, the combination study with bosutinib, a second-generation TKI has the promising results with 8.2 months prolonged OS in R/R Ph+ ALL patients who have not T315I mutation[78].

Secondly, the CD20 surface receptor is responsible for the higher relapse and lower OS because of its role in cell cycle and apoptosis. CD20 linked monoclonal antibodies are rituximab, ofatumumab, obinutuzumab and REGN1979 causing highly effective antibody-mediated cytotoxicity for the pre-B ALL, Ph- ALL or chronic lymphocytic leukemia (CLL) [7]. REGN1979 is engineered to target not only CD20 but also CD3 surface receptors to activate the immune response of T-cells to B-cells. The first results revealed that this biallelic antibody stimulates the decline of B-cells[79].

Furthermore, CD19 has mostly expressed receptor in the B-lineage family and recruited for surface immunoglobulin on the B-cell in order to activate proliferation-related pathways such as PI3 kinase, SRC-family kinases and c-myc[80-82]. CD-19 targeted monoclonal antibodies: coltuximab ravtansine (SAR3419), Denintuzumab mafodotin (SGN-CD19A) and ADCT-402 are developed to treat R/R ALL patients. Additionally, like REGN1979, blinatumomab may target CD19-positive B-ALL cells leading to activation of CD3 positive T cells. Besides the significant results on R/R Ph- ALL, the blinatumomab application to R/R Ph+ ALL patients treated with second and/or third-generation TKIs revealed similar results with the Ph-negative patients. Four of ten blinatumomab-treated patients with T315I mutation achieved the complete remission of the disease and the prolonged OS of them was 7.1 months[83]. There are several ongoing studies, which try to increase the efficacy of this treatment with the effective TKIs [84].

Since antibodies have a higher affinity to bind their specific antigen epitopes, they can be utilized to target mostly expressed receptors in cancerous cells. R/R Ph- ALL patients experienced better results instead of classical treatment ways. The recent studies brought in the influence of monoclonal antibodies on Ph+ ALL patients treated with currently used TKIs. The future studies will lead to an increase in CR of these diseases.

1.1.2.2.2. Chimeric Antigen Receptor (CAR) T-cells

CAR T cells are the engineered form of T lymphocytes to transcribe the receptors which are targets of an anti-CD19 segment and fused with activator signaling molecules of the T-cell receptor. These T-cells are obtained from the patient's blood and they merge the cytotoxic activity of T-cells and the antibody's antigen specificity[85]. First generated CAR-T cells, which have expressed CD19 or CD20 receptors did not achieve the significant anti-tumor activity while second and third-generation CAR-T cells have the ability to rise the elimination of cancerous cells due to their co-stimulatory domains. The fourth and last generation CAR-T cells contain the cytokine-expressing region to increase the survival and expansion[86]. The clinical studies including effective CAR-T cell application for the R/R Ph- ALL patients have increased the OS and life qualities of the patients. However, this type of study is not frequently used to treat R/R Ph+ ALL due to the fact that TKIs are highly effective for the treatment of Ph+ ALL patients. On the other hand, a study about relapsed patients carrying T315I mutation illustrated that CD19-targeted CAR-T cells are likely to be applied relapsed patients with ponatinib or alone to eliminate the BCR-ABL transcripts with higher efficacy[87]. Another case study about a triple combination of third-generation TKI, blinatumomab monoclonal antibody and CD19-targeted CAR-T cell therapy revealed a promising result contributing the development of subsequent combinational usage. A Ph+ patient who had relapsed following by CD19 targeted CAR-T cell treatment had had a quick and considerable response to ponatinib combination with blinatumomab. However, the patient died after twelve months of the treatment because of the central nervous system relapse of ALL[88].

Although there are many treatment options for R/R ALL patients, the application of the right combination and time plays a crucial role in their lifetimes and life qualities. Thus, it is necessary to develop new strategies targeted only cancerous cells with distinctive features to eliminate them effectively.

1.2. Sphingolipid Metabolism

Sphingolipids are very common molecules in all eukaryotes and several prokaryotes[89]. The sphingolipid family comprises several major classes; sphingoid bases, sphingomyelins, and glycosphingolipids. The sphingosine bases are the building blocks of sphingolipids and sphingosine is the mostly seen member in mammals and can be converted to other lipid molecules[90]. The sphingoid bases are used to derive ceramide constructed by using hydrophobic sphingoid bases and fatty acid in the varied chain length by linking to the backbone through an amide bond. Ceramide has significant roles in the regulation of permeable eukaryotic membranes and internal cellular signaling for differentiation, cell adhesion, migration and cell cycle arrest. Besides their messenger roles, ceramides function in the regulation of proliferation, inflammation and apoptosis[91].

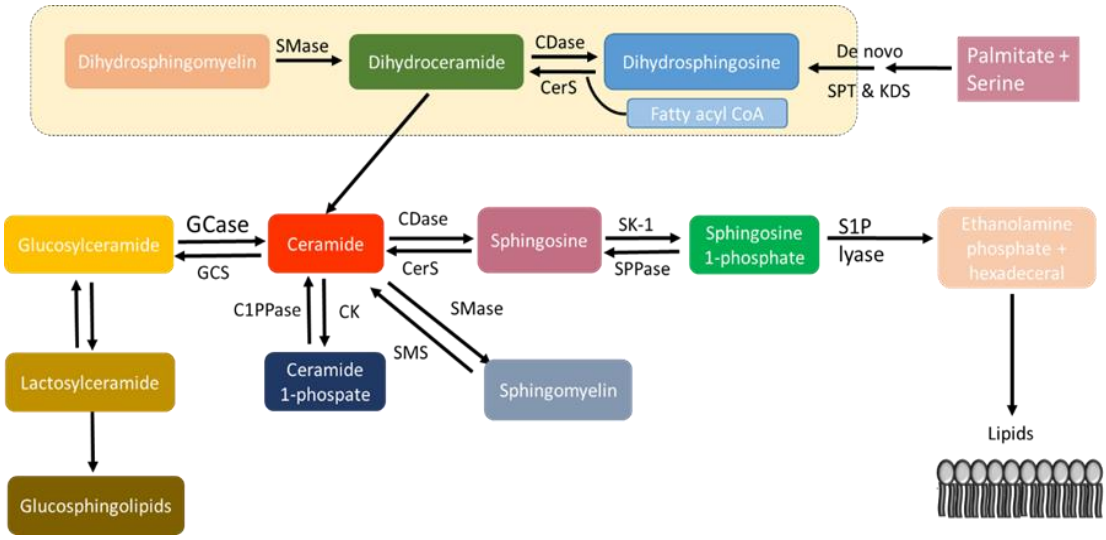

Figure 1. 3. Sphingolipid Metabolism

1.2.1. Bioactive Sphingolipids

The studies about sphingolipids revealed their importance in the regulation of cell growth in various aspects for the cells and they identified that "bioactivity" of lipid can be explained that the changes in lipid levels lead to significant results in cellular events[92]. The main bioactive sphingolipids including sphingosine, ceramide and sphingosine-1-phosphate are highly functional in the modulation of proliferation, survival, apoptosis, migration, inflammation, differentiation, cell cycle and cytoskeleton rearrangement[90].

Ceramides are central lipid molecules for all sphingolipids and generated in mammals through *de novo* synthesis, sphingomyelin metabolism or salvage pathway (Figure 1.3). The first ceramide-generation step includes the reaction of L-serine and palmitoyl-CoA under the regulation of serine palmitoyltransferase (SPT) in the endoplasmic reticulum (ER)[93]. Following several pathways regulated by sphingolipid metabolizing enzymes, ceramides are synthesized as central molecules and then metabolized to the sphingolipids in order to function in their specific regions for their roles[94]. In the sphingomyelin cycle, ceramide is generated followed by the hydrolysis of sphingomyelin (SM) located in the plasma membrane through the sphingomyelinase (SMase) activity[95]. These ceramide-generating enzymes also play roles in the regulation of apoptosis and cell cycle arrest. The reversible reaction, which includes the conversion of ceramide to SM, takes place in Golgi following by transportation of ceramide by ceramide transfer protein (CERT) [95-96]. In the salvage pathway, glycosphingolipids have lost their hydrophilic portions to produce intermediates; galactosylceramide (Gal-Cer) and Glucosylceramide (GluCer) that are immediately converted into ceramide with their specific enzymes[97]. Therefore, the ceramide level is regulated by three different ways to continue the function of the central-piece molecule during the various cellular events. Furthermore, GluCer is generated by utilizing from ceramide under glucosylceramide synthase (GCS) enzyme activity. GCS is able to transfer glucose to ceramide by using UDP-glucose to generate GluCer. The GCS based cancer studies revealed that GluCer promotes tumor growth[98] and the elevated GluCer increases the drug resistance level of melanoma and breast cancer to the drugs of chemotherapy[99]. The first study about drug resistance interaction of GCS revealed that imatinib-resistant K562 CML cells have rocketed mRNA and protein levels of GCS to eliminate the ceramide accumulation[100]. Additionally, GCS overexpression results in a sharp decrease in the cellular ceramide levels and glucosylceramide accumulation and thereby reducing apoptosis and promoting survival of drug-resistant MEC-2 CLL cells[101].

Sphingosine is a pro-survival bioactive lipid molecule derived from ceramide by ceramidase activity. Sphingosine plays roles in the induction of cell death and inhibition of cell proliferation. Sphingosine is phosphorylated to convert another major bioactive sphingolipid, sphingosine-1-phosphate (S1P) by activities of sphingosine kinase-1 and -2 (SK-1 and -2 or SphK 1/2) [93, 95]. It is indicated in the literature that unlike sphingosine, S1P is involved in the modulation of proliferation, survival, cell growth, migration and inflammation by binding G-protein-coupled receptors (GPCRs) on the cell surface [102].

These S1P receptors are divided into five groups, S1P1-5 and the binding of S1P to these receptors depends on the cancer type[102-103]. The level of S1P in the cancerous cells are highly increased and thus, these cells show higher resistance to apoptosis[104]. Sphingosine and S1P are functional to establish a balance with ceramide in the regulation of cell fate under both normal and stress conditions. While ceramide is responsible for the modulation of apoptosis, S1P activates the proliferation and resistance-related pathways.

1.2.2. Roles of Ceramides and Ceramide Synthases in Cancer Cells

Cellular stress is likely to activate several death-related pathways such as ceramide synthesis and ceramide conversion from sphingosine and/or S1P molecules. Endogenous ceramide synthesis is carried out by ceramide synthases (CERS1-6) which are recruited as the rate-limiting enzymes. These enzymes located mainly in near ER also generate ceramide by using sphingosine as a substrate in the salvage pathway. Ceramides with various chain lengths from 14 to 26 carbons play roles in varied cellular pathways of both normal and cancer cells. Thus, they are attractive targets to eliminate their functions by specific inhibitors in cancer cells. Identification of CerS-regulating pathways leads to the clarification of various roles of ceramides in cancer metabolism. Understanding of interactions and functions of CerS (1-6) with other lipids and proteins in cancer cells is crucial to find better treatment options[93].

Ceramide synthase 1 (CerS1) is mainly expressed in the human brain and skin tissues and plays role in the production of long-chain C18:0-ceramide by *de novo* synthesis and salvage pathway[105-106]. A study about head and neck squamous cell carcinoma (HNSCC) states that CerS1 mRNA and C18-ceramide levels are lower in patients compared to healthy control tissues and CerS1 overexpression induces apoptosis of these cells in vitro through restoring the C18-ceramide level[107]. The further study revealed that its suppression is regulated at its promoter region by histone deacetylase 1 (HDAC1)-dependent inhibition of a transcription factor, Sp1[108]. Additionally, C18-ceramide generated by overexpressed CerS1 triggers the deacetylation of Sp3 transcription factor by the activity of HDAC1. Thus, both molecules to inhibit its transcription wrap human telomerase reverse transcriptase (hTERT) promoter region and thereby resulting in the apoptosis of A549 human lung adenocarcinoma cells[93, 109]. Emerging evidence states that imatinib-treated K562 cells had experienced an increased

level of apoptosis due to the higher activity of CerS1 and C18-ceramide level. The drug-resistance K562 cells increased the S1P generation instead of the ceramide to overcome the negative effects of the drug on cellular proliferation[110]. Furthermore, dasatinib-treated K562 sensitive cells overexpressed CerS1 mRNA and thereby resulting in the apoptosis of the cells[111]. In addition to drug-related cytotoxicity, acute myeloid leukemia (AML) cells containing FMS-like tyrosine kinase 3 (FLT3) mutation have been treated with FLT3 inhibitors and the overexpressed CerS1 and its product C18-ceramide moved to mitochondria to activate mitophagy, an autophagy subtype with damaged mitochondria. Interestingly, due to the application of exogenous C18-ceramide analog, the AML cells experience the ceramide-associated lethal mitophagy[112]. The obtained results indicate that suppression of CerS1/C18-ceramide after drug treatment causes drug resistance whereas their higher expression levels result in lethal mitophagy[105].

CerS2 is known to be ubiquitously expressed in all tissues among the CerS enzymes and predominantly expressed in kidney, liver, lung, heart, brain, breast and adipose tissues[93]. The CerS2 expression, which is mainly located in ER increases the generation of long-chain ceramides ranging from C20 to C26 [105]. The growing number of studies suggest that the absence of CerS2 activity is associated with the accelerated development of varied cancer types and thus, CerS2 is classified as a tumor-suppressor protein. The level of CerS2 expression and the long-chain ceramide products are crucial for the coordination of proliferation and growth of hepatocytes. CerS2 lower expression associated with the poor prognosis and tumor progression of hepatocellular carcinoma (HCC)[113]. CerS2 overexpression causes the migration ability of MDA-MB-231 cells that have remarkable ability to be invasive and migrate whereas MCF7 cells with CerS2 knockdown have considerably increased ability to migrate and being invasive[114]. In addition to these results, there was strong evidence indicating the tumor suppressor effect of CerS2 on ovarian, breast, and lung cancer patients, which restored CerS2 expression can be ensured by abrogating the miR-9 interaction so that C24 ceramide level was increased in these cells. Therefore, the proliferation and metastasis abilities of the cell lines inhibited whereas the apoptosis rates in these cell lines were accelerated[115]. The detail studies about how CerS2 inhibits the proliferation revealed that CerS2 overexpression stimulates the G0/G1 cell-cycle arrest through the p21/p53-dependent pathway in papillary thyroid cancer cells[116]. Conversely, CerS2 is mainly expressed and generated C24 and C24:1-ceramide molecules in some cancer types such as human breast and colorectal cancer (CRC) tissues. Although studies state that CerS2 inhibits tumor

progression in several cancer types, CerS2 can contribute to the improvement of chemo-resistance in various cancers[105]. Two studies using different cell lines of bladder cancer obtained different results. The downregulation of CerS2 mediated by siRNA enhanced the migration ability of RT4 and T24 cell lines[117] whereas this downregulation declined the migration ability of UMUC1 cells[118]. The partially resistant p53-deficient and p53-expressing HCT116 colon cancer cells increased levels of CerS2 and its products after 5-fluorouracil (5-FU) and oxaliplatin treatments[119]. A study revealed that CerS2 downregulation increased the C16 ceramide level using C24 and C24:1 ceramides so that the apoptotic rate of cisplatin/UV radiation exposed HeLa cells enhanced[120]. Collectively, CerS2 has dual roles in several cancers and it can act as either a tumor suppressor or a driver molecule for enhanced chemo-resistance.

CerS3 is predominantly expressed in testis tissues and mildly in skin whereas its expression is limited in other tissues. CerS3 might generate varied ceramide molecules containing a wide range of carbon numbers from C18 to C26[105]. Despite a lack of information about its primary function, CerS3 deletion in male mice germ cells increased their apoptosis and inhibited spermatogenesis[121]. Due to the limited and controversial results, there is no clear interaction between CerS3 and cancer progression.

CerS4 is mainly found in mice skin tissues and the CerS4 deficiency in adult mice caused the hair loss[122]. CerS4 overexpressed in nearly all human tissues and its protein level is highest in testis tissues whereas other tissues such as ovary, lymph nodes, spleen and vagina have a lower level of CerS4 protein. CerS4 regulates the C18 and C20 ceramide synthesis mainly found in ER within a cell[105]. The cancerous cells have higher CerS4 expression compared to non-cancerous cells such as liver cancer tissues[123] and the levels of C18 and C20 ceramide are increased in the estrogen receptor (EsR) positive breast cancer tissues[124]. Conversely, exogenous CerS4 overexpression leads to C18- and C20-ceramide synthesis and thereby decreasing proliferation and inducing apoptosis of human colon and breast cancer tissues[125]. During the tumor progression through the metastatic stage, CerS4 mRNA levels are gradually decreased in HNSCC and renal cell carcinoma patients and CerS4 knockdown stimulates the migration ability of lung cancer cells *in vitro* and induces the metastatic ability of murine mammary cancer cells to the liver *in vivo*[126]. Collectively, CerS4 has several roles in the regulation of proliferation and metastasis abilities of cancerous cells.

CerS5 is predominantly expressed in the human brain and in almost all mice tissues. CerS5 generates mainly C14- and C16 ceramides and less C18 ceramide and

found -mainly- in the ER and nucleus[105]. Drug-induced CerS5 upregulation results in higher C16- ceramide generation and thereby resulting in apoptosis of MCF7 breast cancer cells by directing Bax to mitochondria[127]. Moreover, artificial overexpression of CerS5 and its product C16-ceramide trigger apoptosis of HeLa cells after ionizing radiation[128]. A high level of CerS5 is found in CRC patients and this higher expression decreases the overall survival and increases the recurrence rate within 5 years [129]. Besides, CerS5 is also highly expressed in breast cancer tissues and it enhances tumor cell proliferation with higher estrogen activity[130-131]. When the literature is checked, there is a clear correlation between two suppressor molecules; p53 and ceramide [132]. The article states that CerS5 is under the control of p53 to response to the chemotherapeutic application in HCT116 cells [119]. The μ-irradiation increased the p53 activation in Molt-4 LXSN leukemia cells and thereby resulting in the overexpression of CerS5 mRNA and higher de novo synthesis of C16-ceramide[133]. Conversely, CerS5 exogenous expression repressed the p53 promoter activity in HEK293 cells[134] whereas artificial C16-ceramide application to HCT116 cells enhances p53 transcription[135]. Indeed, endogenously enhanced C16-ceramide level increases the p53 stabilization by binding and its activation in varied cancer types[136]. The discovery of clear interaction between p53 and CerS5/C16-ceramide might provide the better treatment way for various cancer types.

CerS6 is mainly localized in the ER and is found in almost all human tissues. This enzyme plays a role in the synthesis of C14- and C16-ceramide molecules[105]. CerS6 is predominantly expressed in EsR-positive breast cancer compared to negative breast cancer cells and the levels of C16-ceramide and CerS6 expression are higher in the metastatic breast cancer tissues[124]. The enhanced CerS6 expression in human non-small-cell lung cancer (NSCLC) results in the increase of their invasive and metastatic abilities by decreasing the miR-101 level in these tissues[137]. Another study revealed that knockdown of CerS6 decreases proliferation, invasion and migration of gastric cancer cells in in vitro and *in vivo* experiments. A mechanism was demonstrated that CerS6 overexpression in these cells downregulates the upregulation of SOCS2 (suppressor of cytokine signaling 2) that belongs to the SOCS family of JAK-STAT signaling inhibitors. Thus, the cells may not activate JAK-STAT signaling and enhance the expression levels of cell cycle-related genes cyclins A and B and metastasis-associated genes MMP-2 and -9 [138]. Additionally, CerS6 expression gradually decreased during Epithelial-Mesenchymal Transition (EMT) in various cancers and an artificial increase of C16-ceramide level results in the decreased fluidity of plasma membrane and inhibition of

migration ability of mesenchymal breast cancer tissues[139]. CerS6 expression increases the chemosensitivity of cancer cells through drug-based activation of death-related receptors such as Fas receptor (CD95). CD95 that is a member of tumor necrosis factor (TNF) receptor superfamily is activated by drug-induced CerS6 expression and thereby resulting in the apoptosis of liver, pancreatic and ovarian cancer cells [140]. The exogenous overexpression of CerS6 is likely to interact with CD95 to inhibit its assembly with Fas-associated protein with death domain (FADD) and thereby preventing the drug-triggered apoptosis through the extrinsic pathway in ALL cells. The downregulation CerS6 causes the increased sensitivity of these cells to a drug, ABT-737 through increased CD95/FADD interaction[141]. Collectively, CerS6 plays roles in the enhanced proliferation and migration abilities of various cancer cells.

1.2.3. Roles of Sphingosine-1-Phosphate in Cancer Cells

Following the excess ceramide synthesis or completing the function, it is converted into sphingosine through ceramidases (CDases) and then sphingosine is phosphorylated by SK-1 or SK-2 to yield sphingosine-1-phosphate (S1P)[142]. S1P plays roles in the autocrine or paracrine signaling secreting outside from cancerous cells by ATP-binding cassette sub-family C member 1 or 2 (ABCC1 or ABCC2) (such as in breast cancer cells) and activating five specialized GPCRs, also named as S1PR1–5 [142-143].

SK-1 and-2 are the members of diacylglycerol kinase family and SK-1 is localized generally in the cytosol whereas SK-2 is found predominantly in the nuclear membrane and in the cytoplasm. The clinical and *in vitro* studies declared that both SK-1 and -2 play crucial roles in the stimulation of cell survival and oncogenic signaling pathways depending on their subcellular localization for S1P generation[144]. S1PR signaling has important roles in several cancer types including the inhibition of apoptosis, induction of proliferation and migration[143, 145]. Similarly, this signaling enhanced the drug resistance through the inhibition of caspase-3 signaling and serine/threonine-protein phosphatase 2A (PP2A) and increasing stability of BCR-ABL in the drug resistance CML cells [146].

S1P secreted from SPNS2 (protein spinster homologue 2) in endothelial cells increases tumor metastasis by decelerating the cytotoxic T cell function through regulating S1PR functions on the cancer cells and/or these immune cells [147-148]. Furthermore, SK-1-associated S1P in MB49 murine bladder cancer cells activates S1PR2

signaling and thereby resulting in the inhibition of breast cancer metastasis-suppressor 1 (BRMS1) expression, namely a master suppressor of metastasis. Thus, S1P-triggered S1PR2 brings about enhanced lung metastasis of these cells. As a treatment option, a monoclonal antibody Sphingomab that directly interacts with S1P to prevent its signaling inhibits the lung metastasis of these murine bladder cancer cells. This study revealed that S1P has a crucial role in providing communication way between cancer cells and immune cells to escape from their regulation and cancer cells, therefore, become metastatic [148].

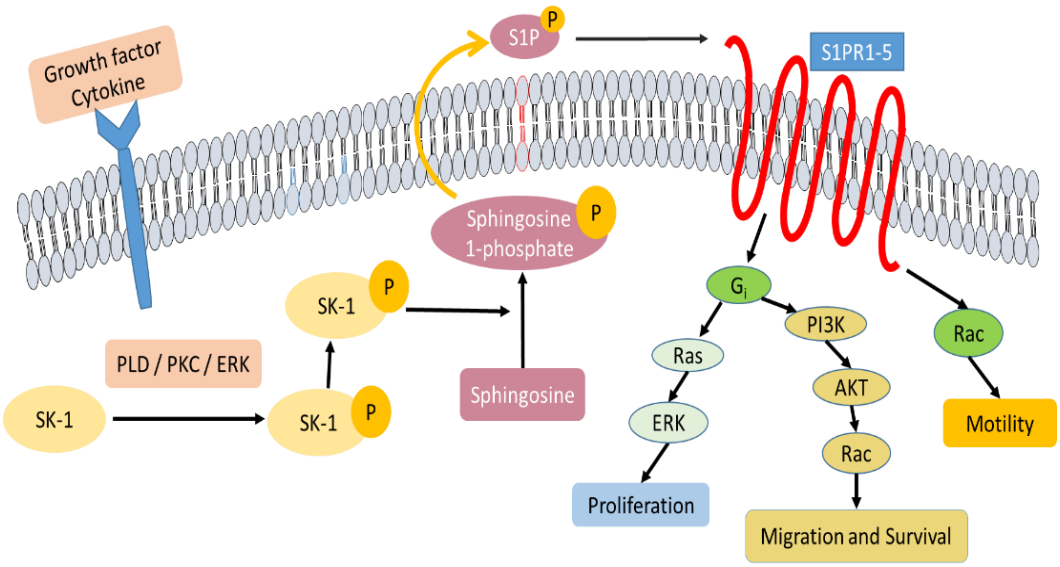

Figure 1. 4. Sphingosine-1 Phosphate Signalling

On the other hand, S1P produced by SK-2 can function in the cytoplasm by binding to TNF receptor-associated factor 2 (TRAF2) to induce NF-κB signaling in HeLa and HEK293 cells for proliferation and immune responses[149]. SK-2 generated S1P near the nuclear envelope inhibits TERT degradation by directly binding to its catalytic subunit and increases the TERT stability by mimicking the TERT phosphorylation. The inhibition of SK-2 causes the suppression of cancer growth through TERT degradation[150].

1.2.4. The Sphingolipid Rheostat: Ceramide vs S1P

The sphingolipid rheostat provided by ceramide and sphingosine-1-phosphate as biological balance in a cell determines the fate of either cancerous or normal cells. The dynamic balance can shift through the increase in the ceramide or S1P levels. If the

balance goes towards ceramide due to enhanced cellular stress caused by radiation or chemotherapy application, the cells experience the apoptosis. Conversely, the shifting towards S1P increases the cellular proliferation, chemo-resistance and anti-apoptotic abilities of the cells[151]. Following the increase or decrease of ceramide and/or S1P in the cytoplasm and environment of the cells, they experience some changes in the several cellular events, which are mentioned above in this chapter.

1.3. Natural Products: Flavonoids

The traditional plants, vegetables and fruits are known to be sources of numerous compounds, which are likely to use for the treatment of several death-causing diseases including cancer. The scientific *in vitro* and *in vivo* studies demonstrate that flavonoids are ubiquitous polyphenols naturally occurred in the plants and they might have crucial roles including the prevention and inhibition of the progression of many diseases. Flavonoids are the secondary metabolites in the plants, which have several features such as anti-oxidant, anti-inflammatory, anti-viral/bacterial, anti-cancer and anti-aging. Apigenin is a member of this family, which has strong features in the inhibition on varied cancer types with different functions[152-153].

1.3.1. Structure and Metabolism of Apigenin

Apigenin is the most abundant natural flavonoid found in several dietary plants such as fruits and vegetables. Apigenin is named as 4',5,7-trihydroxyflavone with the chemical structure $C_{15}H_{10}O_5$ and its molecular mass is 270.24 g/mol [154-155]. Its 2D chemical structure is demonstrated in Figure 1.5 [156].

The "apigenin" name originates from Apium genus in Apiaceae family that is a sub-family of aromatic flowering plants such as carrot, parsley and celery [157]. Apigenin is found as a secondary metabolite in dietary plants, which contain the glycosylated site in its original form. Thus, it becomes more soluble and stable in organic solvents [158]. Apigenin is mainly found in significant amounts in various dietary vegetables and fruits such as parsley, celery, chamomile, oranges, thyme, onions and honey [154, 157]. Tang et al. have determined the apigenin distribution in the plants in detail with their common and scientific names and content as mg/kg dry weight [159].

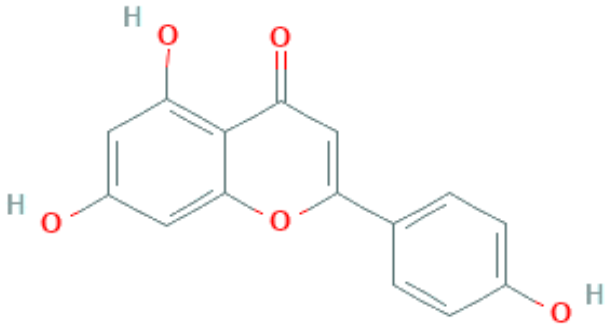

Figure 1. 5. 2D chemical structure of Apigenin

The first study about apigenin in the literature stated its positive effect on histamine release within the 1950s [154, 160]. The anti-mutagenic and tumor inhibitory effects were reported for the first time by Birt et al. [161]. In the following years, apigenin has been widely investigated in numerous studies as a potent chemo-preventive agent against various cancers.

1.3.2. Apigenin and Cancer

The effects of apigenin on cell lines, mouse models or human tumor tissues of various cancer types have been studied in a wide range. The recent studies about the anti-cancer effects of apigenin on different cancer types were reviewed in this part.

Apigenin which is a natural compound found in several plants triggers the oxidative stress and shows anti-cancer effects on hepatocellular carcinoma through regulating reactive oxygen and nitrogen species[162] as well as apigenin promotes oxidative stress in several types of cervical cancer cells [163]. Nevertheless, apigenin regulates the glucose metabolism in cancer cells through inhibiting Glucose transporter 1 (GLUT1) expression that improves the better response in treatment [164-166].

Several studies stated that apigenin inhibits the cell proliferation and growth of various cancers; breast cancer[167], prostate cancer[168], CRC[169], choriocarcinoma[170], malignant mesothelioma[171], glioblastoma[172], bladder cancer[173], HCC[174], colon cancer[175], osteosarcoma[176], and melanoma[177] in dose and/or time-dependently. A recent study demonstrated that apigenin inhibits the proliferation of HCC HepG2 and renal cell carcinoma cells in a dose and time-dependent manner and apigenin also inhibits tumor growth and the tumorigenesis in xenograft mice models respectively [178-179].

Apigenin induces directly apoptosis regulating signaling pathways in breast cancer[180-181], colon cancer[182-183], NSCLC [184] and esophageal carcinoma[185]. It is recently shown that apigenin induces ROS generation and activating caspases in HCC cells. Indeed, it promoted death receptor 5 (DR5) expression and enhanced TRAIL-mediated apoptosis in a dose-dependent manner[186]. Another study showed its apoptotic and autophagic effects on HCC cells by regulating PI3K/Akt/mTOR signaling pathway. Apigenin enhanced apoptosis decreasing the phosphorylation levels of Akt and mTOR and promoting the cleavage of PARP, caspase-3 and -9, increasing Bax gene expression whereas decreasing Bcl-2 expression[178].

Several studies demonstrated that apigenin induces cell cycle arrest in prostate cancer[168], bladder cancer [173] and melanoma[177]. Apigenin enhances cell cycle arrest at the G2/M phase through regulating cell cycle-related factors: ATM, Chk2, Cdc25c, Cdc2, Cyclin B1 in renal cell carcinoma[179]. Other studies also indicated that apigenin induces cell cycle arrest at the G2/M phase in MDA-MB-231 breast cancer cells[167] as well as in glioblastoma cells[172].

In addition to its cytotoxic, cytostatic and apoptotic effects, apigenin inhibits the migration, invasion and metastasis abilities of several cancer cells including prostate cancer[187], CRC[169], osteosarcoma cells[176], lung cancer[188] and melanoma cells[177]. Dai J et al. showed that apigenin inhibited invasion, migration and metastasis in CRC cells by repressing Neural precursor cell expressed developmentally down-regulated 9 (NEDD9)/Src/Akt signaling pathway in both *in vitro* and *in vivo*[189]. Other studies showed that apigenin inhibited invasion, EMT and metastasis of HCC and colon cancer cells via downregulating NF-κB and Snail signaling in both *in vitro* and *in vivo* studies [174, 190]. Indeed, apigenin inhibits SPOCK1-snail/slug axis in both *in vitro* and *in vivo* to prevent these abilities in prostate cancer cells[191].

It has been proved that apigenin inhibits the stem cell features of cancer cells through regulating related signaling pathways such as Wnt, YAP/TAZ, cMet and PI3K/Akt/Nf-kB[192-194]. For instance, a study demonstrated that apigenin inhibits the tumorigenic properties and stem cell features of triple-negative breast cancer cells through disrupting the YAP/TAZ signaling pathway and its protein-protein interaction with TEAD, which is crucial for maintaining of cancer stem cells [194]. Another study indicated that apigenin abolishes the expression of hypoxia-induced stem-cell markers such as CD105, CD44, and VEGF in head and neck squamous cell carcinoma [195].

Huge pieces of evidence demonstrate the apigenin either overcomes the drug resistance in several types of cancer cells or enhances the therapeutic effects of chemotherapeutic drugs. Combination treatment of apigenin and cetuximab was more effective than only chemotherapy drug application in both nasopharyngeal carcinoma cells and mice [196]. Apigenin and gefitinib treatment can be a promising strategy in NSCLC due to the fact that apigenin inhibits several oncogenic signaling pathways[164]. Apigenin elevated the anti-cancer effects of cisplatin in different cancer cells through modulation of p53 by ERK/MAPK pathway[197]. Indeed, studies showed that apigenin enhances 5-FU in HCC and solid Ehrlich carcinoma[198-199]. Besides, studies showed that apigenin sensitizes the resistant HCC cells to doxorubicin through suppressing the miR-101/Nrf2 pathway [200]. Gao et al. also showed that apigenin enhances doxorubicin sensitivity in HCC cells via regulating miR-520b/ATG7 axis in both cells and xenograft mice model [201]. In addition to this, apigenin overcomes the drug resistance in adriamycin-resistant breast cancer cells through regulating the STAT3 signaling pathway [202] and apigenin also enhances the effects of cisplatin on prostate cancer stem cells [203].

1.4. Aim of the Study

Ph+ ALL is a type of ALL which is a hematological disorder characterized by the Philadelphia chromosome and its product BCR-ABL oncoprotein that mediate the crucial roles in the determination of cellular fate. In spite of the fact that there are current targeted treatment strategies for Ph+ ALL patients, the overall survival of these patients is still worse. Therefore, novel strategies combined with current targeted treatment ways are necessities not only for Ph+ ALL patients but also for whole cancer patients. Besides, the bioactive sphingolipids participate in the regulation of several biological processes to determine the responses against cellular stress. Thus, these sphingolipids are considered as therapeutic targets to overcome their anti-therapeutic responses.

In addition to the roles of both BCR-ABL and sphingolipids during the tumorigenesis, the studies indicated that flavonoids might contribute to the bioactive sphingolipids-associated cell death in varied cancer cells. Take an example for this interaction; resveratrol is likely to trigger cell death elevating the levels of ceramide compounds in prostate cancer [204] while it modulates the bioactive sphingolipid genes in order to stimulate apoptosis in AML HL-60 cell line dose-dependently [205]. As expected,

resveratrol has the ability to promote apoptosis via modulation of the SK-1 pathway in Ph+ K562 cells [206]. There has been only one study, which indicates the interaction of apigenin with SK-1 generated S1P signaling pathway through inducing apoptosis *in vitro* and *in vivo* studies of rat heart tissues [207]. According to the background information, we hypothesized that apigenin might have cytotoxic, cytostatic and apoptotic effects on Philadelphia chromosome-positive acute lymphoblastic leukemia SD-1 cells whereas the lower effect of apigenin on non-cancerous lung Beas-2B cells. Apigenin has a great potential to induce the apoptosis of SD-1 cells and it will cause to stop their proliferation abilities arresting them at G2/M transition. Furthermore, apigenin might have possible therapeutic potential to modulate the bioactive sphingolipids genes. Drug-induced overexpression of them will elevate the levels of ceramide molecules and thereby resulting in the apoptosis of SD-1 cells with the higher rates in a dose-dependent manner.

In this study, the cytotoxic, cytostatic and apoptotic effects of apigenin on Ph+ ALL cells will be determined by MTT cell viability assay, Trypan blue dye exclusion assay, Annexin V/PI dual staining, JC-1 dye-based measurement of mitochondrial membrane potential loss and cell cycle analysis for the first time. Moreover, the possible interaction between BCR-ABL and bioactive sphingolipids in apigenin treated SD-1 cells will be investigated for the first time as well.

CHAPTER 2

MATERIALS AND METHODS

2.1. Materials

The materials including cell lines, chemicals for the propagation of cells and apigenin whose therapeutic potential was investigated, primers and antibodies to be used in this study were listed below by making them in a proper group to follow easily.

2.1.1. Cell Lines

The Philadelphia chromosome-positive cell line SD-1 (ACC-366, DSMZ code) was obtained from the German Collection of Microorganisms and Cell Cultures (DSMZ), Germany. Non-cancerous epithelial lung Beas-2B cell line (ATCC® CRL-9609™) which was obtained before from American Type of Culture Collection (ATCC), USA and stored in the -80°C stock fridge was used in this project.

2.1.2. Chemicals

Apigenin was obtained from Sigma, USA and its stock solution was prepared by using Dimethyl sulfoxide (DMSO) which obtained from Sigma-Aldrich, UK as 10 mM in 1.5 mL Eppendorf tube and this tube was stored at -20°C fridge.

RPMI Medium 1640 (1X), DMEM High glucose (1X), Fetal Bovine Serum (FBS), Phosphate Buffer Saline (PBS) (10X), and DNAse/RNAse free distilled water were obtained from Gibco by Life Technologies, UK. Penicillin-Streptomycin (100X), L-glutamine (100X) and 0.25 mM Trypsin-EDTA were obtained from Euroclone, Italy.

6X DNA Loading Dye, GeneRuler 50bp DNA Ladder and 10mM dNTP Mix were obtained from Thermo Scientific, USA. Agarose for DNA electrophoresis was obtained from Genaxxon Bioscience, Germany. 10X Tris-Acetate EDTA (TAE) buffer was obtained from Vivantis Incorporation, USA.

Bovine Serum Albumin (BSA) was obtained from ChemCruz, Santa Cruz Biotechnology, USA. Pierce Bicinchoninic Acid Protein Assay kit was obtained from Thermo Scientific, USA.

Trans-Blot Turbo Mini-Size Transfer Stacks, Trans-Blot Turbo Mini-Size PDVF Membrane, 10X TGS Buffer for SDS-PAGE, Trans-Blot Turbo 5X Transfer Buffer, 10% TGX Stain-Free FastCast Acrylamide Kit, Blotting-Grade Blocker (Non-fat dry milk), 10x TBS (Tris-Buffered Saline), Clarity Western ECL Substrate, TEMED, Ammonium Persulfate, 4X Laemmli Sample Buffer and 2- Mercapto ethanol were obtained from Bio-Rad, USA. Tween-20 was obtained from Sigma-Aldrich, USA. Protein markers were obtained from Euroclone, Italy.

FITC Annexin V Apoptosis Detection Kit I was obtained from BD Pharmigen, BD Biosciences.

MitoProbe JC-1 Assay (Mitochondrial Membrane Potential Detection) kit for flow cytometry was obtained from Invitrogen, USA.

2, 5, 10 and 25 mL serological pipettes were obtained from Costar, USA

15 mL and 50 mL Falcon tubes were obtained from Isolab, Germany

6-, 12-, 24- and 96-well plates were obtained from Corning, USA.

25cm^2 and 75 cm^2 tissue culture flasks were obtained from Sarstedt, Germany.

10, 200 and 1000 µL tips were obtained from Axygen, Cornin, USA and they used in the experiments after properly autoclaved at autoclave machine.

2.1.3. Primers

Sphingosine kinase (SK)-1 and 2; Ceramide synthase (CERS)-1, 2, 4, 5, 6 and β-actin primers shown in Table 2.1 were obtained from Sentebiolab Biotech, Ankara, Turkey. Following the obtaining of them, they were dissolved in the indicated volumes of nuclease-free water by the manufacturer to reach 100 µM and then, they were aliquoted to obtain 10 µM working solution and stored at 4°C in the icebox.

2.1.4. Antibodies

The antibodies used in this study were purchased from various companies and their brands and dilution ranges were listed in Table 2.2.

Table 2.1. Primers used in this study

Primer Name	Primer Nucleotide Sequence
SK-1 Forward	5'- AGGCTGAAATCTCCTTCACGC -3'
SK-1 Reverse	5'- GTCTCCAGACATGACCACCAG -3'
SK-2 Forward	5'- ATGGACACCTTGAAGCAGAGG -3'
SK-2 Reverse	5'- CTGGGTAGGAGCCAAACTCG -3'
CERS-1 Forward	5'- ACGCTACGCTATACATGGACAC -3'
CERS-1 Reverse	5'- AGGAGGAGACGATGAGGATGAG -3'
CERS-2 Forward	5'- AGTAGAGCTTTTGTCCCGGC -3'
CERS-2 Reverse	5'- GCTGGCTTCTCGGAACTTCT -3'
CERS-4 Forward	5'- CTTCGTGGCGGTCATCCTG -3'
CERS-4 Reverse	5'- TGTAACAGCAGCACCAGAGAG -3'
CERS-5 Forward	5'- TCAGGGGAAAGGTATCGAAGG -3'
CERS-5 Reverse	5'- CTGCCTCCCATGTGACCATT -3'
CERS-6 Forward	5'- GGGATCTTAGCCTGGTTCTGG -3'
CERS-6 Reverse	5'- GCCTCCTCCGTGTTCTTCAG -3'
β-actin Forward	5'- ATTGGCAATGAGCGGTTCC -3'
β-actin Reverse	5'- GGTAGTTTCGTGGATGCCACA -3'

Table 2.2. Antibodies used in this study

Primary Antibody	Brand	Dilution	Secondary antibody	Dilution
SK-1	Abcam	1:1000 in 5% non-fat dry milk in 1% TBST-20	Goat Anti-Rabbit, Bio-Rad	1:3000 in 5% non-fat dry milk in 1% TBST-20
SK-2	Sigma Aldrich	2 µg/mL in 5% non-fat dry milk in 1% TBST-20	Goat Anti-Mouse, Bio-Rad	1:3000 in 5% non-fat dry milk in 1% TBST-20
GCS	Sigma Aldrich	2 µg/mL in 5% non-fat dry milk in 1% TBST-20	Goat Anti-Mouse, Bio-Rad	1:3000 in 5% non-fat dry milk in 1% TBST-20
GAPDH	ProteinTech	1:15000 in 5% non-fat dry milk in 1% TBST-20	Goat Anti-Mouse, Bio-Rad	1:3000 in 5% non-fat dry milk in 1% TBST-20

2.2. Methods

2.2.1. Cell Lines and Culture Conditions

SD-1 cells were grown in RPMI 1640 medium containing 15% heat-inactivated fetal bovine serum (FBS), 1% L-glutamine and 1% Penicillin-Streptomycin in 75cm^2 tissue culture flasks. The cells were incubated in a CO_2 incubator (Thermo Scientific, USA) at 37°C in the presence of 5% CO_2. Beas-2B cells were cultured in DMEM high glucose medium containing 10% FBS, 1% L-glutamine and 1% Penicillin-Streptomycin in 25 cm^2 tissue culture flasks. The cells were incubated in a CO_2 incubator (Thermo Scientific, USA) at 37°C in presence of 5% CO_2. The media were refreshed two days.

2.2.2. Thawing Frozen Cells

Cells were removed from frozen storage and quickly thawed in a palm to obtain the highest percentage of viable cells. As soon as the ice crystals melted, the content was taken into a sterile 15 mL-Falcon tube containing 2 mL of complete medium. The cryogenic vial was washed with 1 mL of culture medium two times and the remaining content was transferred into this Falcon tube. The cells were centrifuged, and the supernatant was removed quickly and carefully. The culture medium was added into the 15 mL of Falcon tube and the cells were cultured in the well of 6-well plate.

2.2.3. Maintenance of SD-1 Cell Line

Cell suspension (about 10 mL) was taken from the tissue culture flask into a 15 mL Falcon tube. The cells were centrifuged at 500rpm for 5 min. After centrifugation, the supernatant was removed, and the pellet was re-suspended in 10mL of RPMI 1640. 30μL of Trypan blue (0.04% in PBS) dye was added into 0.5 mL Eppendorf tubes and 30μL of re-suspended cell medium was transferred into this Eppendorf tube. Next, 10μL of this cell-dye mixture was placed into the Neubauer Haemocytometer with a coverslip.

Based on its instructions, the cells were counted in the four squares of glass slide under 10X magnification of Zeiss Light Microscopy and the average of four squares is multiplied with the dilution factor and 10^4 from the instruction. The multiplication result

is the average cell number per mL. The multiplication of this cell number with a total medium gives the total number of cells. SD-1 culture medium was prepared based on the cell culture concentration (450.000 cells in 1 mL or 4.5 million cells in 10 mL) and this medium was transferred into a new 75cm^2 tissue culture flask. The cell culture medium was refreshed every two days and the concentration was kept as 450.000 cells in 1 mL.

2.2.4. Maintenance of Beas-2B Cell Line

Following more than 90% confluence of Beas-2B cells in 25 cm^2 tissue culture flask, their medium in the culture flask was removed and cells were washed with 2 mL of 1X PBS. Then, PBS was removed after shaking the culture flask and 1 mL of 0.25 mM Trypsin-EDTA solution was put into the flask. The cells were incubated at 5% CO_2 at 37°C in the incubator until they are wholly suspended. The suspended cells were collected with 2 mL complete medium from the flask to a 15 mL falcon and then, this falcon was centrifuged at 1000 rpm for 5 minutes. Following the centrifugation, the supernatant was discarded carefully, and the pellet was re-suspended in 3 mL of fresh complete medium. 30 µL of this solution was placed into 500 µL-Eppendorf tube that contains 30 µL of Trypan blue dye (0.04% dissolved in PBS). The cells and dye were mixed and 10 µL of the mixture was put into a Neubauer Hemacytometer to count the cell number.

Based on its instructions, the cells were counted in the four squares of glass slide under 10X magnification of Zeiss Light Microscopy and the average of these four squares is multiplied with the dilution factor and 10^4 from an instruction. The multiplication result is the average cell number per mL. The multiplication of this cell number with a total medium of 3 mL gives the total number of cells. After cell counting, Beas-2B cells were seeded into 25 cm^2 culture flask as 1x10^6 in 5 mL complete DMEM high glucose medium.

2.2.5. Freezing Cells

Cells were frozen in case they may be needed for further studies. High numbers of cells were required for this purpose. The freezing mixes were prepared to freeze these cells. Freezing mix 1 includes 6 mL of Serum-free media and 4 mL of fetal bovine serum (FBS) while freezing mix 2 contains 8 mL of Serum-free media and 2 mL of DMSO. Cells cultured in 75cm^2 tissue culture flask in 10 mL of complete media were harvested

and the content of the flask was poured into Falcon tube. The cells were centrifuged at 500 rpm for 5 minutes. After removing supernatant, the pellet was re-suspended in 1mL of Freezing mix 1 and counted based on trypan blue counting instructions. For instance, if the counting number is $10x10^6$, the cell pellet should be re-suspended with an extra 1.5 mL of Freezing mix 1 because each cryogenic vials contain $2x10^6$ cells in 1mL of freezing solution. After trypan blue counting, cryogenic vials were labeled with the name of cells, passage number, and freezing date. Based on the counting results, the cells with 2 $x10^6$ cells in 500µL of Freezing mix 1 were transferred into the labeled cryogenic vials. Next, 500µL of Freezing mix 2 containing FBS and DMSO was added into the cryogenic vials. These vials were placed into storage boxes and stored in -80°C fridge.

2.2.6. Preparation of Agent and Its Application to SD-1 Cells

25 mg Apigenin (Synonym: 4′,5,7-Trihydroxyflavone) powder was obtained from Sigma-Aldrich, USA. 3.6 mg of apigenin whose molecular weight (MA) is 270.24 g/mol was dissolved in 1332 µL DMSO to obtain a 10 mM stock solution. The dissolving volume of DMSO was determined by the general molarity (M) equation using mole (n) and volume (V). All drug solutions were stored at –20°C and dark. In the application of the drug, the 10 mM Apigenin stock solution was used to prepare the other concentrations (10-100 µM) in order to determine the IC50 value. Other concentrations were prepared by taking determined volume and mixing with the volumes of complete medium.

2.2.7. Measurement of Cell Survival by MTT Cell Proliferation Assay

The concentrations of apigenin that inhibited 50% of cell growth (IC50) were determined from absorbance values obtained by 3-(4, 5-Dimethylthiazol-2-yl)-2-5-diphenyltetrazolium bromide (MTT). The cells proliferated during two-day incubation were counted using Neubauer Hematocytometer and the cells were diluted with the completed medium based on the calculation for the cell number. The needed cell number was determined by multiplying the well number while medium volume was determined by multiplying the well number with 100µL completed medium. Thus, 1×10^4 cells/well for SD-1 and 5×10^3 cells/well for Beas-2B cells were plated into 96-well plates containing 100µL medium and then, apigenin concentrations were prepared with the completed

medium to obtain the determined concentrations. The prepared agents were applied to each well and each well plate for each agent was incubated at 37°C in 5% CO_2 for 48 h. They were then treated with 20µL MTT (5 mg/ml). After 4 hour-incubation of MTT dye, the well plates for each agent were centrifuged at 1400 rpm for 10 minutes at 4°C. The solutions found in each well were discarded directly and sharply. Next, 100 µL of DMSO was added into each well using multichannel micropipette, the plates were incubated at room temperature for 10 minutes under shaking conditions. Then, the plate was read in a microplate reader (Thermo Scientific, Multiskan GO, Finland) at 570 nm and 670 nm. Finally, IC50 concentrations of the compounds were determined from cell survival plots.

2.2.8. Determination of Cell Survival by Trypan Blue Dye Exclusion Assay

After propagation of SD-1 cells for 48h, the cells were collected into the tube and centrifuged as mentioned above. Next, the cells were counted with the Neubauer glass slide using the indicated volume of Trypan blue dye. SD-1 cells were taken as $3x10^5$ in the calculated volumes from the 15-mL falcon bearing the counted cells. These cells were seeded into the wells of 24-well plate with three replicates for each dosage used in MTT assay and then wells were fulfilled up to 1 mL of the completed medium. The calculated volumes of 10 mM of Apigenin were added into the wells of 24-well plate and the well plate was incubated at 5% CO_2, 37°C in the CO_2 incubator for 48 hours. After incubation time, cells in the wells were suspended at least ten times with 1000mL micropipette and 30 µL of this solution was placed into the 250 µL-PCR tubes which have already filled with 30 µL of Trypan blue dye. The solution was pipetted several times with 10µL micropipette and 10 µL of the mixed solution was placed into a hemocytometer. Its four corner regions were counted under microscope. The triplicate results of each dosage used in MTT were used to obtain average points for each dosage in one assay.

2.2.9. Detection of Apoptosis by FITC Annexin V Apoptosis Detection Kit I

The possible apoptotic effect of apigenin on SD-1 cells was determined by using Annexin-V/PI Double Staining by BD Flow Cytometry. SD-1 cells with $3x10^5$ cells/mL

concentration were seeded as $6x10^5$ cells in 2 mL of completed RPMI 1640 medium in the wells of the 6-well plate. Apigenin was applied as 10-, 20-, and 40 µM with double controls which do not contain any agent. Next, the cells in 6-well-plate were incubated at 5% CO_2, 37°C in the incubator (Thermo Scientific, USA) for 24 and 48 hours. Following the incubation times, agent-exposed cells were collected into the 15 mL falcons and the falcons were centrifuged at 1000 rpm for 10 minutes. After centrifugation, the supernatant was discarded carefully and cells were dissolved in 1 mL of cold 1X PBS immediately. At this point, the control groups were divided into two 15 mL falcon tubes. Then, the falcons were centrifuged again at 1000 rpm for 10 minutes and the supernatant was discarded using 1000 µL micropipette. The pellets were dissolved in 200 µL of Annexin binding buffer and 2 µL of Annexin and/or 2 µL of PI dyes were added into the samples defined below Figure 2.1. Following the 15 minutes incubation of the cells at room temperature, they were analyzed at flow cytometry (BD FACS Canto, USA).

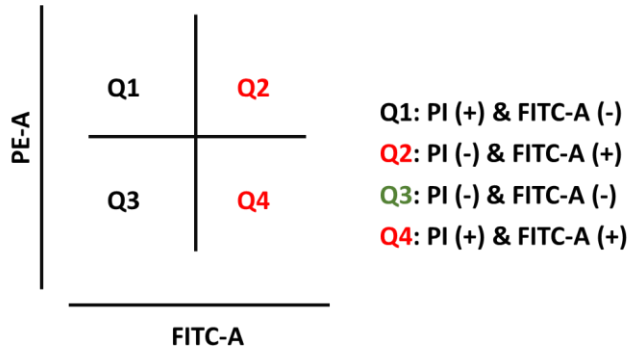

Figure 2.1. Types of Samples dyed with only Annexin V, only PI, Both or Non-stained Phosphatidylserine normally localizes in the inner membrane of the cells and it might go to the outer membrane by flip-flop due to the apoptosis of the cells. Conversely, DNA fragments in the nucleus due to the cellular stress can be visualized by the interaction with PI dye. The results in Q2 indicate the late apoptosis of the cells while Q4 determines what percentage of the cells are in the early apoptosis stage. The results in the Q1 states the necroptosis cell percentage whereas Q3 indicates the percentage of the alive cells.

The cells in the falcon tubes were analyzed in two channels by flow cytometry, BD FACS Canto, USA in BIOMER subunit of TAM in IZTECH. These cells are analyzed based on the interactions of the used dyes such as firs interaction between Annexin V dye (FITC-A) and phosphatidylserine in the outer membrane of the cells and second interaction between (PI) Propodium Iodide dye and DNA fragments in a nucleus of a cell.

2.2.10. Detection of Mitochondrial Membrane Potential using JC-1 Dye

The possible apoptotic influence of apigenin on SD-1 cells was determined by using JC-1 Mitochondrial Membrane Potential Kit by flow cytometry. SD-1 cells were seeded as $6x10^5$ cells in 2 mL of completed medium in the wells of 6-well plate. Apigenin agent was exposed onto the cells as 0-10-20-40 µM and the 6-well-plate was incubated at 5% CO_2, 37 °C in the incubator for 48 hours. After 48 incubation time, 100µL JC-1 staining solution prepared by adding 50µL of JC-1 dye into 450µL of completed medium was applied to each well and it was mixed gently. The plate was incubated at 5% CO_2, 37°C in the incubator for 20 minutes. At the end of incubation, cells were collected into the 15 mL falcon tubes and centrifuged at 1000rpm for 5 minutes. After centrifugation, the supernatant was discarded carefully, and SD-1 cells were dissolved sensitively in 1mL JC-1 assay buffer prepared by dissolving one of cell-based assay buffer tablets in 100mL sterilized distilled water. The falcons were centrifuged again at 1000rpm for 5 minutes and supernatant was discarded using 1000µL micropipette after centrifugation. The pellets were dissolved in 500µL JC-1 assay buffer and mitochondrial membrane potential was detected by flow cytometry (BD FACS Canto).

2.2.11. Determination of Cell Cycle Profile

The cytostatic effect of apigenin on SD-1 cells was determined by using PI staining by Flow Cytometry. SD-1 cells were seeded as $6x10^5$ cells in 2mL complete RPMI 1640 medium in the wells of 6-well plates. Apigenin was exposed as 0-10-20-40 µM with DMSO whose volume is the same with the highest apigenin concentration and this plate was incubated at 5% CO_2, 37°C in the incubator for 48 hours. After incubation time, cells were collected into the falcon tubes and centrifuged at 1000rpm for 5 minutes. Following the centrifugation, supernatants were discarded, and the pellets were dissolved in 1mL of cold PBS. These tubes were incubated on ice for 15 minutes and then 4mL of -20°C absolute ethanol was added into each falcon. These falcon tubes were incubated at -20°C for at least 24 hours. In the measurement day, falcon tubes were centrifuged at 1000 rpm for 10 minutes. Supernatants were discarded sensitively, and the pellets were dissolved in 5mL of cold 1X PBS. Next, the falcon tubes were centrifuged at 1000 rpm for 10 minutes again. Then, supernatants were discarded, and the pellets were dissolved

in 1mL PBS-0.1% TritonX 100 using 1000 µL-micropipette. Then, 100µL RNase A was added into each falcon and these were incubated at 5% CO_2, 37°C in the incubator for 30 minutes. After completing the incubation time, 100µL of PI dye was added into each falcon tube and the falcon tubes were incubated at room temperature for 10 minutes. Finally, cell cycle profiles of apigenin-exposed cells were examined by flow cytometry.

2.2.12. Determination of Effects of Apigenin on Expression Levels of Bioactive Sphingolipid Genes

The effect of apigenin on the expression levels of sphingolipid genes in SD-1 cells was determined by RT-PCR. The sequences of primers were described in Table 2.1.

SD-1 cells were seeded in 8 mL complete medium as $3x10^5$ cells/mL in 100 mm Petri dishes. Apigenin was applied to the cells as 0-10-20-40 µM and Petri dishes were incubated at 5% CO_2, 37°C in the incubator for 48 hours. At the end of incubation time, agent applied SD-1 cells were collected into 15mL falcon tubes and they were centrifuged at 1000rpm for 5 minutes. Following the centrifugation, supernatants were discarded sensitively, and the pellets were dissolved in 1 mL of 1X PBS using 1000µL micropipette. These solutions were transferred into the Eppendorf tubes and they were centrifuged at 1000rpm for 5 minutes. Finally, the supernatants were discarded immediately and the tubes with cell pellets were stored in -80 °C fridge for the total RNA isolation process.

2.2.12.1. Total RNA Isolation from Cells

Macherey-Nagel NucleoSpin®RNA isolation kit was used to isolate the total RNA from Apigenin-exposed and control SD-1 cells as described by the manufacturer's instruction. All steps in this protocol were performed at room temperature. Following gathering cells into the Eppendorf tubes, pellets were well dissolved in 350µL lysis buffer of the isolation kit and 3,5µL β-mercaptoethanol was added into each tube. The mixed solutions were added into the violet filter placed into the collection tubes and the tubes were centrifuged at 11,000g for 1 minute. The flow-through of each tube was discarded and 350µL of 70% ethanol was added into each tube. Then, lysates were homogenized by up-down pipetting. The samples were loaded to a new blue filter (spin column) in a new collection tube and centrifuged at 11,000g for 30 seconds. The spin columns were

placed into new collection tubes and 350µL of Membrane Desalting Buffer (MDB) was added to spin columns. The columns were centrifuged again at 11,000g for 1 minute. DNase reaction mixture was prepared by mixing 10µL of reconstituted rDNase with 90 µL Reaction Buffer for ready-to-use rDNase. Then, 95µL of DNase reaction mixtures were added directly to the center of the spin columns. The columns were incubated at room temperature for 15 minutes. After the incubation process, 200µL of Buffer RAW2 was added to each column and columns were centrifuged at 11,000g for 30 seconds to inactivate the rDNase with Buffer RAW2. Next, blue filters were placed into new collection tubes and 600µL of Buffer RA3 was added into each filter. The columns were centrifuged at 11,000g for 30 seconds. After centrifuge, 250µL of Buffer RA3 was added to the center of the columns and columns were centrifuged again at 11,000g for 2 minutes. The columns were placed into nuclease-free tubes and 50µL of RNase-free water was added to each column for elution. They were incubated at room temperature for 5 minutes and then, were centrifuged at 11,000g for 1 minute to elute total RNAs.

Following total RNA isolation, RNAs were quantified by NanoDrop ND1000 Spectrometer, Thermo Fischer, USA. The ratio between readings at 260 nm and 280 nm (A260/A280) provides an estimation of RNA samples' purity. Generally, pure RNA has a ratio of ~2.0. Finally, if RNAs do not use in PCR directly, RNAs can be stored at -80ºC.

2.2.12.2. cDNA Synthesis from Total RNA

Total RNAs isolated from Apigenin-exposed and control SD-1 cells were converted to cDNA through Thermo Scientific RevertAid Reverse Transcriptase Kit, the USA following the manufacturer's manual in two steps.

The first step includes the elimination of the secondary structures of isolated RNAs. Template RNA and primers were added into the nuclease-free tubes on ice as indicated order and volumes in Table 2.4. The volume of template RNA was calculated to take 1 µg based on the RNA ratio. The tubes were centrifuged briefly and incubated at 65 °C for 5 minutes in BIO-RAD T100^{TM} Thermal Cycler to become total RNAs linear.

The second step contains the main conversion reaction from linear RNA to cDNA. Following the incubation, 7.5 µL of master mix prepared according to Table 2.5 was added into each tube on ice, mixed gently and centrifuged briefly. Based on the manufacturer instructions, tubes were placed into the BIO-RAD T100^{TM} Thermal Cycler

and incubated at 25°C for 10 minutes followed by at 42°C for 60 minutes. Then, the termination reaction was performed at 70°C for 10 min and samples were placed onto ice immediately. At the end of the incubation process in the thermal cycler, if cDNAs are not used in RT-PCR directly, cDNAs can be stored at -20°C.

Table 2.3. Components of the first step of the cDNA conversion reaction

Components	Final Concentration	Volume
Template RNA (Total RNA)	1 µg	Based on the RNA ratio
Primer (Random hexamer)	0,2 µg (100 pmol)	1 µL
DEPC- treated water		to 12,5 µL
Total Volume		12,5 µL

Table 2.4. Master Mix of the second step of the cDNA conversion reaction

Components	Final Concentration	Volume
5X Reaction Buffer	1 X	4 µL
Thermo Scientific™ RiboLock RNase Inhibitor	20 U	0,5 µL
dNTP Mix (10 mM each)	1 mM each	2 µL
RevertAid Reverse Transcriptase	200 U	1 µL
Total Volume		20 µL

2.2.12.3. Real-Time Polymerase Chain Reaction (RT-PCR)

In the beginning, gradient PCR was performed by several temperatures provided by the manufacturer and then, agarose gel electrophoresis was performed to visualize and understand the most feasible annealing temperatures for each primer. After an indication of annealing temperature of each primer, RT-PCR was performed by using the Roche RT-PCR machine to determine the effects of apigenin on expression levels of *CERS 1-6* except *CerS-3, SK-1* and *SK-2* genes by using Thermo Scientific DyNAmo HS SYBR Green qPCR Kits, USA. Moreover, β-actin was used as a positive internal control in this

experiment to determine the changes. Based on the manufacturer's instruction, 20 µL of the master mix was prepared for each well and placed into the wells of 96-well-plate RT-PCR plate on ice as indicated order and volumes shown in Table 2.6. Then, RT-PCR was performed Roche RT-PCR for each gene based on the determined PCR conditions of each primer shown below in Table 2.7-10. After obtaining the bands in gradient PCR for several bioactive sphingolipids such as ceramide synthases, Sphingosine Kinase 1 or 2 and glucosylceramide synthase, they are grouped based on their annealing temperatures for efficient RT-PCR application. First, the primer concentrations and cDNA amount were investigated by doing several RT-PCR experiments for each pair of primers to eliminate the primer dimerization of the samples. Then, optimized values shown below were used to determine the changes in the expression levels of bioactive sphingolipids in SD-1 cells after 48 hour-treatment of 10-20-40 µM apigenin concentrations.

Table 2.5. Master Mix of RT-PCR

Components	**Final Concentration**	**Volume**
2X Master mix	1X	10 µL
Forward Primer	0.3 µM	0.6 µL
Reverse Primer	0.3 µM	0.6 µL
Template DNA	< 10 ng/µL	2 µL into wells of 96-well-plate
Nuclease free water	-	6.8 µL
Total Volume		20 µL

Table 2.6. RT-PCR Conditions for CerS-1 and CerS-5

Steps	**Temperature**	**Time**	**Cycle**
Initial Denaturation	95 ºC	15 minutes	1 cycle
Denaturation	94 ºC	10 seconds	40 cycles
Annealing	50 ºC	20 seconds	
Extension	72 ºC	30 seconds	
Melting Curve	95 ºC	1 minute	1 cycle
	55 ºC	2 minutes	
	95 ºC	Continue	
Cooling	40 ºC	10 minutes	1 cycle

Table 2.7. RT-PCR Conditions of CerS-2, CerS-4 and Beta-actin

Steps	Temperature	Time	Cycle
Initial Denaturation	95 ºC	15 minutes	1 cycle
Denaturation	94 ºC	10 seconds	40 cycles
Annealing	52 ºC	20 seconds	
Extension	72 ºC	30 seconds	
Melting Curve	95 ºC	1 minute	1 cycle
	57 ºC	2 minutes	
	95 ºC	Continuous	
Cooling	40 ºC	10 minutes	1 cycle

Table 2.8. RT-PCR Conditions of CerS-6

Steps	Temperature	Time	Cycle
Initial Denaturation	95 ºC	15 minutes	1 cycle
Denaturation	94 ºC	10 seconds	40 cycles
Annealing	60 ºC	20 seconds	
Extension	72 ºC	30 seconds	
Melting Curve	95 ºC	1 minute	1 cycle
	65 ºC	2 minutes	
	95 ºC	Continue	
Cooling	40 ºC	10 minutes	1 cycle

Table 2.9. RT-PCR Conditions of SK-1 and SK-2

Steps	Temperature	Time	Cycle
Initial Denaturation	95 ºC	15 minutes	1 cycle
Denaturation	94 ºC	10 seconds	40 cycles
Annealing	58 ºC	20 seconds	
Extension	72 ºC	30 seconds	
Melting Curve	95 ºC	1 minute	1 cycle
	63 ºC	2 minutes	
	95 ºC	Continue	
Cooling	40 ºC	10 minutes	1 cycle

2.2.13. Western Blotting Analyses

Western Blotting (WB) was performed in several steps to determine the effects of apigenin on SK-1, SK-2, and GCS protein levels in apigenin exposed and control SD-1 cells. GAPDH was used as a positive internal control.

2.2.13.1. Total Protein Isolation from Cells

The protein levels of proteins of interest were detected by Western blot analysis. Firstly, SD-1 cells were seeded into 10 cm^2 Petri dishes as 10 mL completed medium with $3x10^5$ cells/mL concentration. Petri dishes were exposed with apigenin as 0-, 10-, 20-, and 40 µM and then incubated at 5% CO_2, 37°C in the incubator for 48 hours. The cells were collected into falcon tubes after incubation. Tubes were centrifuged at 800 rpm for 5 min and the supernatants were removed. Then, cell pellets were resuspended with 1 mL PBS and cell solutions were transferred into 1.5 mL Eppendorf tubes. These were centrifuged at 1000 rpm for 5 min and the supernatants were discarded. The cell pellet volume was indicated by comparing volumes of distilled water samples. Three times higher of Lysis Buffer were added into cell pellets by pipetting. The samples were centrifuged at 14.000 rpm for 30 min at 4°C. Then, supernatants were taken into a sterile 1.5 mL Eppendorf tubes and protein concentrations in each sample were determined by Bicinchoninic Acid (BCA) Protein Assay. The Eppendorf tubes were incubated at -80°C.

2.2.13.2. Determination of Protein Concentration by Bicinchoninic Acid (BCA) Protein Assay

Bicinchoninic acid protein assay comprises two reagents and its working reagent was prepared by mixing 50 parts of Reagent A with 1 part of Reagent B in an Eppendorf Tube. The working reagent was vortexed until it was light green in color. 200 µL of BCA working reagent was taken into the wells of 96-well plate. 10 µL of protein samples that are diluted as 1:10 with using Lysis buffer and Bovine Serum Albumin (BSA) standards were added into the BCA working solution and the 96-well plate was shaken gently. This well plate was incubated at 37°C for 30 minutes and the well plate was then read at 595 nm. Firstly, the absorbance value-BSA standards graphic was drawn and then, protein

samples' concentrations were calculated according to BSA standard graphic and absorbance values of protein samples. The concentrations in the samples are in µg/µL.

Table 2.10. Standard BSA curve for the determination of protein concentrations.

Bovine Serum Albumin Standards (mg/mL)	**Required Volume (µL) From Main Stock (2 mg/mL)**	**Required Volume (µL) from dH_2O**
2	25	0
1.5	18.75	6.25
1	12.5	12.5
0.75	9.38	15.62
0.5	6.25	18.75
0.25	3.13	21.87
0	0	25

This table indicates the required volumes of stock Bovine Serum Albumin and distilled water for the preparation of Bovine Serum Albumin standards indicated on the left.

2.2.13.3. SDS Polyacrylamide Gel Electrophoresis (SDS-PAGE)

The protein concentrations of all unknown samples were calculated based on the standard curve of BSA protein. The protein samples were then diluted by lysis buffer to prepare 20 µg in the 15 µL of lysis buffer. The samples were completed with β-mercaptoethanol added 4X Laemmli Buffer (1:9 dilution rate) up to 20 µL of volume, so that the final concentration of protein is the same for all samples. Next, the protein samples were denatured at 95 ºC for 10 minutes by using Dry Block Heating temperature.

Bio-Rad 10% TGX Stain-Free FastCast Acrylamide kit was used to make SDS-PAGE in order to separate the proteins. In this separation process, resolver solution (separating gel) and sealing gel were prepared following the instruction manuals with some changes. 3 ml of Resolver A solution and 3 ml of Resolver B solution were added into the 15 ml falcon tube and mixed well. 500 µL of this solution was transferred into the 1.5 ml Eppendorf tube for sealing gel preparation. 10 µL of 10% APS which is stored at 4◦C was added into this Eppendorf tube. Next, 1 µL of TEMED was added immediately into this tube. Because TEMED increases the polymerization rate, this whole solution for

sealing gel was added into WB System, which is already assembled immediately. 30 µL of 10% APS which is stored at 4°C was added into the remaining resolver A and B mixture for separating gel. 3 µL of TEMED was added immediately into this falcon tube. In this step, the solution was mixed by 5 ml serologic pipette and approximately 6 mL of resolver solution was transferred into the WB system immediately until the first line of the system.

Stacker solution or collecting gel was prepared with adding 1 mL of Stacker A solution and 1 mL of Stacker B solution into the 15 ml falcon tube. 10 µL of 10% APS which is stored at 4°C was added into the 15 ml falcon tube. 2 µL of TEMED was added immediately into this falcon tube. In this step, the solution was mixed by a 5 ml serologic pipette and 2 mL of Stacker Solution was transferred into the WB system immediately until the border of the WB system. Finally, 10 wells comb (1 mm comb; Well width: 5.08 mm) was inserted into the WB system and it was allowed for 30 minutes polymerization.

The gel within two glasses was placed into the WB system carefully and this WB system was placed into the Mini Tank of WB. Mini Tank was fulfilled with 1X Bio-Rad (Tris/Glycine/SDS) running buffer until the chamber assembly and 10 wells comb was removed without disrupting gel area. 5 µL of Euro-Clone Pre-stained Standard protein marker and 20 of µL protein samples were loaded into the wells. It was checked whether the inside of WB system is full of 1X (Tris/Glycine/SDS) running buffer. Finally, the gel with company recommendation: 200V for 45 minutes was started to separate the proteins.

2.2.13.4. Transfer of Proteins from Gel to PVDF Membrane

Proteins separated in SDS-PAGE were transferred from Bio-Rad 10% SDS-polyacrylamide gel to Bio-Rad PVDF membrane using a machine named Bio-Rad Trans-Blot Turbo Transfer System. The membrane was wetted with absolute methanol for 5 minutes and washed with 1X Transfer Buffer under shaking conditions at room temperature. Two pieces of transfer stack (slightly bigger than gel) were washed with 1X Transfer Buffer for 5 minutes. Then, the first transfer stack was placed into the cassette and this transfer stack was smoothened by using a cylindrical tube. The activated PVDF membrane was placed onto the transfer stack and then, SDS-PAGE was placed onto the PVDF membrane. The gel and membrane were smoothened by using the cylindrical tube. The last transfer stack was placed onto the PVDF gel carefully. The upper part of the cassette was placed on this “sandwich” and locked carefully for Bio-Rad’s Trans-Blotting

process. The suitable program was chosen for both higher and lower molecular weights of interested proteins. The whole proteins were transferred to PVDF membrane for 10 minutes at 1.3 mA at room temperature. When the transfer was finished, the membrane was immersed in 5% non-fat dry milk solution at room temperature for 1 hour. After blocking proteins, the membrane was washed with 1X TBS-Tween 20 solution for 10 minutes at room temperature under shaking conditions. The washed membrane was placed into a box and the primary antibody with specific dilution in non-fat dry milk was added into this box. Finally, the box with its own cap was placed into the shaker and incubated with the primary antibody at 4ºC overnight under shaking conditions.

2.2.13.5. Detection of Desired Proteins by Specific Antibodies

After completed incubation time for the first primary antibody, this antibody solution was poured into its 15 mL falcon tubes directly. The membrane was washed three times with 0.1% TBS-Tween20 and each washing takes 10 minutes under shaking conditions. Then, 5 mL of secondary antibody prepared with 1:3000 dilution in 5% non-fat dry milk in 0.1% TBS-Tween20 was applied to the membrane. After 2 hours of incubation at room temperature, the membrane was washed again three times with a 10-minute washing process under shaking conditions. Following the last washing of the membrane, 75 µL of ECL Solution A and ECL Solution B with the same volume were mixed into an Eppendorf tube. The membrane was placed onto a tray without any bubbles and then, the prepared solution was poured onto the specific protein whose location is estimated based on the marker lines and the observed molecular weight as kD provided by the manufacturer. The tray with the activated membrane was placed into the Fusion SL Vilber Vourmat machine and the view of the membrane was snapped immediately. Next, the bands of proteins of interest were visualized under chemiluminescence lights after waiting for the required time for the visualization. Following the obtaining of the bands of related proteins, GAPDH solution prepared as 1:15000 dilution in 5% non-fat dry milk in 0.1% TBS-Tween20 was applied to the membrane as an internal control of the samples. The process for the visualization of GAPDH protein in the sample was the same as the whole process for proteins of interest. Finally, the membrane was wrapped with aluminum folio and stored at -20ºC.

CHAPTER 3

RESULTS AND DISCUSSION

3.1. MTT Cell Proliferation Assay in Apigenin Exposed SD-1 and Beas-2B Cells

The cytotoxic effect of apigenin on Ph+ ALL SD-1 cells was investigated by gradually increasing concentrations (10-100 µM) with non-treated control groups at 24 and 48 hours using MTT dye.

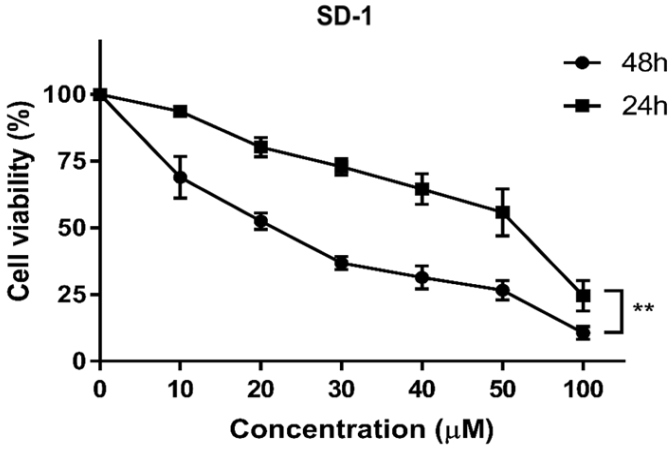

Figure 3.1. The cytotoxic effect of apigenin on SD-1 cell viability at 24 and 48h. SD-1 cells were seeded into the wells of 96-well plate as $1x10^4$ cells per 100 µL in a well. The prepared drug solutions with increasing concentrations were applied to the cells. The experiment was repeated independently three times and statistical analysis was done using a paired t-test, $p<0.05$:*; $p<0.01$:** were considered significant whereas ns is abbreviated from non-significant. The error bars represent the standard deviations (SD).

Apigenin has a significant role in the inhibition of the proliferation of SD-1 cells. Step-wise increasing concentrations of apigenin leads to the determination of the half-maximal inhibitory concentration (IC_{50}) of apigenin at 24 and 48 hours. The IC50 values of apigenin were calculated as 60 µM and 21.5 µM for SD-1 cells at 24 and 48 hours, respectively. The IC_{50} for 24 hour-drug application is approximately 2-fold higher than IC_{50} value for 48 hour-application. Furthermore, the cytotoxic effect on non-cancerous

Beas-2B cells was investigated by gradually increasing apigenin concentrations (10-100 µM) at 48 hours using MTT dye with 5mg/mL main stock concentration.

The cytotoxic effect of apigenin on both cell lines indicates that apigenin is likely to inhibit the proliferation of cancerous cells with the application of low drug concentration. The IC_{50} for SD-1 cells is around 21.5 µM whereas the IC_{50} value for Beas-2B cells could not be determined even though the highest concentration of apigenin for SD-1 cells was applied to non-cancerous Beas-2B cells. Besides, it is clearly seen in Figure 3.2 that the application of 21.5 µM apigenin promotes the proliferation of Beas-2B cells. More than 30 µM apigenin applied Beas-2B cells for 48 hours experienced the elevated apoptosis in Figure 3.2. The 100µM apigenin application that is the highest concentration within the applied doses resulted in the death of approximately 40% of cells compared to the control group.

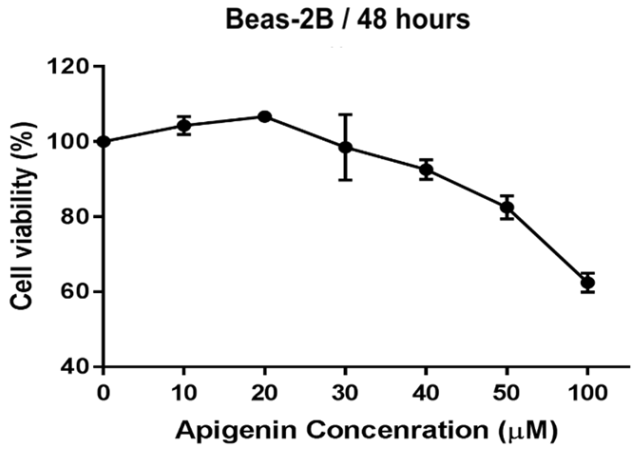

Figure 3.2. The cytotoxic effect of apigenin on Beas-2B cells at 48h. Beas-2B cells were seeded into the wells of 96-well plate as $5x10^3$ cells per 100 µL in a well. The prepared drug solutions with increasing concentrations were applied to the cells. The experiment was repeated independent three times the error bars represent the standard deviations (SD).

In the comparison of cytotoxic effects of apigenin on cancerous and non-cancerous cells, approximately 20 µM are crucial points for each figure of apigenin application. When exact 20 µM is applied to cancerous cells, this concentration causes the death of nearly half-percentage of SD-1 cells whereas this value induces the proliferation of non-cancerous cells to reach their highest value in Figure 3.2 when 20 µM of apigenin is applied to Beas-2B cells for 48 hours.

3.2. Trypan Blue Dye Exclusion Assay to Count SD-1 Cell Viability

The cytotoxic effect of gradually increasing apigenin concentrations (10-100 µM) on SD-1 cells was investigated by counting the alive cells using the Neubauer Hematocytometer based on the instructions of Trypan blue dye exclusion assay.

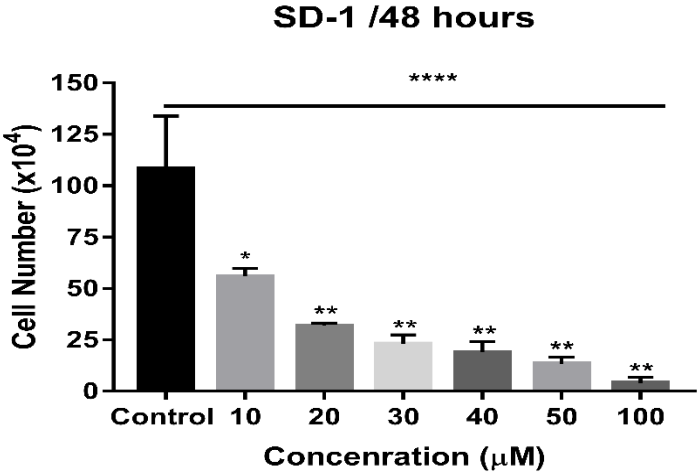

Figure 3.3. The cytotoxic effect of apigenin on cell number of SD-1 cells at 48h. SD-1 cells were seeded into the wells of 24-well plate as $3x10^5$ cells per 1 mL in a well. Then, the increasing drug concentrations were applied to the cells using a 10 mM apigenin stock solution. The experiment was repeated independently three times and statistical analysis was done using an unpaired t-test and *one-way ANOVA*, $p<0.05$:*, $p<0.01$:** and $p<0.0001$:**** were considered significant whereas ns is abbreviated from non-significant. The error bars represent the standard deviations (SD).

The cytotoxic effect of gradually increasing apigenin concentrations on SD-1 cells was investigated by counting the alive cells under a light microscope by using Trypan blue dye (0.04%) dissolved in PBS. Following the centrifugation of whole cells, the alive cells were collected at the bottom of the tubes and they were dissolved with 1mL complete medium. The cell suspension was diluted in a 1:1 dilution with the 0.4% Trypan Blue stock solution. The mixture comprised of trypan blue dye and cells was placed into the specific hematocytometer. Thus, the viability of the cells, which have been treated with different concentrations were determined by counting bright-uncolored cells under a 10X magnified microscope image. The viability of the cells decreased significantly following the drug application for 48 hours. Unlike the results of the MTT cell viability assay, the number of alive cells has rapidly decreased in Figure 3.3 indicating 10 µM apigenin.

3.3. Effects of Apigenin on Apoptosis of SD-1 Cells

The apoptotic effect of increasing apigenin concentration on SD-1 cells was investigated using Annexin V dye for measuring the phosphatidylserine percentage in the outer membrane and PI dye for DNA fragments by flow cytometry.

The apoptotic effect of apigenin on SD-1 cells was investigated by the upward several concentrations of apigenin, which are determined by MTT cell viability assay results following the 24 and 48 hour-drug applications. The used drug concentrations 10, 20 and 40 µM indicate the approximately IC30, IC50, IC70 values of apigenin whose dosages indicate the death percentages of the SD-1 cells compared to the control group. The viability or apoptosis of cells was determined based on the interactions between Annexin V and phosphatidylserine and DNA fragments and propidium iodide. The viability of the cells treated with these determined concentrations decreased significantly as indicated in the Q3 of each quadruplet on the left panel of figure and their apoptotic rates, which are the addition of Q2 and Q4 of each quadruplet raised dramatically following both 24 and 48 hour-apigenin applications in Figure 3.4 and Figure 3.5.

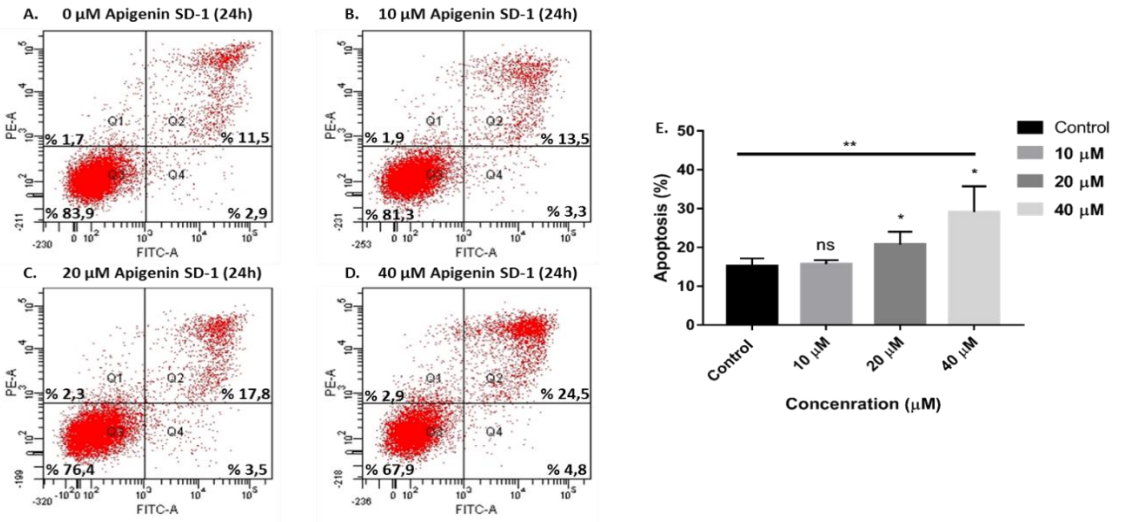

Figure 3.4. The apoptotic effect of apigenin on SD-1 cells at 24h. SD-1 cells were seeded into the wells of the 6-well plate as $6x10^5$ cells per 2 mL in a well. The increasing drug concentrations were applied to the cells using a 10 mM apigenin stock solution. The cells were incubated with the drug concentrations for 24 hours. The experiment was repeated independently three times and statistical analysis was done using a paired t-test and one-way ANOVA, $p<0.05$:* and $p<0.01$:** were considered significant whereas ns is abbreviated from non-significant. The error bars represent the standard deviations (SD).

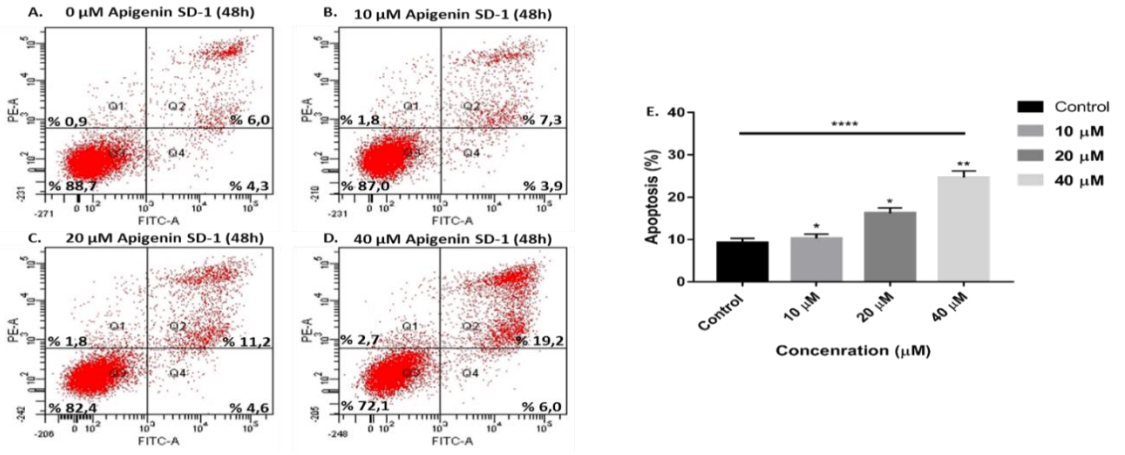

Figure 3.5. The apoptotic effect of apigenin on SD-1 cells at 48h. SD-1 cells were seeded into the wells of the 6-well plate as $6x10^5$ cells per 2 mL in a well. The increasing drug concentrations were applied to the cells using a 10 mM apigenin stock solution. The cells were incubated with these drug concentrations for 48 hours. The experiment was repeated independently three times and statistical analysis was done using the paired t-test and one-way ANOVA. $p<0.05$:*; $p<0.01$:**; $p<0.0001$: **** were considered significant. The error bars represent the standard deviations (SD).

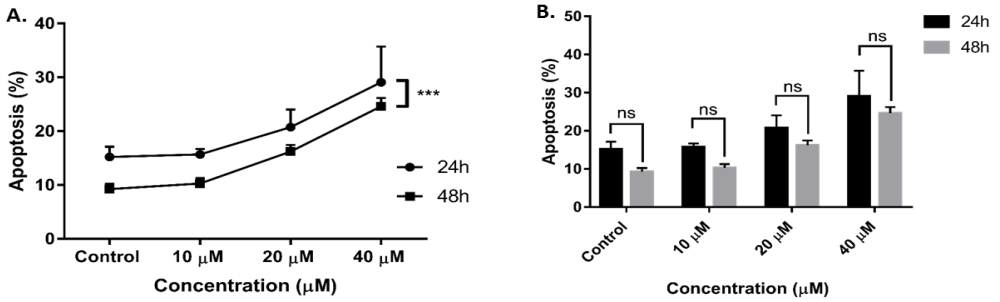

Figure 3.6. The whole and dose-based comparison of time-dependent apoptotic effects of apigenin on SD-1 cells. The experiment was repeated independently three times and statistical analysis was done using paired t-test and one-way ANOVA. $p<0.05$:*; $p<0.01$:**; $p<0.001$:*** were considered significant whereas ns is abbreviated from non-significant. The time-dependent obtained results were compared based on the general trend of result (Figure 3.6A) and dose-by-dose manner of these general trends (Figure 3.6B) by using one-way and two-way ANOVA. The error bars represent the standard deviations (SD).

Collectively, apigenin might participate in the elevated apoptosis rate of SD-1 cells time-and dose-dependent manner. Apigenin may inhibit the cell proliferation within 24 hours instead of 48-hour drug incubation. The time-dependent comparison indicates the significant changes in 24-hour application compared to 48-hour treatment. Moreover, the applied concentrations have similar effects on the apoptosis percentages of cells.

3.4. Effects of Apigenin on Mitochondrial Membrane Potential of SD-1 Cells

The apoptotic effect of increasing apigenin concentrations on SD-1 cells was investigated using JC-1 dye for the measurement of the loss of their mitochondrial membrane potentials (MMPs) by flow cytometry.

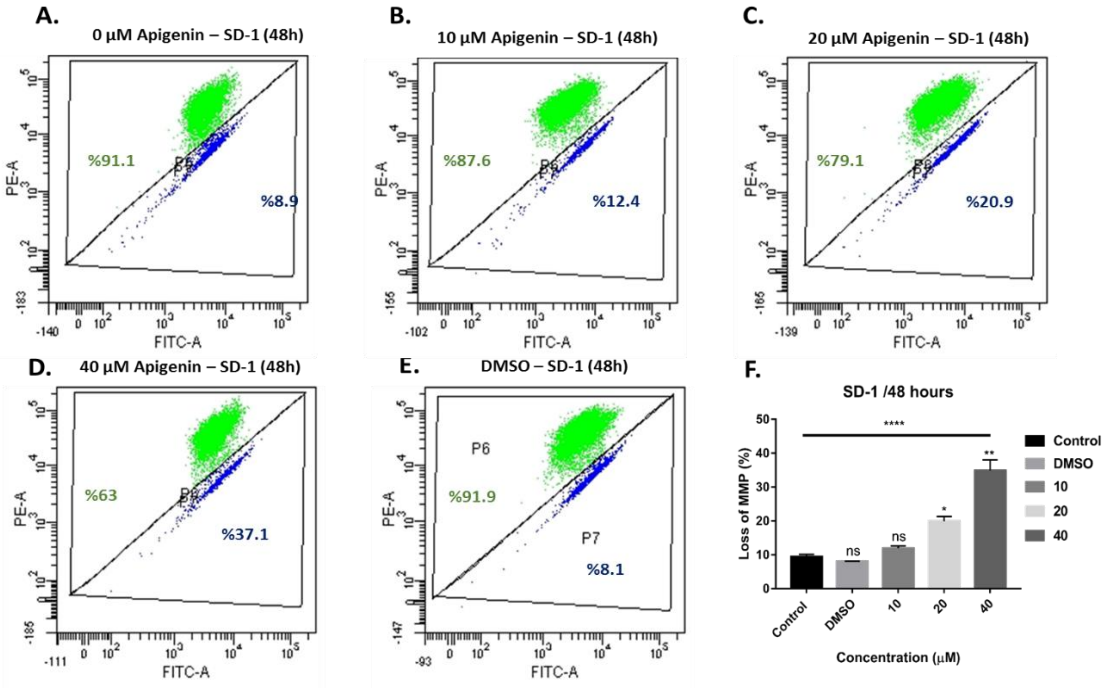

Figure 3.7. The effect of apigenin on the loss of mitochondria membrane potential of SD-1 cells at 48 h. SD-1 cells were seeded into the wells of the 6-well plate as $6x10^5$ cells per 2 mL in a well. The increasing drug concentrations were applied to the cells using a 10 mM apigenin stock solution. The experiment was repeated independently two times and statistical analysis was done using a paired t-test and one-way ANOVA. $p<0.05$:*, $p<0.01$:** and $p<0.0001$:**** were considered significant whereas ns is abbreviated from non-significant. The error bars represent the standard deviations (SD).

The flow cytometry results indicated that loss of mitochondrial membrane potential of SD-1 cells gradually increased while elevating the apigenin concentrations, which are IC_{30}, IC_{50} and IC_{70} values determined by the results of MTT cell viability assay. Indeed, the DMSO applied category has a similar loss of MMP compared to the control group even if DMSO volume per 2mL is the same with 40µM apigenin applied cell category. The graph shows the percentage of mitochondrial membrane potential loss of SD-1 cells according to the statistical analysis of two independent experiments.

Loss of mitochondrial membrane potential significantly increased in SD-1 cells following the step-wise increase of apigenin concentration (Figure 3.7F). Control and DMSO applied groups have approximately 9% of mitochondrial membrane potential loss whereas the other drug applied categories have experienced the elevated percentages of the MMP loss. It can be stated that this data correlates with the Annexin V-PI dual staining assay results of apigenin exposed SD-1 cells and apigenin has an apoptotic effect on several cancer types including Ph-positive ALL SD-1 cell line.

3.5. Effects of Apigenin on Cell Cycle Profiles of SD-1 Cells

The cytostatic effects of increasing apigenin concentrations on the cell cycle profile of the SD-1 cells were investigated using PI staining protocol for the measurement of the changes in the cell cycle phases by flow cytometry.

The cytostatic effect of apigenin on the cell cycle phases of SD-1 cells was investigated by the upward several concentrations of apigenin, which are IC30, IC50 and IC70 values determined by the results of MTT cell viability assay following the 24 and 48 hour-drug applications. This investigation states that increasing drug concentrations have potential effects on 48 hour-drug incubated SD-1 cells in terms of the arresting of them in the different cell cycle phases.

In addition to the effects of apigenin on cell proliferation and apoptosis of SD-1 cells, apigenin has also the ability to change their cell cycle profiles by arresting them at the G2/M phase. Control cells without any treatment are arrested at the G1 phase with 57.56%, at the G2 phase with 0.29 % and S phase 42.13%. (Figure 3.8.A) while DMSO applications with the same volume of 40 μM apigenin application has the cell cycle arrest at G1 stage with 59.55%, at G2 phase with 3.48% and at S phase 36.97% (Figure 3.8B) at the end of 48-hour drug application. 10 μM apigenin can affect the cell cycle profile of SD-1 cells more than DMSO does by increasing the G2 phase percentage to 10.65% and decreasing the G1 phase to 56% and S phase to 33.35%. Indeed, 20 μM apigenin applied SD-1 cells are mostly arrested at the G1 phase with 63.08 while G2 phase with 15.09% and S phase with 21.83% respectively (Figure 3.8C). Moreover, 40 μM apigenin exposed SD-1 cells are primarily arrested at the G2 phase of the cell cycle with % 27.53 while SD-1 cells were found at G1 and S phase with 60.39% and 12.08% (Figure 3.8D).

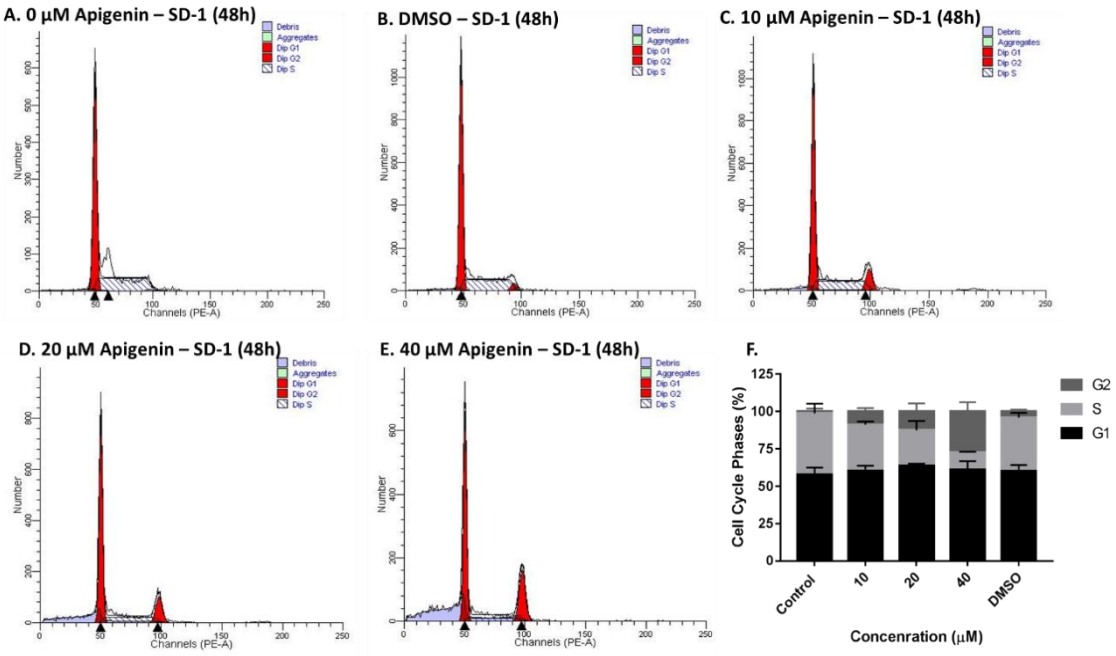

Figure 3.8. The effect of apigenin on cell cycle profile of SD-1 cells. SD-1 cells were seeded into the wells of the 6-well plate as $6x10^5$ cells per 2 mL in a well. The determined drug concentrations that are IC_{30}, IC_{50} and IC_{70} values were applied to the cells using a 10 mM apigenin stock solution. Moreover, DMSO was added to the analyses to compare the effects of drugs and DMSO. The experiment was repeated independently three times and the error bars represent the standard deviations (SD).

The overall results of three independent experiments demonstrate that a 48-hour apigenin application enhances the cell cycle arrest in SD-1 cells in a dose-dependent manner significantly at the G2 phase. The graph demonstrates the changes in the percentages of cell cycle phases in response to the increasing concentration of apigenin (Figure 3.8F). Additionally, there is no significant change in response to the DMSO application which is the same with the DMSO volume of the highest drug application.

3.6. Expression Analyses of Bioactive Sphingolipids in Apigenin Exposed SD-1 Cells

After determination of cytotoxic, cytostatic and apoptotic effects of apigenin on SD-1 cells, its effects on the expression levels of bioactive sphingolipids were investigated by RT-PCR followed by the total RNA isolation and cDNA conversion of whole RNAs. The isolation method for total RNA from the indicated apigenin concentrations-applied SD-1 cells was followed and cDNA conversion was done using

the reverse transcriptase enzyme. The expression levels of CerS-1, -2, -4, -5 and -6 and SK-1 and -2 genes were determined by three repeats on each RT-PCR experiment, which are normalized to the internal positive control Beta-actin gene.

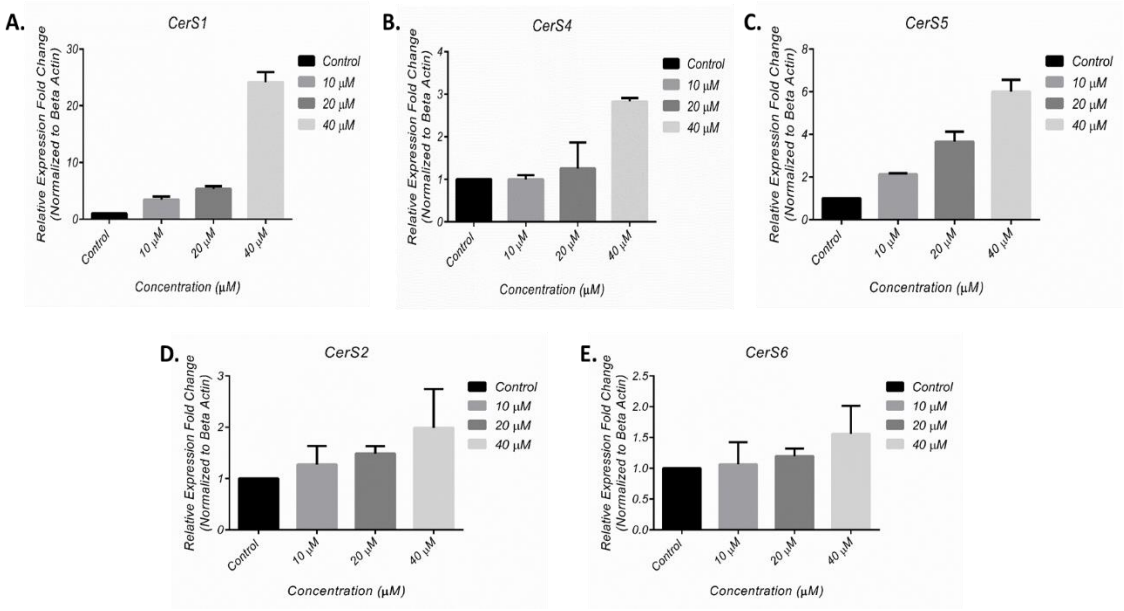

Figure 3.9. The expression levels of Ceramide Synthase genes following apigenin applications. The effects of apigenin on the expression levels of CerS-1, -2, -4, -5 and -6 genes of Ph+ ALL SD-1 cells were determined by RT-PCR. The experiments were performed as two different experiments (n=2) including three technical replicates. The beta-actin gene was used as a positive internal control. The error bars represent the standard deviations (SD). Statistical analysis was done using ordinary one-way ANOVA for each CerS gene, $p<0.05$:* and $p<0.001$:*** were considered significant for the changes in CerS-1, CerS-4 and CerS-5 expression levels respectively whereas the changes in CerS-2 and CerS-6 expression levels were non-significant. Figures 3.9A, B, C, D and E indicate the expression levels of CerS-1, -2, -4, -5 and -6 genes in apigenin applied SD-1 cells for 48 hours.

The recent studies reviewed in the section of bioactive sphingolipids state that exogenous expression of ceramide synthase genes is crucial to modulate the apoptosis-related pathways. Ceramide synthases are highly expressed and cause drug resistance in various cancer cells. Therefore, they are considered as targets for the treatment of the patients. Their apigenin-induced expressions in SD-1 cells might cause an elevated level of apoptosis in these cells. At this point, the increased levels of CerS genes may lead to overexpression of ceramide molecules which are synthesized by these Ceramide synthase enzymes. Secondly, the increase in the mRNA levels of these enzymes may cause the activation of the apoptosis-associated pathways. In this regulation, CerS-1, -4 and -5 are

highly expressed in order to increase the de-novo synthesis of ceramide chains compared to other Ceramide synthase genes. Their elevated levels in stepwise increased apigenin concentrations reach nearly 24-, 2.84- and 6-fold increase in 40 µM applied SD-1 cells relative to Beta-actin expression levels respectively. The increase in these CerS genes is statistically significant compared to other *CerS-2* and *-6* genes.

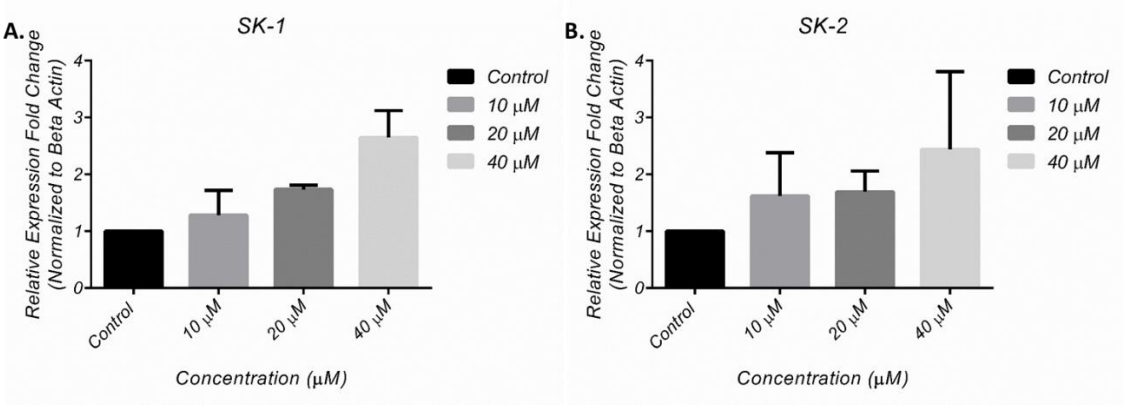

Figure 3.10. The expression levels of Sphingosine Kinase 1 and 2 genes. The effects of apigenin on the expression levels of Sphingosine Kinase 1 and 2 genes of Ph+ ALL SD-1 cells were determined by RT-PCR. The experiments were performed as two different experiments (n=2) including three technical replicates. The beta-actin gene was used as a positive internal control. The error bars represent the standard deviations (SD). Statistical analysis was done using ordinary one-way ANOVA for SK-1 and -2 genes. $p<0.05$:* was considered significant for the change in SK-1 expression level whereas the change in SK-2 was non-significant. Figures 3.10A and B indicate the expression levels of *SK-1* and *-2* genes respectively in apigenin applied SD-1 cells for 48 hours.

The studies reviewed in the section of bioactive sphingolipids state that SK-1 and -2 expressions are crucial to modulate the drug resistance and inhibit the apoptosis-related pathways. SK-1 and -2 are liable to prevent the ceramide-based apoptosis by balancing ceramide-S1P levels so that cancerous cells can overcome the drug-induced apoptosis. Therefore, their apigenin-induced expressions in SD-1 cells might cause an elevated level of drug-resistance in these cells. At this point, the increased levels of CerS genes may lead to overexpression of ceramide molecules whereas SK-1 and 2 enzymes have been converting this ceramide to S1P in order to trigger proliferation-associated pathways. In this regulation, SK-1 and 2 have been expressed approximately 3 and 2.5 fold more respectively (relative to Beta-actin expression levels) in 40 µM applied SD-1 cells to decrease the detrimental effects of apigenin on SD-1 cells.

3.7. Protein Levels of Bioactive Sphingolipid Genes in Apigenin Exposed SD-1 Cells

Following the determination of the expression levels of ceramide synthase and sphingosine kinase genes at the mRNA level, the effects of apigenin on the protein levels of bioactive sphingolipids were investigated by western blotting analyses.

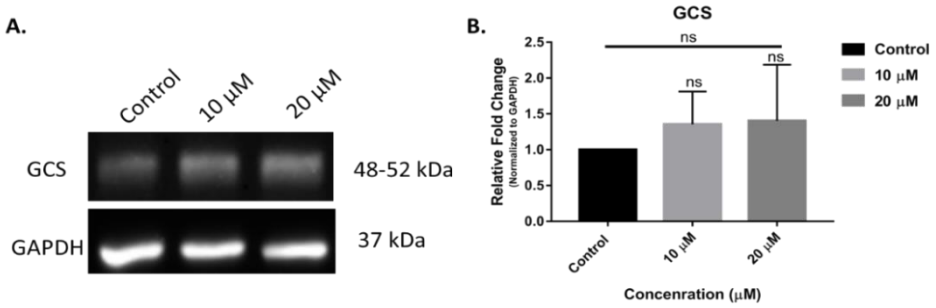

Figure 3.11. The protein levels of Glucosylceramide synthase (GCS). The effects of apigenin on the expression levels of GCS protein of SD-1 cells were determined by western blotting. The experiments were performed as two different experiments (n=2) and GAPDH was used as a positive internal control. Statistical analysis of dose application compared to control was done using a paired t-test while statistical analysis of whole columns was done using ordinary one-way ANOVA for GCS. The error bars represent the standard deviations (SD). Figures 3.11A indicates the experimental view of the GCS levels while Figure 3.11B illustrates the statistical changes in GCS protein levels of apigenin applied SD-1 cells for 48 hours.

The protein isolation from the indicated apigenin concentrations-applied SD-1 cells was followed as indicated above and SDS-PAGE gel was prepared based on the instruction's order with some changes. Although the protein levels of CerS-1, -2, -4, -5 and -6 were not visualized because of the lack of specific antibodies in the market for SD-1 cells, the protein levels of GCS and SK-1 and -2 were determined by two repeats on each western blotting normalized to the internal positive control GAPDH protein. Figure 11 indicates the effect of apigenin on the protein level of GCS in apigenin exposed SD-1 cells after 48 hours. There is a slight increase in the protein levels of GCS in 10 and 20 µM apigenin applied SD-1 cells. However, this increment is no statistically meaningful. According to the studies; Baran et al., 2011 and Huang, Tu, and Freter, 2018, GCS overexpression is related to the proliferation and drug resistance of cancer cells. The probable increase in the protein level of GCS after 48 hour-application might be eliminated by apigenin so that SD-1 cells underwent the programmed cell death.

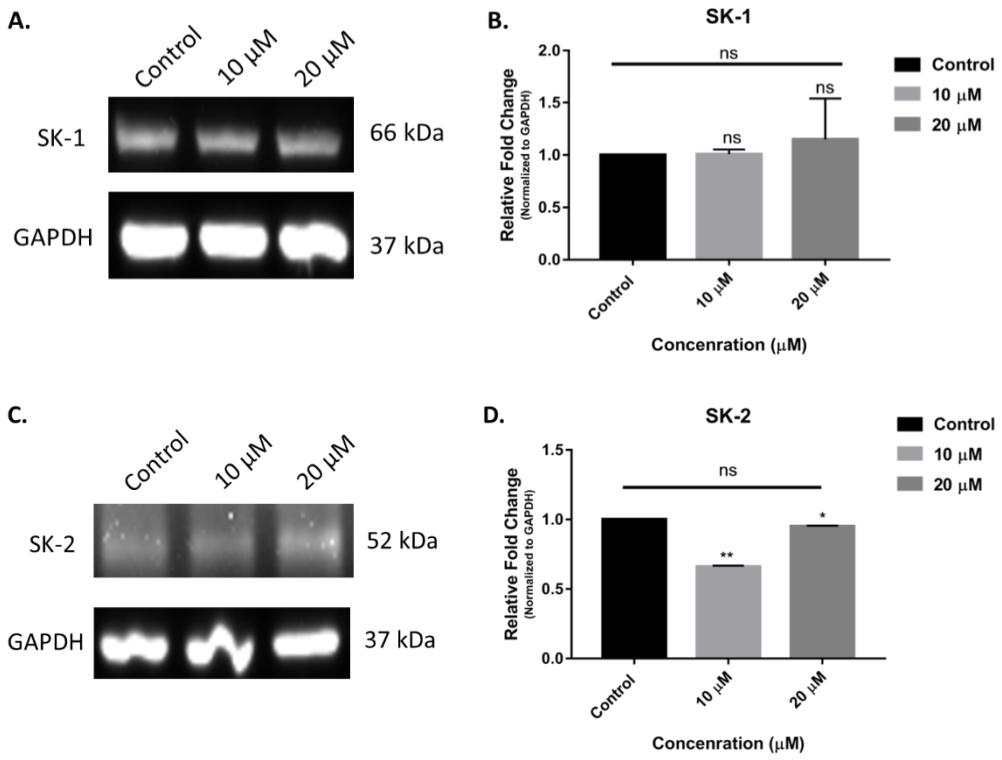

Figure 3.12. The protein level of Sphingosine Kinase-1 and -2. The effects of apigenin on the protein levels of SK-1 and -2 of SD-1 cells were determined by western blotting. The experiments were performed as two different experiments (n=2) and GAPDH was used as a positive internal control. Statistical analysis of dose application compared to control was done using a paired t-test and the changes in protein levels were ns; $p<0.05$:*; $p<0.01$:**. Statistical analysis of whole columns was done using ordinary one-way ANOVA for SK-1 and -2 and the changes in the protein level were non-significant. The error bars represent the standard deviations (SD). Figures 3.12A-B indicate the experimental and statistical changes in the SK-1 level while Figure 3.12C-D illustrates the experimental and statistical changes in the SK-2 protein level in apigenin applied SD-1 cells for 48 hours.

In addition to the investigation of the protein levels of GCS after 48 hour-apigenin application, the effects of apigenin on the protein levels of SK-1 and -2 were determined using the western blotting analysis. In these experiments, there is no significant change in their protein levels when the overall results are compared to each other. Although there is a significant change in the expression level of SK-1 at the mRNA level, there is no significant change in its protein levels. On the other hand, there is no statistically significant change in the expression levels of SK-2 at the mRNA level as well as in the protein level of SK-2. In spite of the fact that the protein level of SK-2 was decreased significantly in 10μM apigenin application and it was increased in 20μM apigenin application compared to 10μM apigenin application.

CHAPTER 4

CONCLUSION

ALL is a hematologic disorder characterized by an elevated number of immature lymphoblasts in peripheral blood and bone marrow. ALL has several genetic abnormalities and one of them -mostly observed- is BCR/ABL translocation arisen from reciprocal translocation of the regions within chromosome 9 and 22. This fusion protein has several abilities such as auto-phosphorylation and the aberrant tyrosine kinase activity to regulate various pathways associated with proliferation, anti-apoptotic and drug resistance. In spite of the fact that current targeted treatment strategies include the elimination of BCR/ABL activity or increase the effectiveness of monoclonal antibodies and CAR-T cells, complete remission, overall survival and mortality of Ph+ ALL patients are still challenging compared to other cancer patients. Therefore, new strategies combined with current targeted treatments are a necessity for Ph+ ALL patients who are categorized as a high-risk group of ALL.

The bioactive sphingolipids that are highly effective class of lipids in cancer studies have been investigated in detail. Since these bioactive sphingolipids are likely to regulate crucial biological processes for cell fate, they gain importance as a therapeutic target to eliminate or accelerate their functions. The chemotherapeutic agents or inhibitors of bioactive sphingolipids have been improved for novel cancer treatment strategies. The traditional culture-based studies revealed that the dietary foods and their contents are highly effective to pull through the worse stage of cancer. The flavonoids, which are plant metabolites in these cousins contribute to the induction of bioactive sphingolipids-related cell death, inhibition of cell proliferation and suppression of metastatic cells in tumor progression. Only one study showed that apigenin triggers apoptosis by increasing de novo synthesis of ceramide in rat heart tissues. Furthermore, apigenin may inhibit cellular proliferation by increasing the endogenous ceramide level and decreasing the sphingosine kinase activities to reduce S1P production.

According to this background information, we hypothesized that apigenin might have anti-proliferative and pro-apoptotic effects on Ph+ ALL SD-1 cell line without diminishing the non-cancerous cells such as lung Beas-2B cell line. In this hypothesis, it

is stated that apigenin may increase the de novo synthesis of bioactive sphingolipid genes to elevate the ceramide level in the cytoplasm for a possible therapeutic potential.

To begin with, the cytotoxic effects of apigenin on SD-1 and BEAS-2B cells were determined by MTT cell proliferation assay and it was found that step-wise increase of apigenin concentration had a detrimental effect on SD-1 cells in time and dose-dependent manner. However, apigenin has a proliferative effect on Beas-2B cells. Next, Trypan blue dye exclusion assay revealed that apigenin influences the proliferation rate of SD-1 cells negatively and it gives rise to a rapid decrease in the viability of cells. Moreover, Annexin V-PI dual staining and JC-1 dye-based loss of mitochondrial membrane potential analyses correlated with other results and indicated that the apoptotic effect of gradually increasing concentrations stimulates the apoptosis percentages of SD-1 cells for 48 hours. Besides, the investigation of cytostatic effects of apigenin on Ph+ ALL cells using PI staining brings about that apigenin functions in the cell cycle arrest of these cells at G2 phase while these cells were also arrested at S phase by a high dose of apigenin.

In addition to these cytotoxic, cytostatic and apoptotic studies, the roles of bioactive sphingolipids in the cellular fate of SD-1 cells following the 48 hour-drug application were determined by RT-PCR. The results state that apigenin has the therapeutic potential to increase the expression levels of ceramide synthase genes and their end-products various carbon-bearing ceramides which are functional to balance the proliferation and apoptosis. RT-PCR results revealed that apigenin triggers the artificial expression of sphingolipid genes especially CerS-1, CerS-4 and CerS-5 to elevate apoptosis in SD-1 cells during the 48-hour incubation.

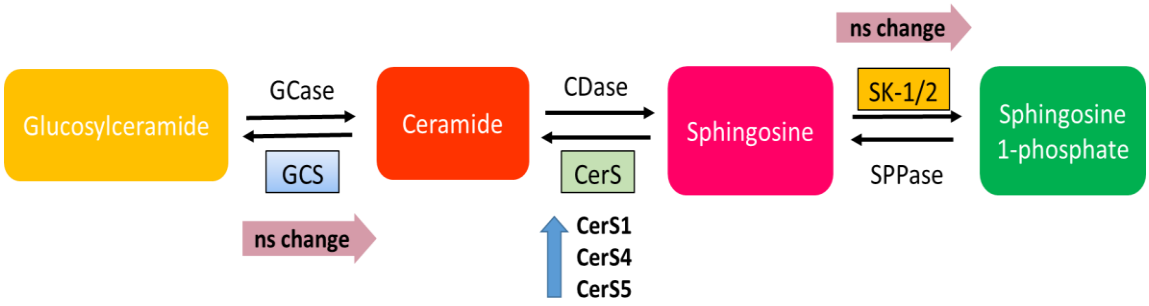

Figure 3. 13. The overall effect of apigenin on bioactive sphingolipid genes

The mRNA level expressions of bioactive sphingolipids were determined by RT-PCR and the protein levels of some bioactive sphingolipids were confirmed by western

blotting analysis. The protein levels of SK-1 and -2 and GCS were investigated after 48-hour apigenin treatment to SD-1 cells in Petri dishes. When the protein levels of drug applied SD-1 cells are compared to the control columns, there is no statistically significant change in their protein levels though there are slight increases or decreases in Figures 11 and 12.

Collectively, apigenin has cytotoxic effects on SD-1 cells by increasing apoptosis-related ceramide synthase genes including CerS1, 4 and 5 expression levels at mRNA level and suppressing the activities of the proliferation-related sphingolipid metabolizing molecules including SK-1 and -2 at both mRNA and protein levels and GCS genes at its protein level.

To put on a nutshell, the cytotoxic, apoptotic and cytostatic effects of apigenin on Ph+ ALL SD-1 cells were investigated for the first time in this study. Furthermore, the regulatory functions of bioactive sphingolipid genes on the apigenin applied Ph+ ALL SD-1 cells were determined for the first time as well.

REFERENCES

1. National Cancer Institute Adult Acute Lymphoblastic Leukemia Treatment (PDQ®)–Patient Version. https://www.cancer.gov/types/leukemia/patient/adult-all-treatment-pdq#_1.

2. American Cancer Society What Is Acute Lymphocytic Leukemia (ALL)? https://www.cancer.org/cancer/acute-lymphocytic-leukemia/about/what-is-all.html#.

3. Bray, F.; Ferlay, J.; Soerjomataram, I.; Siegel, R. L.; Torre, L. A.; Jemal, A., Global cancer statistics 2018: GLOBOCAN estimates of incidence and mortality worldwide for 36 cancers in 185 countries. *CA Cancer J Clin* 2018**,** *68* (6), 394-424.

4. National Cancer Institute, S., Epidemiology, and End Results Program, Cancer Stat Facts: Leukemia. https://seer.cancer.gov/statfacts/html/leuks.html.

5. The Global Cancer Observatory, C. T., International Agency for Research on Cancer, World Health Organization, Turkey Fact Sheets. http://gco.iarc.fr/today/data/factsheets/populations/792-turkey-fact-sheets.pdf.

6. American Cancer Society Key Statistics for Acute Lymphocytic Leukemia (ALL). https://www.cancer.org/cancer/acute-lymphocytic-leukemia/about/key-statistics.html.

7. Terwilliger, T.; Abdul-Hay, M., Acute lymphoblastic leukemia: a comprehensive review and 2017 update. *Blood Cancer J* 2017**,** *7* (6), e577.

8. Iacobucci, I.; Mullighan, C. G., Genetic Basis of Acute Lymphoblastic Leukemia. *J Clin Oncol* 2017**,** *35* (9), 975-983.

9. Mohseni, M.; Uludag, H.; Brandwein, J. M., Advances in biology of acute lymphoblastic leukemia (ALL) and therapeutic implications. *American journal of blood research* 2018**,** *8* (4), 29-56.

10. Kato, M.; Manabe, A., Treatment and biology of pediatric acute lymphoblastic leukemia. *Pediatr Int* 2018**,** *60* (1), 4-12.

11. Santiago, R.; Vairy, S.; Sinnett, D.; Krajinovic, M.; Bittencourt, H., Novel therapy for childhood acute lymphoblastic leukemia. *Expert Opin Pharmacother* 2017**,** *18* (11), 1081-1099.

12. Kang, Z. J.; Liu, Y. F.; Xu, L. Z.; Long, Z. J.; Huang, D.; Yang, Y.; Liu, B.; Feng, J. X.; Pan, Y. J.; Yan, J. S.; Liu, Q., The Philadelphia chromosome in leukemogenesis. *Chin J Cancer* 2016**,** *35*, 48.

13. Nowell, P. C., Discovery of the Philadelphia chromosome: a personal perspective. *J Clin Invest* 2007**,** *117* (8), 2033-5.

14. Hermans, A.; Heisterkamp, N.; von Linden, M.; van Baal, S.; Meijer, D.; van der Plas, D.; Wiedemann, L. M.; Groffen, J.; Bootsma, D.; Grosveld, G., Unique fusion of bcr and c-abl genes in Philadelphia chromosome positive acute lymphoblastic leukemia. *Cell* 1987**,** *51* (1), 33-40.

15. Barnes, D. J.; Melo, J. V., Cytogenetic and molecular genetic aspects of chronic myeloid leukaemia. *Acta Haematol* 2002**,** *108* (4), 180-202.

16. Groffen, J.; Stephenson, J. R.; Heisterkamp, N.; de Klein, A.; Bartram, C. R.; Grosveld, G., Philadelphia chromosomal breakpoints are clustered within a limited region, bcr, on chromosome 22. *Cell* 1984**,** *36* (1), 93-9.

17. Chissoe, S. L.; Bodenteich, A.; Wang, Y. F.; Wang, Y. P.; Burian, D.; Clifton, S. W.; Crabtree, J.; Freeman, A.; Iyer, K.; Jian, L.; et al., Sequence and analysis of the human ABL gene, the BCR gene, and regions involved in the Philadelphia chromosomal translocation. *Genomics* 1995**,** *27* (1), 67-82.

18. Rumpold, H.; Webersinke, G., Molecular pathogenesis of Philadelphia-positive chronic myeloid leukemia - is it all BCR-ABL? *Current cancer drug targets* 2011**,** *11* (1), 3-19.

19. Pane, F.; Frigeri, F.; Sindona, M.; Luciano, L.; Ferrara, F.; Cimino, R.; Meloni, G.; Saglio, G.; Salvatore, F.; Rotoli, B., Neutrophilic-chronic myeloid leukemia: a distinct disease with a specific molecular marker (BCR/ABL with C3/A2 junction) [see comments]. *Blood* 1996**,** *88* (7), 2410-2414.

20. Laurent, E.; Talpaz, M.; Kantarjian, H.; Kurzrock, R., The BCR Gene and Philadelphia Chromosome-positive Leukemogenesis. *Cancer Research* 2001**,** *61* (6), 2343-2355.

21. Reuther, G. W.; Fu, H.; Cripe, L. D.; Collier, R. J.; Pendergast, A. M., Association of the protein kinases c-Bcr and Bcr-Abl with proteins of the 14-3-3 family. *Science* 1994**,** *266* (5182), 129.

22. McWhirter, J. R.; Galasso, D. L.; Wang, J. Y., A coiled-coil oligomerization domain of Bcr is essential for the transforming function of Bcr-Abl oncoproteins. *Molecular and cellular biology* 1993**,** *13* (12), 7587-95.

23. Chuang, T. H.; Xu, X.; Kaartinen, V.; Heisterkamp, N.; Groffen, J.; Bokoch, G. M., Abr and Bcr are multifunctional regulators of the Rho GTP-binding protein family. *Proceedings of the National Academy of Sciences of the United States of America* 1995**,** *92* (22), 10282-6.

24. Peiris, M. N.; Li, F.; Donoghue, D. J., BCR: a promiscuous fusion partner in hematopoietic disorders. *Oncotarget* 2019**,** *10* (28), 2738-2754.

25. Reckel, S.; Gehin, C.; Tardivon, D.; Georgeon, S.; Kukenshoner, T.; Lohr, F.; Koide, A.; Buchner, L.; Panjkovich, A.; Reynaud, A.; Pinho, S.; Gerig, B.; Svergun, D.; Pojer, F.; Guntert, P.; Dotsch, V.; Koide, S.; Gavin, A. C.; Hantschel, O., Structural and

functional dissection of the DH and PH domains of oncogenic Bcr-Abl tyrosine kinase. *Nature communications* 2017**,** *8* (1), 2101.

26. Cutler, J. A.; Tahir, R.; Sreenivasamurthy, S. K.; Mitchell, C.; Renuse, S.; Nirujogi, R. S.; Patil, A. H.; Heydarian, M.; Wong, X.; Wu, X.; Huang, T. C.; Kim, M. S.; Reddy, K. L.; Pandey, A., Differential signaling through p190 and p210 BCR-ABL fusion proteins revealed by interactome and phosphoproteome analysis. *Leukemia* 2017**,** *31* (7), 1513-1524.

27. Takeda, N.; Shibuya, M.; Maru, Y., The BCR-ABL oncoprotein potentially interacts with the xeroderma pigmentosum group B protein. *Proceedings of the National Academy of Sciences of the United States of America* 1999**,** *96* (1), 203-7.

28. Ridley, A. J.; Hall, A., The small GTP-binding protein rho regulates the assembly of focal adhesions and actin stress fibers in response to growth factors. *Cell* 1992**,** *70* (3), 389-99.

29. Abelson, H. T.; Rabstein, L. S., Lymphosarcoma: virus-induced thymic-independent disease in mice. *Cancer Res* 1970**,** *30* (8), 2213-22.

30. Dorey, K.; Engen, J. R.; Kretzschmar, J.; Wilm, M.; Neubauer, G.; Schindler, T.; Superti-Furga, G., Phosphorylation and structure-based functional studies reveal a positive and a negative role for the activation loop of the c-Abl tyrosine kinase. *Oncogene* 2001**,** *20* (56), 8075-84.

31. Pendergast, A. M.; Muller, A. J.; Havlik, M. H.; Maru, Y.; Witte, O. N., BCR sequences essential for transformation by the BCR-ABL oncogene bind to the ABL SH2 regulatory domain in a non-phosphotyrosine-dependent manner. *Cell* 1991**,** *66* (1), 161-71.

32. Xu, W.; Harrison, S. C.; Eck, M. J., Three-dimensional structure of the tyrosine kinase c-Src. *Nature* 1997**,** *385* (6617), 595-602.

33. Barila, D.; Superti-Furga, G., An intramolecular SH3-domain interaction regulates c-Abl activity. *Nature genetics* 1998**,** *18* (3), 280-2.

34. Ren, R.; Ye, Z. S.; Baltimore, D., Abl protein-tyrosine kinase selects the Crk adapter as a substrate using SH3-binding sites. *Genes Dev* 1994**,** *8* (7), 783-95.

35. Wang, J. Y., The capable ABL: what is its biological function? *Molecular and cellular biology* 2014**,** *34* (7), 1188-97.

36. Sawyers, C. L.; McLaughlin, J.; Goga, A.; Havlik, M.; Witte, O., The nuclear tyrosine kinase c-abl negatively regulates cell growth. *Cell* 1994**,** *77* (1), 121-131.

37. Taagepera, S.; McDonald, D.; Loeb, J. E.; Whitaker, L. L.; McElroy, A. K.; Wang, J. Y. J.; Hope, T. J., Nuclear-cytoplasmic shuttling of C-ABL tyrosine kinase. *Proceedings of the National Academy of Sciences* 1998**,** *95* (13), 7457.

38. Miao, Y. J.; Wang, J. Y., Binding of A/T-rich DNA by three high mobility group-like domains in c-Abl tyrosine kinase. *J Biol Chem* 1996**,** *271* (37), 22823-30.

39. Heisterkamp, N.; Voncken, J. W.; Senadheera, D.; Gonzalez-Gomez, I.; Reichert, A.; Haataja, L.; Reinikainen, A.; Pattengale, P. K.; Groffen, J., Reduced oncogenicity of p190 Bcr/Abl F-actin-binding domain mutants. *Blood* 2000**,** *96* (6), 2226-32.

40. Steelman, L. S.; Pohnert, S. C.; Shelton, J. G.; Franklin, R. A.; Bertrand, F. E.; McCubrey, J. A., JAK/STAT, Raf/MEK/ERK, PI3K/Akt and BCR-ABL in cell cycle progression and leukemogenesis. *Leukemia* 2004**,** *18* (2), 189-218.

41. Puil, L.; Liu, J.; Gish, G.; Mbamalu, G.; Bowtell, D.; Pelicci, P. G.; Arlinghaus, R.; Pawson, T., Bcr-Abl oncoproteins bind directly to activators of the Ras signalling pathway. *The EMBO journal* 1994**,** *13* (4), 764-73.

42. Niki, M.; Di Cristofano, A.; Zhao, M.; Honda, H.; Hirai, H.; Van Aelst, L.; Cordon-Cardo, C.; Pandolfi, P. P., Role of Dok-1 and Dok-2 in leukemia suppression. *The Journal of experimental medicine* 2004**,** *200* (12), 1689-95.

43. Hickey, F. B.; England, K.; Cotter, T. G., Bcr-Abl regulates osteopontin transcription via Ras, PI-3K, aPKC, Raf-1, and MEK. *Journal of leukocyte biology* 2005**,** *78* (1), 289-300.

44. Ilaria, R. L., Jr.; Van Etten, R. A., P210 and P190(BCR/ABL) induce the tyrosine phosphorylation and DNA binding activity of multiple specific STAT family members. *J Biol Chem* 1996**,** *271* (49), 31704-10.

45. Gesbert, F.; Griffin, J. D., Bcr/Abl activates transcription of the Bcl-X gene through STAT5. *Blood* 2000**,** *96* (6), 2269-76.

46. Samanta, A.; Perazzona, B.; Chakraborty, S.; Sun, X.; Modi, H.; Bhatia, R.; Priebe, W.; Arlinghaus, R., Janus kinase 2 regulates Bcr-Abl signaling in chronic myeloid leukemia. *Leukemia* 2011**,** *25* (3), 463-72.

47. Sayed, D.; Badrawy, H.; Gaber, N.; Khalaf, M. R., p-Stat3 and bcr/abl gene expression in chronic myeloid leukemia and their relation to imatinib therapy. *Leuk Res* 2014**,** *38* (2), 243-50.

48. Hu, Y.; Liu, Y.; Pelletier, S.; Buchdunger, E.; Warmuth, M.; Fabbro, D.; Hallek, M.; Van Etten, R. A.; Li, S., Requirement of Src kinases Lyn, Hck and Fgr for BCR-ABL1-induced B-lymphoblastic leukemia but not chronic myeloid leukemia. *Nature genetics* 2004**,** *36* (5), 453-61.

49. Sattler, M.; Mohi, M. G.; Pride, Y. B.; Quinnan, L. R.; Malouf, N. A.; Podar, K.; Gesbert, F.; Iwasaki, H.; Li, S.; Van Etten, R. A.; Gu, H.; Griffin, J. D.; Neel, B. G., Critical role for Gab2 in transformation by BCR/ABL. *Cancer cell* 2002**,** *1* (5), 479-92.

50. Sattler, M.; Salgia, R.; Okuda, K.; Uemura, N.; Durstin, M. A.; Pisick, E.; Xu, G.; Li, J. L.; Prasad, K. V.; Griffin, J. D., The proto-oncogene product p120CBL and the

adaptor proteins CRKL and c-CRK link c-ABL, p190BCR/ABL and p210BCR/ABL to the phosphatidylinositol-3' kinase pathway. *Oncogene* 1996**,** *12* (4), 839-46.

51. Kharas, M. G.; Janes, M. R.; Scarfone, V. M.; Lilly, M. B.; Knight, Z. A.; Shokat, K. M.; Fruman, D. A., Ablation of PI3K blocks BCR-ABL leukemogenesis in mice, and a dual PI3K/mTOR inhibitor prevents expansion of human BCR-ABL+ leukemia cells. *The Journal of clinical investigation* 2008**,** *118* (9), 3038-3050.

52. Badura, S.; Tesanovic, T.; Pfeifer, H.; Wystub, S.; Nijmeijer, B. A.; Liebermann, M.; Falkenburg, J. H.; Ruthardt, M.; Ottmann, O. G., Differential effects of selective inhibitors targeting the PI3K/AKT/mTOR pathway in acute lymphoblastic leukemia. *PloS one* 2013**,** *8* (11), e80070.

53. Goldman, J. M., Chronic myeloid leukemia: a historical perspective. *Seminars in hematology* 2010**,** *47* (4), 302-11.

54. Hamad, A.; Sahli, Z.; El Sabban, M.; Mouteirik, M.; Nasr, R., Emerging therapeutic strategies for targeting chronic myeloid leukemia stem cells. *Stem Cells Int* 2013**,** *2013*, 724360.

55. Takeuchi, J.; Kyo, T.; Naito, K.; Sao, H.; Takahashi, M.; Miyawaki, S.; Kuriyama, K.; Ohtake, S.; Yagasaki, F.; Murakami, H.; Asou, N.; Ino, T.; Okamoto, T.; Usui, N.; Nishimura, M.; Shinagawa, K.; Fukushima, T.; Taguchi, H.; Morii, T.; Mizuta, S.; Akiyama, H.; Nakamura, Y.; Ohshima, T.; Ohno, R., Induction therapy by frequent administration of doxorubicin with four other drugs, followed by intensive consolidation and maintenance therapy for adult acute lymphoblastic leukemia: the JALSG-ALL93 study. *Leukemia* 2002**,** *16* (7), 1259-66.

56. Woessner, D. W.; Lim, C. S.; Deininger, M. W., Development of an effective therapy for chronic myelogenous leukemia. *Cancer journal (Sudbury, Mass.)* 2011**,** *17* (6), 477-86.

57. Druker, B. J.; Tamura, S.; Buchdunger, E.; Ohno, S.; Segal, G. M.; Fanning, S.; Zimmermann, J.; Lydon, N. B., Effects of a selective inhibitor of the Abl tyrosine kinase on the growth of Bcr-Abl positive cells. *Nature medicine* 1996**,** *2* (5), 561-6.

58. Yilmaz, M.; Kantarjian, H.; Ravandi-Kashani, F.; Short, N. J.; Jabbour, E., Philadelphia chromosome-positive acute lymphoblastic leukemia in adults: current treatments and future perspectives. *Clinical advances in hematology & oncology : H&O* 2018**,** *16* (3), 216-223.

59. Weisberg, E.; Manley, P. W.; Cowan-Jacob, S. W.; Hochhaus, A.; Griffin, J. D., Second generation inhibitors of BCR-ABL for the treatment of imatinib-resistant chronic myeloid leukaemia. *Nat Rev Cancer* 2007**,** *7* (5), 345-56.

60. Druker, B. J.; Lydon, N. B., Lessons learned from the development of an abl tyrosine kinase inhibitor for chronic myelogenous leukemia. *J Clin Invest* 2000**,** *105* (1), 3-7.

61. Lombardo, L. J.; Lee, F. Y.; Chen, P.; Norris, D.; Barrish, J. C.; Behnia, K.; Castaneda, S.; Cornelius, L. A.; Das, J.; Doweyko, A. M.; Fairchild, C.; Hunt, J. T.; Inigo, I.; Johnston, K.; Kamath, A.; Kan, D.; Klei, H.; Marathe, P.; Pang, S.; Peterson, R.; Pitt, S.; Schieven, G. L.; Schmidt, R. J.; Tokarski, J.; Wen, M. L.; Wityak, J.; Borzilleri, R. M., Discovery of N-(2-chloro-6-methyl- phenyl)-2-(6-(4-(2-hydroxyethyl)- piperazin-1-yl)-2-methylpyrimidin-4- ylamino)thiazole-5-carboxamide (BMS-354825), a dual Src/Abl kinase inhibitor with potent antitumor activity in preclinical assays. *Journal of medicinal chemistry* 2004**,** *47* (27), 6658-61.

62. Lindauer, M.; Hochhaus, A., Dasatinib. *Recent results in cancer research. Fortschritte der Krebsforschung. Progres dans les recherches sur le cancer* 2010**,** *184*, 83-102.

63. Fabarius, A.; Giehl, M.; Rebacz, B.; Kramer, A.; Frank, O.; Haferlach, C.; Duesberg, P.; Hehlmann, R.; Seifarth, W.; Hochhaus, A., Centrosome aberrations and G1 phase arrest after in vitro and in vivo treatment with the SRC/ABL inhibitor dasatinib. *Haematologica* 2008**,** *93* (8), 1145-54.

64. Porkka, K.; Khoury, H. J.; Paquette, R. L.; Matloub, Y.; Sinha, R.; Cortes, J. E., Dasatinib 100 mg once daily minimizes the occurrence of pleural effusion in patients with chronic myeloid leukemia in chronic phase and efficacy is unaffected in patients who develop pleural effusion. *Cancer* 2010**,** *116* (2), 377-86.

65. Jabbour, E.; Cortes, J.; Kantarjian, H., Long-term outcomes in the second-line treatment of chronic myeloid leukemia: a review of tyrosine kinase inhibitors. *Cancer* 2011**,** *117* (5), 897-906.

66. Shah, N. P.; Tran, C.; Lee, F. Y.; Chen, P.; Norris, D.; Sawyers, C. L., Overriding Imatinib Resistance with a Novel ABL Kinase Inhibitor. *Science* 2004**,** *305* (5682), 399.

67. Cowan-Jacob, S. W.; Fendrich, G.; Floersheimer, A.; Furet, P.; Liebetanz, J.; Rummel, G.; Rheinberger, P.; Centeleghe, M.; Fabbro, D.; Manley, P. W., Structural biology contributions to the discovery of drugs to treat chronic myelogenous leukaemia. *Acta Crystallogr D Biol Crystallogr* 2007**,** *63* (Pt 1), 80-93.

68. Deininger, M. W., Nilotinib. *Clinical Cancer Research* 2008**,** *14* (13), 4027.

69. Maekawa, T.; Ashihara, E.; Kimura, S., The Bcr-Abl tyrosine kinase inhibitor imatinib and promising new agents against Philadelphia chromosome-positive leukemias. *Int J Clin Oncol* 2007**,** *12* (5), 327-40.

70. Jabbour, E.; Cortes, J.; Kantarjian, H., Treatment selection after imatinib resistance in chronic myeloid leukemia. *Targeted oncology* 2009**,** *4* (1), 3-10.

71. Kim, D. Y.; Joo, Y. D.; Lim, S. N.; Kim, S. D.; Lee, J. H.; Lee, J. H.; Kim, D. H.; Kim, K.; Jung, C. W.; Kim, I.; Yoon, S. S.; Park, S.; Ahn, J. S.; Yang, D. H.; Lee, J. J.; Lee, H. S.; Kim, Y. S.; Mun, Y. C.; Kim, H.; Park, J. H.; Moon, J. H.; Sohn, S. K.; Lee, S. M.; Lee, W. S.; Kim, K. H.; Won, J. H.; Hyun, M. S.; Park, J.; Lee, J. H.; Shin, H. J.; Chung, J. S.; Lee, H.; Eom, H. S.; Lee, G. W.; Cho, Y. U.; Jang, S.; Park, C. J.; Chi, H.

S.; Lee, K. H., Nilotinib combined with multiagent chemotherapy for newly diagnosed Philadelphia-positive acute lymphoblastic leukemia. *Blood* 2015**,** *126* (6), 746-56.

72. O'Hare, T.; Shakespeare, W. C.; Zhu, X.; Eide, C. A.; Rivera, V. M.; Wang, F.; Adrian, L. T.; Zhou, T.; Huang, W. S.; Xu, Q.; Metcalf, C. A., 3rd; Tyner, J. W.; Loriaux, M. M.; Corbin, A. S.; Wardwell, S.; Ning, Y.; Keats, J. A.; Wang, Y.; Sundaramoorthi, R.; Thomas, M.; Zhou, D.; Snodgrass, J.; Commodore, L.; Sawyer, T. K.; Dalgarno, D. C.; Deininger, M. W.; Druker, B. J.; Clackson, T., AP24534, a pan-BCR-ABL inhibitor for chronic myeloid leukemia, potently inhibits the T315I mutant and overcomes mutation-based resistance. *Cancer cell* 2009**,** *16* (5), 401-12.

73. Pfeifer, H.; Wassmann, B.; Pavlova, A.; Wunderle, L.; Oldenburg, J.; Binckebanck, A.; Lange, T.; Hochhaus, A.; Wystub, S.; Bruck, P.; Hoelzer, D.; Ottmann, O. G., Kinase domain mutations of BCR-ABL frequently precede imatinib-based therapy and give rise to relapse in patients with de novo Philadelphia-positive acute lymphoblastic leukemia (Ph+ ALL). *Blood* 2007**,** *110* (2), 727-34.

74. Zhou, T.; Commodore, L.; Huang, W. S.; Wang, Y.; Thomas, M.; Keats, J.; Xu, Q.; Rivera, V. M.; Shakespeare, W. C.; Clackson, T.; Dalgarno, D. C.; Zhu, X., Structural mechanism of the Pan-BCR-ABL inhibitor ponatinib (AP24534): lessons for overcoming kinase inhibitor resistance. *Chemical biology & drug design* 2011**,** *77* (1), 1-11.

75. Jabbour, E.; Kantarjian, H.; Ravandi, F.; Thomas, D.; Huang, X.; Faderl, S.; Pemmaraju, N.; Daver, N.; Garcia-Manero, G.; Sasaki, K.; Cortes, J.; Garris, R.; Yin, C. C.; Khoury, J. D.; Jorgensen, J.; Estrov, Z.; Bohannan, Z.; Konopleva, M.; Kadia, T.; Jain, N.; DiNardo, C.; Wierda, W.; Jeanis, V.; O'Brien, S., Combination of hyper-CVAD with ponatinib as first-line therapy for patients with Philadelphia chromosome-positive acute lymphoblastic leukaemia: a single-centre, phase 2 study. *The Lancet. Oncology* 2015**,** *16* (15), 1547-1555.

76. Phelan, K. W.; Advani, A. S., Novel Therapies in Acute Lymphoblastic Leukemia. *Curr Hematol Malig Rep* 2018**,** *13* (4), 289-299.

77. Hendriks, D.; Choi, G.; de Bruyn, M.; Wiersma, V. R.; Bremer, E., Chapter Seven - Antibody-Based Cancer Therapy: Successful Agents and Novel Approaches. In *International Review of Cell and Molecular Biology*, Galluzzi, L., Ed. Academic Press: 2017; Vol. 331, pp 289-383.

78. Jain, N.; Cortes, J. E.; Ravandi, F.; Konopleva, M.; Alvarado, Y.; Kadia, T.; Wierda, W. G.; Borthakur, G.; Naqvi, K.; Pemmaraju, N.; DiNardo, C. D.; Daver, N.; Yilmaz, M.; Patel, K.; Bull Linderman, D.; Garris, R.; Jabbour, E. J.; Kantarjian, H. M., Inotuzumab Ozogamicin in Combination with Bosutinib for Patients with Relapsed or Refractory Ph+ ALL or CML in Lymphoid Blast Phase. *Blood* 2017**,** *130* (Supplement 1), 143-143.

79. Smith, E. J.; Olson, K.; Haber, L. J.; Varghese, B.; Duramad, P.; Tustian, A. D.; Oyejide, A.; Kirshner, J. R.; Canova, L.; Menon, J.; Principio, J.; MacDonald, D.; Kantrowitz, J.; Papadopoulos, N.; Stahl, N.; Yancopoulos, G. D.; Thurston, G.; Davis, S.,

A novel, native-format bispecific antibody triggering T-cell killing of B-cells is robustly active in mouse tumor models and cynomolgus monkeys. *Scientific reports* 2015**,** *5*, 17943.

80. Otero, D. C.; Omori, S. A.; Rickert, R. C., Cd19-dependent activation of Akt kinase in B-lymphocytes. *J Biol Chem* 2001**,** *276* (2), 1474-8.

81. Fujimoto, M.; Poe, J. C.; Jansen, P. J.; Sato, S.; Tedder, T. F., CD19 amplifies B lymphocyte signal transduction by regulating Src-family protein tyrosine kinase activation. *Journal of immunology (Baltimore, Md. : 1950)* 1999**,** *162* (12), 7088-94.

82. Chung, E. Y.; Psathas, J. N.; Yu, D.; Li, Y.; Weiss, M. J.; Thomas-Tikhonenko, A., CD19 is a major B cell receptor-independent activator of MYC-driven B-lymphomagenesis. *J Clin Invest* 2012**,** *122* (6), 2257-66.

83. Martinelli, G.; Boissel, N.; Chevallier, P.; Ottmann, O.; Gokbuget, N.; Topp, M. S.; Fielding, A. K.; Rambaldi, A.; Ritchie, E. K.; Papayannidis, C.; Sterling, L. R.; Benjamin, J.; Stein, A., Complete Hematologic and Molecular Response in Adult Patients With Relapsed/Refractory Philadelphia Chromosome-Positive B-Precursor Acute Lymphoblastic Leukemia Following Treatment With Blinatumomab: Results From a Phase II, Single-Arm, Multicenter Study. *J Clin Oncol* 2017**,** *35* (16), 1795-1802.

84. Abou Dalle, I.; Jabbour, E.; Short, N. J.; Ravandi, F., Treatment of Philadelphia Chromosome-Positive Acute Lymphoblastic Leukemia. *Curr Treat Options Oncol* 2019**,** *20* (1), 4.

85. Batlevi, C. L.; Matsuki, E.; Brentjens, R. J.; Younes, A., Novel immunotherapies in lymphoid malignancies. *Nature reviews. Clinical oncology* 2016**,** *13* (1), 25-40.

86. Rafei, H.; Kantarjian, H. M.; Jabbour, E. J., Recent advances in the treatment of acute lymphoblastic leukemia. *Leukemia & lymphoma* 2019, 1-16.

87. Yang, F.; Yang, X.; Bao, X.; Kang, L.; Zhou, L.; Wu, X.; Tang, X.; Fu, Z.; Ma, X.; Sun, A.; Zhang, J.; Qiu, H.; Wu, D., Anti-CD19 chimeric antigen receptor T-cells induce durable remission in relapsed Philadelphia chromosome-positive ALL with T315I mutation. *Leukemia & lymphoma* 2019, 1-8.

88. El Chaer, F.; Holtzman, N. G.; Sausville, E. A.; Law, J. Y.; Lee, S. T.; Duong, V. H.; Baer, M. R.; Koka, R.; Singh, Z. N.; Hardy, N. M.; Emadi, A., Relapsed Philadelphia Chromosome-Positive Pre-B-ALL after CD19-Directed CAR-T Cell Therapy Successfully Treated with Combination of Blinatumomab and Ponatinib. *Acta Haematol* 2019**,** *141* (2), 107-110.

89. Heung, L. J.; Luberto, C.; Del Poeta, M., Role of Sphingolipids in Microbial Pathogenesis. *Infection and Immunity* 2006**,** *74* (1), 28.

90. Hannun, Y. A.; Obeid, L. M., Sphingolipids and their metabolism in physiology and disease. *Nat Rev Mol Cell Biol* 2018**,** *19* (3), 175-191.

91. Uchida, Y., Ceramide signaling in mammalian epidermis. *Biochimica et Biophysica Acta (BBA) - Molecular and Cell Biology of Lipids* 2014**,** *1841* (3), 453-462.

92. Hannun, Y. A.; Obeid, L. M., Principles of bioactive lipid signalling: lessons from sphingolipids. *Nat Rev Mol Cell Biol* 2008**,** *9* (2), 139-50.

93. Wegner, M. S.; Schiffmann, S.; Parnham, M. J.; Geisslinger, G.; Grosch, S., The enigma of ceramide synthase regulation in mammalian cells. *Prog Lipid Res* 2016**,** *63*, 93-119.

94. Pewzner-Jung, Y.; Ben-Dor, S.; Futerman, A. H., When do Lasses (longevity assurance genes) become CerS (ceramide synthases)?: Insights into the regulation of ceramide synthesis. *J Biol Chem* 2006**,** *281* (35), 25001-5.

95. Adan-Gokbulut, A.; Kartal-Yandim, M.; Iskender, G.; Baran, Y., Novel agents targeting bioactive sphingolipids for the treatment of cancer. *Current medicinal chemistry* 2013**,** *20* (1), 108-22.

96. Kudo, N.; Kumagai, K.; Tomishige, N.; Yamaji, T.; Wakatsuki, S.; Nishijima, M.; Hanada, K.; Kato, R., Structural basis for specific lipid recognition by CERT responsible for nonvesicular trafficking of ceramide. *Proceedings of the National Academy of Sciences of the United States of America* 2008**,** *105* (2), 488-93.

97. Tettamanti, G., Ganglioside/glycosphingolipid turnover: new concepts. *Glycoconjugate journal* 2004**,** *20* (5), 301-17.

98. Perales, M.; Cervantes, F.; Cobo, F.; Montserrat, E., Non-Hodgkin's lymphoma associated with Gaucher's disease. *Leukemia & lymphoma* 1998**,** *31* (5-6), 609-612.

99. Lucci, A.; Cho, W. I.; Han, T. Y.; Giuliano, A. E.; Morton, D. L.; Cabot, M. C., Glucosylceramide: a marker for multiple-drug resistant cancers. *Anticancer Res* 1998**,** *18* (1B), 475-480.

100. Baran, Y.; Bielawski, J.; Gunduz, U.; Ogretmen, B., Targeting glucosylceramide synthase sensitizes imatinib-resistant chronic myeloid leukemia cells via endogenous ceramide accumulation. *Journal of cancer research and clinical oncology* 2011**,** *137* (10), 1535-1544.

101. Huang, C.; Tu, Y.; Freter, C. E., Fludarabine-resistance associates with ceramide metabolism and leukemia stem cell development in chronic lymphocytic leukemia. *Oncotarget* 2018**,** *9* (69), 33124-33137.

102. Spiegel, S.; Milstien, S., Sphingosine-1-phosphate: an enigmatic signalling lipid. *Nat Rev Mol Cell Biol* 2003**,** *4* (5), 397-407.

103. Pyne, S.; Lee, S. C.; Long, J.; Pyne, N. J., Role of sphingosine kinases and lipid phosphate phosphatases in regulating spatial sphingosine 1-phosphate signalling in health and disease. *Cellular signalling* 2009**,** *21* (1), 14-21.

104. Payne, S. G.; Milstien, S.; Spiegel, S., Sphingosine-1-phosphate: dual messenger functions. *FEBS letters* 2002**,** *531* (1), 54-7.

105. Brachtendorf, S.; El-Hindi, K.; Grosch, S., Ceramide synthases in cancer therapy and chemoresistance. *Prog Lipid Res* 2019**,** *74*, 160-185.

106. Mizutani, Y.; Kihara, A.; Igarashi, Y., Mammalian Lass6 and its related family members regulate synthesis of specific ceramides. *The Biochemical journal* 2005**,** *390* (Pt 1), 263-71.

107. Koybasi, S.; Senkal, C. E.; Sundararaj, K.; Spassieva, S.; Bielawski, J.; Osta, W.; Day, T. A.; Jiang, J. C.; Jazwinski, S. M.; Hannun, Y. A.; Obeid, L. M.; Ogretmen, B., Defects in cell growth regulation by C18:0-ceramide and longevity assurance gene 1 in human head and neck squamous cell carcinomas. *Journal of Biological Chemistry* 2004**,** *279* (43), 44311-44319.

108. Meyers-Needham, M.; Ponnusamy, S.; Gencer, S.; Jiang, W.; Thomas, R. J.; Senkal, C. E.; Ogretmen, B., Concerted functions of HDAC1 and microRNA-574-5p repress alternatively spliced ceramide synthase 1 expression in human cancer cells. *EMBO Molecular Medicine* 2012**,** *4* (2), 78-92.

109. Wooten-Blanks, L. G.; Song, P.; Senkal, C. E.; Ogretmen, B., Mechanisms of ceramide-mediated repression of the human telomerase reverse transcriptase promoter via deacetylation of Sp3 by histone deacetylase 1. *The FASEB Journal* 2007**,** *21* (12), 3386-3397.

110. Baran, Y.; Salas, A.; Senkal, C. E.; Gunduz, U.; Bielawski, J.; Obeid, L. M.; Ogretmen, B., Alterations of ceramide/sphingosine 1-phosphate rheostat involved in the regulation of resistance to imatinib-induced apoptosis in K562 human chronic myeloid leukemia cells. *J Biol Chem* 2007**,** *282* (15), 10922-34.

111. Gencer, E. B.; Ural, A. U.; Avcu, F.; Baran, Y., A novel mechanism of dasatinib-induced apoptosis in chronic myeloid leukemia; ceramide synthase and ceramide clearance genes. *Annals of Hematology* 2011**,** *90* (11), 1265-1275.

112. Dany, M.; Gencer, S.; Nganga, R.; Thomas, R. J.; Oleinik, N.; Baron, K. D.; Szulc, Z. M.; Ruvolo, P.; Kornblau, S.; Andreeff, M.; Ogretmen, B., Targeting FLT3-ITD signaling mediates ceramide-dependent mitophagy and attenuates drug resistance in AML. *Blood* 2016**,** *128* (15), 1944-1958.

113. Ruan, H.; Wang, T.; Yang, C.; Jin, G.; Gu, D.; Deng, X.; Wang, C.; Qin, W.; Jin, H., Co-expression of LASS2 and TGF-β1 predicts poor prognosis in hepatocellular carcinoma. *Scientific reports* 2016**,** *6*, 32421.

114. Fan, S. H.; Wang, Y. Y.; Lu, J.; Zheng, Y. L.; Wu, D. M.; Zhang, Z. F.; Shan, Q.; Hu, B.; Li, M. Q.; Cheng, W., CERS2 suppresses tumor cell invasion and is associated with decreased V-ATPase and MMP-2/MMP-9 activities in breast cancer. *Journal of cellular biochemistry* 2015**,** *116* (4), 502-13.

115. Meng, J.; Chen, S.; Han, J. X.; Tan, Q.; Wang, X. R.; Wang, H. Z.; Zhong, W. L.; Qin, Y.; Qiao, K. L.; Zhang, C.; Gao, W. F.; Lei, Y. Y.; Liu, H. J.; Liu, Y. R.; Zhou, H. G.; Sun, T.; Yang, C., Derepression of co-silenced tumor suppressor genes by nanoparticle-loaded circular ssDNA reduces tumor malignancy. *Science translational medicine* 2018**,** *10* (442).

116. Zeng, F.; Huang, L.; Cheng, X.; Yang, X.; Li, T.; Feng, G.; Tang, Y.; Yang, Y., Overexpression of LASS2 inhibits proliferation and causes G0/G1 cell cycle arrest in papillary thyroid cancer. *Cancer cell international* 2018**,** *18*, 151.

117. Wang, H.; Zuo, Y.; Ding, M.; Ke, C.; Yan, R.; Zhan, H.; Liu, J.; Wang, W.; Li, N.; Wang, J., LASS2 inhibits growth and invasion of bladder cancer by regulating ATPase activity. *Oncol Lett* 2017**,** *13* (2), 661-668.

118. Aldoghachi, A. F.; Baharudin, A.; Ahmad, U.; Chan, S. C.; Ong, T. A.; Yunus, R.; Razack, A. H.; Yusoff, K.; Veerakumarasivam, A., Evaluation of CERS2 Gene as a Potential Biomarker for Bladder Cancer. *Dis Markers* 2019**,** *2019*, 3875147.

119. Brachtendorf, S.; Wanger, R. A.; Birod, K.; Thomas, D.; Trautmann, S.; Wegner, M.-S.; Fuhrmann, D. C.; Brüne, B.; Geisslinger, G.; Grösch, S., Chemosensitivity of human colon cancer cells is influenced by a p53-dependent enhancement of ceramide synthase 5 and induction of autophagy. *Biochimica et Biophysica Acta (BBA) - Molecular and Cell Biology of Lipids* 2018**,** *1863* (10), 1214-1227.

120. Sassa, T.; Suto, S.; Okayasu, Y.; Kihara, A., A shift in sphingolipid composition from C24 to C16 increases susceptibility to apoptosis in HeLa cells. *Biochimica et Biophysica Acta (BBA) - Molecular and Cell Biology of Lipids* 2012**,** *1821* (7), 1031-1037.

121. Rabionet, M.; Bayerle, A.; Jennemann, R.; Heid, H.; Fuchser, J.; Marsching, C.; Porubsky, S.; Bolenz, C.; Guillou, F.; Gröne, H.-J.; Gorgas, K.; Sandhoff, R., Male meiotic cytokinesis requires ceramide synthase 3-dependent sphingolipids with unique membrane anchors. *Human Molecular Genetics* 2015**,** *24* (17), 4792-4808.

122. Peters, F.; Vorhagen, S.; Brodesser, S.; Jakobshagen, K.; Brüning, J. C.; Niessen, C. M.; Krönke, M., Ceramide Synthase 4 Regulates Stem Cell Homeostasis and Hair Follicle Cycling. *Journal of Investigative Dermatology* 2015**,** *135* (6), 1501-1509.

123. Chen, J.; Li, X.; Ma, D.; Liu, T.; Tian, P.; Wu, C., Ceramide synthase-4 orchestrates the cell proliferation and tumor growth of liver cancer in vitro and in vivo through the nuclear factor-kappaB signaling pathway. *Oncol Lett* 2017**,** *14* (2), 1477-1483.

124. Schiffmann, S.; Sandner, J.; Birod, K.; Wobst, I.; Angioni, C.; Ruckhäberle, E.; Kaufmann, M.; Ackermann, H.; Lötsch, J.; Schmidt, H.; Geisslinger, G.; Grösch, S., Ceramide synthases and ceramide levels are increased in breast cancer tissue. *Carcinogenesis* 2009**,** *30* (5), 745-752.

125. Hartmann, D.; Lucks, J.; Fuchs, S.; Schiffmann, S.; Schreiber, Y.; Ferreirós, N.; Merkens, J.; Marschalek, R.; Geisslinger, G.; Grösch, S., Long chain ceramides and very long chain ceramides have opposite effects on human breast and colon cancer cell growth. *The International Journal of Biochemistry & Cell Biology* 2012**,** *44* (4), 620-628.

126. Gencer, S.; Oleinik, N.; Kim, J.; Panneer Selvam, S.; De Palma, R.; Dany, M.; Nganga, R.; Thomas, R. J.; Senkal, C. E.; Howe, P. H.; Ogretmen, B., TGF-β receptor I/II trafficking and signaling at primary cilia are inhibited by ceramide to attenuate cell migration and tumor metastasis. *Science Signaling* 2017**,** *10* (502), eaam7464.

127. Jin, J.; Mullen, T. D.; Hou, Q.; Bielawski, J.; Bielawska, A.; Zhang, X.; Obeid, L. M.; Hannun, Y. A.; Hsu, Y. T., AMPK inhibitor Compound C stimulates ceramide production and promotes Bax redistribution and apoptosis in MCF7 breast carcinoma cells. *Journal of lipid research* 2009**,** *50* (12), 2389-97.

128. Mesicek, J.; Lee, H.; Feldman, T.; Jiang, X.; Skobeleva, A.; Berdyshev, E. V.; Haimovitz-Friedman, A.; Fuks, Z.; Kolesnick, R., Ceramide synthases 2, 5, and 6 confer distinct roles in radiation-induced apoptosis in HeLa cells. *Cellular signalling* 2010**,** *22* (9), 1300-1307.

129. Fitzgerald, S.; Sheehan, K. M.; Espina, V.; O'Grady, A.; Cummins, R.; Kenny, D.; Liotta, L.; O'Kennedy, R.; Kay, E. W.; Kijanka, G. S., High CerS5 expression levels associate with reduced patient survival and transition from apoptotic to autophagy signalling pathways in colorectal cancer. *The Journal of Pathology: Clinical Research* 2015**,** *1* (1), 54-65.

130. Wegner, M.-S.; Wanger, R. A.; Oertel, S.; Brachtendorf, S.; Hartmann, D.; Schiffmann, S.; Marschalek, R.; Schreiber, Y.; Ferreirós, N.; Geisslinger, G.; Grösch, S., Ceramide synthases CerS4 and CerS5 are upregulated by 17β-estradiol and GPER1 via AP-1 in human breast cancer cells. *Biochemical Pharmacology* 2014**,** *92* (4), 577-589.

131. Moro, K.; Kawaguchi, T.; Tsuchida, J.; Gabriel, E.; Qi, Q.; Yan, L.; Wakai, T.; Takabe, K.; Nagahashi, M., Ceramide species are elevated in human breast cancer and are associated with less aggressiveness. *Oncotarget* 2018**,** *9* (28), 19874-19890.

132. Jeffries, K. A.; Krupenko, N. I., Chapter Seven - Ceramide Signaling and p53 Pathways. In *Advances in Cancer Research*, Chalfant, C. E.; Fisher, P. B., Eds. Academic Press: 2018; Vol. 140, pp 191-215.

133. Panjarian, S.; Kozhaya, L.; Arayssi, S.; Yehia, M.; Bielawski, J.; Bielawska, A.; Usta, J.; Hannun, Y. A.; Obeid, L. M.; Dbaibo, G. S., De novo N-palmitoylsphingosine synthesis is the major biochemical mechanism of ceramide accumulation following p53 up-regulation. *Prostaglandins & Other Lipid Mediators* 2008**,** *86* (1), 41-48.

134. Jiang, Z.; Li, F.; Wan, Y.; Han, Z.; Yuan, W.; Cao, L.; Deng, Y.; Peng, X.; Chen, F.; Fan, X.; Liu, X.; Dai, G.; Wang, Y.; Zeng, Q.; Shi, Y.; Zhou, Z.; Chen, Y.; Xu, W.; Luo, S.; Chen, S.; Ye, X.; Mo, X.; Wu, X.; Li, Y., LASS5 Interacts with SDHB and

Synergistically Represses p53 and p21 Activity. *Current Molecular Medicine* 2016**,** *16* (6), 582-590.

135. Rénert, A.-F.; Leprince, P.; Dieu, M.; Renaut, J.; Raes, M.; Bours, V.; Chapelle, J.-P.; Piette, J.; Merville, M.-P.; Fillet, M., The Proapoptotic C16-ceramide-Dependent Pathway Requires the Death-Promoting Factor Btf in Colon Adenocarcinoma Cells. *Journal of Proteome Research* 2009**,** *8* (10), 4810-4822.

136. Fekry, B.; Jeffries, K. A.; Esmaeilniakooshkghazi, A.; Szulc, Z. M.; Knagge, K. J.; Kirchner, D. R.; Horita, D. A.; Krupenko, S. A.; Krupenko, N. I., C 16-ceramide is a natural regulatory ligand of p53 in cellular stress response. *Nature communications* 2018**,** *9* (1), 4149.

137. Suzuki, M.; Cao, K.; Kato, S.; Komizu, Y.; Mizutani, N.; Tanaka, K.; Arima, C.; Tai, M. C.; Yanagisawa, K.; Togawa, N.; Shiraishi, T.; Usami, N.; Taniguchi, T.; Fukui, T.; Yokoi, K.; Wakahara, K.; Hasegawa, Y.; Mizutani, Y.; Igarashi, Y.; Inokuchi, J.; Iwaki, S.; Fujii, S.; Satou, A.; Matsumoto, Y.; Ueoka, R.; Tamiya-Koizumi, K.; Murate, T.; Nakamura, M.; Kyogashima, M.; Takahashi, T., Targeting ceramide synthase 6-dependent metastasis-prone phenotype in lung cancer cells. *J Clin Invest* 2016**,** *126* (1), 254-65.

138. Uen, Y.-H.; Fang, C.-L.; Lin, C.-C.; Hseu, Y.-C.; Hung, S.-T.; Sun, D.-P.; Lin, K.-Y., Ceramide synthase 6 predicts the prognosis of human gastric cancer: It functions as an oncoprotein by dysregulating the SOCS2/JAK2/STAT3 pathway. *Molecular Carcinogenesis* 2018**,** *57* (12), 1675-1689.

139. Edmond, V.; Dufour, F.; Poiroux, G.; Shoji, K.; Malleter, M.; Fouqué, A.; Tauzin, S.; Rimokh, R.; Sergent, O.; Penna, A.; Dupuy, A.; Levade, T.; Theret, N.; Micheau, O.; Ségui, B.; Legembre, P., Downregulation of ceramide synthase-6 during epithelial-to-mesenchymal transition reduces plasma membrane fluidity and cancer cell motility. *Oncogene* 2015**,** *34* (8), 996-1005.

140. Walker, T.; Mitchell, C.; Park, M. A.; Yacoub, A.; Graf, M.; Rahmani, M.; Houghton, P. J.; Voelkel-Johnson, C.; Grant, S.; Dent, P., Sorafenib and Vorinostat Kill Colon Cancer Cells by CD95-Dependent and -Independent Mechanisms. *Molecular Pharmacology* 2009**,** *76* (2), 342.

141. Verlekar, D.; Wei, S.-J.; Cho, H.; Yang, S.; Kang, M. H., Ceramide synthase-6 confers resistance to chemotherapy by binding to CD95/Fas in T-cell acute lymphoblastic leukemia. *Cell death & disease* 2018**,** *9* (9), 925.

142. Maceyka, M.; Spiegel, S., Sphingolipid metabolites in inflammatory disease. *Nature* 2014**,** *510* (7503), 58-67.

143. Takabe, K.; Kim, R. H.; Allegood, J. C.; Mitra, P.; Ramachandran, S.; Nagahashi, M.; Harikumar, K. B.; Hait, N. C.; Milstien, S.; Spiegel, S., Estradiol induces export of sphingosine 1-phosphate from breast cancer cells via ABCC1 and ABCG2. *J Biol Chem* 2010**,** *285* (14), 10477-86.

144. Ogretmen, B., Sphingolipid metabolism in cancer signalling and therapy. *Nat Rev Cancer* 2018**,** *18* (1), 33-50.

145. Hisano, Y.; Kobayashi, N.; Yamaguchi, A.; Nishi, T., Mouse SPNS2 functions as a sphingosine-1-phosphate transporter in vascular endothelial cells. *PloS one* 2012**,** *7* (6), e38941.

146. Salas, A.; Ponnusamy, S.; Senkal, C. E.; Meyers-Needham, M.; Selvam, S. P.; Saddoughi, S. A.; Apohan, E.; Sentelle, R. D.; Smith, C.; Gault, C. R.; Obeid, L. M.; El-Shewy, H. M.; Oaks, J.; Santhanam, R.; Marcucci, G.; Baran, Y.; Mahajan, S.; Fernandes, D.; Stuart, R.; Perrotti, D.; Ogretmen, B., Sphingosine kinase-1 and sphingosine 1-phosphate receptor 2 mediate Bcr-Abl1 stability and drug resistance by modulation of protein phosphatase 2A. *Blood* 2011**,** *117* (22), 5941-5952.

147. van der Weyden, L.; Arends, M. J.; Campbell, A. D.; Bald, T.; Wardle-Jones, H.; Griggs, N.; Velasco-Herrera, M. D.; Tuting, T.; Sansom, O. J.; Karp, N. A.; Clare, S.; Gleeson, D.; Ryder, E.; Galli, A.; Tuck, E.; Cambridge, E. L.; Voet, T.; Macaulay, I. C.; Wong, K.; Spiegel, S.; Speak, A. O.; Adams, D. J., Genome-wide in vivo screen identifies novel host regulators of metastatic colonization. *Nature* 2017**,** *541* (7636), 233-236.

148. Ponnusamy, S.; Selvam, S. P.; Mehrotra, S.; Kawamori, T.; Snider, A. J.; Obeid, L. M.; Shao, Y.; Sabbadini, R.; Ogretmen, B., Communication between host organism and cancer cells is transduced by systemic sphingosine kinase 1/sphingosine 1-phosphate signalling to regulate tumour metastasis. *EMBO Mol Med* 2012**,** *4* (8), 761-75.

149. Alvarez, S. E.; Harikumar, K. B.; Hait, N. C.; Allegood, J.; Strub, G. M.; Kim, E. Y.; Maceyka, M.; Jiang, H.; Luo, C.; Kordula, T.; Milstien, S.; Spiegel, S., Sphingosine-1-phosphate is a missing cofactor for the E3 ubiquitin ligase TRAF2. *Nature* 2010**,** *465* (7301), 1084-8.

150. Panneer Selvam, S.; De Palma, R. M.; Oaks, J. J.; Oleinik, N.; Peterson, Y. K.; Stahelin, R. V.; Skordalakes, E.; Ponnusamy, S.; Garrett-Mayer, E.; Smith, C. D.; Ogretmen, B., Binding of the sphingolipid S1P to hTERT stabilizes telomerase at the nuclear periphery by allosterically mimicking protein phosphorylation. *Sci Signal* 2015**,** *8* (381), ra58.

151. Selvam, S. P.; Ogretmen, B., Sphingosine kinase/sphingosine 1-phosphate signaling in cancer therapeutics and drug resistance. *Handbook of experimental pharmacology* 2013**,** (216), 3-27.

152. Prochazkova, D.; Bousova, I.; Wilhelmova, N., Antioxidant and prooxidant properties of flavonoids. *Fitoterapia* 2011**,** *82* (4), 513-23.

153. George, V. C.; Dellaire, G.; Rupasinghe, H. P. V., Plant flavonoids in cancer chemoprevention: role in genome stability. *The Journal of nutritional biochemistry* 2017**,** *45*, 1-14.

154. Madunic, J.; Madunic, I. V.; Gajski, G.; Popic, J.; Garaj-Vrhovac, V., Apigenin: A dietary flavonoid with diverse anticancer properties. *Cancer Lett* 2018**,** *413*, 11-22.

155. Zhou, Y.; Zheng, J.; Li, Y.; Xu, D. P.; Li, S.; Chen, Y. M.; Li, H. B., Natural Polyphenols for Prevention and Treatment of Cancer. *Nutrients* 2016**,** *8* (8).

156. National Center for Biotechnology Information, P. D., Apigenin, CID=5280443, Apigenin. https://pubchem.ncbi.nlm.nih.gov/compound/Apigenin (accessed 2019, Novomber 1).

157. Sung, B.; Chung, H. Y.; Kim, N. D., Role of Apigenin in Cancer Prevention via the Induction of Apoptosis and Autophagy. *J Cancer Prev* 2016**,** *21* (4), 216-226.

158. Bak, M. J.; Das Gupta, S.; Wahler, J.; Suh, N., Role of dietary bioactive natural products in estrogen receptor-positive breast cancer. *Seminars in Cancer Biology* 2016**,** *40-41*, 170-191.

159. Tang, D.; Chen, K.; Huang, L.; Li, J., Pharmacokinetic properties and drug interactions of apigenin, a natural flavone. *Expert opinion on drug metabolism & toxicology* 2017**,** *13* (3), 323-330.

160. Spicak, V.; Subrt, F., [Effect of apigenin on histamine liberation]. *Ceskoslovenska fysiologie* **1958,** *7* (3), 263-4.

161. Birt, D. F.; Walker, B.; Tibbels, M. G.; Bresnick, E., Anti-mutagenesis and anti-promotion by apigenin, robinetin and indole-3-carbinol. *Carcinogenesis* 1986**,** *7* (6), 959-963.

162. Banerjee, K.; Mandal, M., Oxidative stress triggered by naturally occurring flavone apigenin results in senescence and chemotherapeutic effect in human colorectal cancer cells. *Redox Biol* 2015**,** *5*, 153-162.

163. Souza, R. P.; Bonfim-Mendonca, P. S.; Gimenes, F.; Ratti, B. A.; Kaplum, V.; Bruschi, M. L.; Nakamura, C. V.; Silva, S. O.; Maria-Engler, S. S.; Consolaro, M. E., Oxidative Stress Triggered by Apigenin Induces Apoptosis in a Comprehensive Panel of Human Cervical Cancer-Derived Cell Lines. *Oxid Med Cell Longev* 2017**,** *2017*, 1512745.

164. Chen, Z.; Tian, D.; Liao, X.; Zhang, Y.; Xiao, J.; Chen, W.; Liu, Q.; Chen, Y.; Li, D.; Zhu, L.; Cai, S., Apigenin Combined With Gefitinib Blocks Autophagy Flux and Induces Apoptotic Cell Death Through Inhibition of HIF-1α, c-Myc, p-EGFR, and Glucose Metabolism in EGFR L858R+T790M-Mutated H1975 Cells. *Frontiers in Pharmacology* 2019**,** *10*.

165. Lee, Y. M.; Lee, G.; Oh, T. I.; Kim, B. M.; Shim, D. W.; Lee, K. H.; Kim, Y. J.; Lim, B. O.; Lim, J. H., Inhibition of glutamine utilization sensitizes lung cancer cells to apigenin-induced apoptosis resulting from metabolic and oxidative stress. *Int J Oncol* 2016**,** *48* (1), 399-408.

166. Bao, Y. Y.; Zhou, S. H.; Lu, Z. J.; Fan, J.; Huang, Y. P., Inhibiting GLUT-1 expression and PI3K/Akt signaling using apigenin improves the radiosensitivity of laryngeal carcinoma in vivo. *Oncol Rep* 2015**,** *34* (4), 1805-14.

167. Tseng, T. H.; Chien, M. H.; Lin, W. L.; Wen, Y. C.; Chow, J. M.; Chen, C. K.; Kuo, T. C.; Lee, W. J., Inhibition of MDA-MB-231 breast cancer cell proliferation and tumor growth by apigenin through induction of G2/M arrest and histone H3 acetylation-mediated p21(WAF1/CIP1) expression. *Environ Toxicol* 2017**,** *32* (2), 434-444.

168. Shukla, S.; Kanwal, R.; Shankar, E.; Datt, M.; Chance, M. R.; Fu, P.; MacLennan, G. T.; Gupta, S., Apigenin blocks IKKalpha activation and suppresses prostate cancer progression. *Oncotarget* 2015**,** *6* (31), 31216-32.

169. Xu, M.; Wang, S.; Song, Y. U.; Yao, J.; Huang, K.; Zhu, X., Apigenin suppresses colorectal cancer cell proliferation, migration and invasion via inhibition of the Wnt/beta-catenin signaling pathway. *Oncol Lett* 2016**,** *11* (5), 3075-3080.

170. Lim, W.; Park, S.; Bazer, F. W.; Song, G., Apigenin Reduces Survival of Choriocarcinoma Cells by Inducing Apoptosis via the PI3K/AKT and ERK1/2 MAPK Pathways. *J Cell Physiol* 2016**,** *231* (12), 2690-9.

171. Masuelli, L.; Benvenuto, M.; Mattera, R.; Di Stefano, E.; Zago, E.; Taffera, G.; Tresoldi, I.; Giganti, M. G.; Frajese, G. V.; Berardi, G.; Modesti, A.; Bei, R., In Vitro and In Vivo Anti-tumoral Effects of the Flavonoid Apigenin in Malignant Mesothelioma. *Front Pharmacol* 2017**,** *8*, 373.

172. Stump, T. A.; Santee, B. N.; Williams, L. P.; Kunze, R. A.; Heinze, C. E.; Huseman, E. D.; Gryka, R. J.; Simpson, D. S.; Amos, S., The antiproliferative and apoptotic effects of apigenin on glioblastoma cells. *J Pharm Pharmacol* 2017**,** *69* (7), 907-916.

173. Shi, M. D.; Shiao, C. K.; Lee, Y. C.; Shih, Y. W., Apigenin, a dietary flavonoid, inhibits proliferation of human bladder cancer T-24 cells via blocking cell cycle progression and inducing apoptosis. *Cancer cell international* 2015**,** *15*, 33.

174. Qin, Y.; Zhao, D.; Zhou, H. G.; Wang, X. H.; Zhong, W. L.; Chen, S.; Gu, W. G.; Wang, W.; Zhang, C. H.; Liu, Y. R.; Liu, H. J.; Zhang, Q.; Guo, Y. Q.; Sun, T.; Yang, C., Apigenin inhibits NF-kappaB and snail signaling, EMT and metastasis in human hepatocellular carcinoma. *Oncotarget* 2016**,** *7* (27), 41421-41431.

175. Shan, S.; Shi, J.; Yang, P.; Jia, B.; Wu, H.; Zhang, X.; Li, Z., Apigenin Restrains Colon Cancer Cell Proliferation via Targeted Blocking of Pyruvate Kinase M2-Dependent Glycolysis. *J Agric Food Chem* 2017**,** *65* (37), 8136-8144.

176. Liu, X.; Li, L.; Lv, L.; Chen, D.; Shen, L.; Xie, Z., Apigenin inhibits the proliferation and invasion of osteosarcoma cells by suppressing the Wnt/beta-catenin signaling pathway. *Oncol Rep* 2015**,** *34* (2), 1035-41.

177. Zhao, G.; Han, X.; Cheng, W.; Ni, J.; Zhang, Y.; Lin, J.; Song, Z., Apigenin inhibits proliferation and invasion, and induces apoptosis and cell cycle arrest in human melanoma cells. *Oncol Rep* 2017**,** *37* (4), 2277-2285.

178. Yang, J.; Pi, C.; Wang, G., Inhibition of PI3K/Akt/mTOR pathway by apigenin induces apoptosis and autophagy in hepatocellular carcinoma cells. *Biomed Pharmacother* 2018**,** *103*, 699-707.

179. Meng, S.; Zhu, Y.; Li, J. F.; Wang, X.; Liang, Z.; Li, S. Q.; Xu, X.; Chen, H.; Liu, B.; Zheng, X. Y.; Xie, L. P., Apigenin inhibits renal cell carcinoma cell proliferation. *Oncotarget* 2017**,** *8* (12), 19834-19842.

180. Seo, H. S.; Ku, J. M.; Choi, H. S.; Woo, J. K.; Jang, B. H.; Go, H.; Shin, Y. C.; Ko, S. G., Apigenin induces caspase-dependent apoptosis by inhibiting signal transducer and activator of transcription 3 signaling in HER2-overexpressing SKBR3 breast cancer cells. *Mol Med Rep* 2015**,** *12* (2), 2977-84.

181. Vrhovac Madunic, I.; Madunic, J.; Antunovic, M.; Paradzik, M.; Garaj-Vrhovac, V.; Breljak, D.; Marijanovic, I.; Gajski, G., Apigenin, a dietary flavonoid, induces apoptosis, DNA damage, and oxidative stress in human breast cancer MCF-7 and MDA MB-231 cells. *Naunyn Schmiedebergs Arch Pharmacol* 2018**,** *391* (5), 537-550.

182. Maeda, Y.; Takahashi, H.; Nakai, N.; Yanagita, T.; Ando, N.; Okubo, T.; Saito, K.; Shiga, K.; Hirokawa, T.; Hara, M.; Ishiguro, H.; Matsuo, Y.; Takiguchi, S., Apigenin induces apoptosis by suppressing Bcl-xl and Mcl-1 simultaneously via signal transducer and activator of transcription 3 signaling in colon cancer. *Int J Oncol* 2018.

183. Wang, B.; Zhao, X. H., Apigenin induces both intrinsic and extrinsic pathways of apoptosis in human colon carcinoma HCT-116 cells. *Oncol Rep* 2017**,** *37* (2), 1132-1140.

184. Chen, M.; Wang, X.; Zha, D.; Cai, F.; Zhang, W.; He, Y.; Huang, Q.; Zhuang, H.; Hua, Z. C., Apigenin potentiates TRAIL therapy of non-small cell lung cancer via upregulating DR4/DR5 expression in a p53-dependent manner. *Scientific reports* 2016**,** *6*, 35468.

185. Zhu, H.; Jin, H.; Pi, J.; Bai, H.; Yang, F.; Wu, C.; Jiang, J.; Cai, J., Apigenin induced apoptosis in esophageal carcinoma cells by destruction membrane structures. *Scanning* 2016**,** *38* (4), 322-8.

186. Kang, C. H.; Molagoda, I. M. N.; Choi, Y. H.; Park, C.; Moon, D. O.; Kim, G. Y., Apigenin promotes TRAIL-mediated apoptosis regardless of ROS generation. *Food Chem Toxicol* 2018**,** *111*, 623-630.

187. Zhu, Y.; Wu, J.; Li, S.; Wang, X.; Liang, Z.; Xu, X.; Xu, X.; Hu, Z.; Lin, Y.; Chen, H.; Qin, J.; Mao, Q.; Xie, L., Apigenin inhibits migration and invasion via modulation of epithelial mesenchymal transition in prostate cancer. *Mol Med Rep* 2015**,** *11* (2), 1004-8.

188. Chang, J. H.; Cheng, C. W.; Yang, Y. C.; Chen, W. S.; Hung, W. Y.; Chow, J. M.; Chen, P. S.; Hsiao, M.; Lee, W. J.; Chien, M. H., Downregulating CD26/DPPIV by apigenin modulates the interplay between Akt and Snail/Slug signaling to restrain metastasis of lung cancer with multiple EGFR statuses. *J Exp Clin Cancer Res* 2018**,** *37* (1), 199.

189. Dai, J.; Van Wie, P. G.; Fai, L. Y.; Kim, D.; Wang, L.; Poyil, P.; Luo, J.; Zhang, Z., Downregulation of NEDD9 by apigenin suppresses migration, invasion, and metastasis of colorectal cancer cells. *Toxicol Appl Pharmacol* 2016**,** *311*, 106-112.

190. Tong, J.; Shen, Y.; Zhang, Z.; Hu, Y.; Zhang, X.; Han, L., Apigenin inhibits epithelial-mesenchymal transition of human colon cancer cells through NF-kappaB/Snail signaling pathway. *Biosci Rep* 2019**,** *39* (5).

191. Chien, M. H.; Lin, Y. W.; Wen, Y. C.; Yang, Y. C.; Hsiao, M.; Chang, J. L.; Huang, H. C.; Lee, W. J., Targeting the SPOCK1-snail/slug axis-mediated epithelial-to-mesenchymal transition by apigenin contributes to repression of prostate cancer metastasis. *J Exp Clin Cancer Res* 2019**,** *38* (1), 246.

192. Erdogan, S.; Doganlar, O.; Doganlar, Z. B.; Serttas, R.; Turkekul, K.; Dibirdik, I.; Bilir, A., The flavonoid apigenin reduces prostate cancer CD44(+) stem cell survival and migration through PI3K/Akt/NF-kappaB signaling. *Life Sci* 2016**,** *162*, 77-86.

193. Kim, B.; Jung, N.; Lee, S.; Sohng, J. K.; Jung, H. J., Apigenin Inhibits Cancer Stem Cell-Like Phenotypes in Human Glioblastoma Cells via Suppression of c-Met Signaling. *Phytother Res* 2016**,** *30* (11), 1833-1840.

194. Li, Y. W.; Xu, J.; Zhu, G. Y.; Huang, Z. J.; Lu, Y.; Li, X. Q.; Wang, N.; Zhang, F. X., Apigenin suppresses the stem cell-like properties of triple-negative breast cancer cells by inhibiting YAP/TAZ activity. *Cell Death Discov* 2018**,** *4*, 105.

195. Ketkaew, Y.; Osathanon, T.; Pavasant, P.; Sooampon, S., Apigenin inhibited hypoxia induced stem cell marker expression in a head and neck squamous cell carcinoma cell line. *Arch Oral Biol* 2017**,** *74*, 69-74.

196. Hu, W. J.; Liu, J.; Zhong, L. K.; Wang, J., Apigenin enhances the antitumor effects of cetuximab in nasopharyngeal carcinoma by inhibiting EGFR signaling. *Biomed Pharmacother* 2018**,** *102*, 681-688.

197. Liu, R.; Ji, P.; Liu, B.; Qiao, H.; Wang, X.; Zhou, L.; Deng, T.; Ba, Y., Apigenin enhances the cisplatin cytotoxic effect through p53-modulated apoptosis. *Oncol Lett* 2017**,** *13* (2), 1024-1030.

198. Gaballah, H. H.; Gaber, R. A.; Mohamed, D. A., Apigenin potentiates the antitumor activity of 5-FU on solid Ehrlich carcinoma: Crosstalk between apoptotic and JNK-mediated autophagic cell death platforms. *Toxicol Appl Pharmacol* 2017**,** *316*, 27-35.

199. Hu, X. Y.; Liang, J. Y.; Guo, X. J.; Liu, L.; Guo, Y. B., 5-Fluorouracil combined with apigenin enhances anticancer activity through mitochondrial membrane potential (DeltaPsim)-mediated apoptosis in hepatocellular carcinoma. *Clin Exp Pharmacol Physiol* 2015**,** *42* (2), 146-53.

200. Gao, A. M.; Zhang, X. Y.; Ke, Z. P., Apigenin sensitizes BEL-7402/ADM cells to doxorubicin through inhibiting miR-101/Nrf2 pathway. *Oncotarget* 2017**,** *8* (47), 82085-82091.

201. Gao, A. M.; Zhang, X. Y.; Hu, J. N.; Ke, Z. P., Apigenin sensitizes hepatocellular carcinoma cells to doxorubic through regulating miR-520b/ATG7 axis. *Chem Biol Interact* 2018**,** *280*, 45-50.

202. Seo, H. S.; Ku, J. M.; Choi, H. S.; Woo, J. K.; Lee, B. H.; Kim, D. S.; Song, H. J.; Jang, B. H.; Shin, Y. C.; Ko, S. G., Apigenin overcomes drug resistance by blocking the signal transducer and activator of transcription 3 signaling in breast cancer cells. *Oncol Rep* 2017**,** *38* (2), 715-724.

203. Erdogan, S.; Turkekul, K.; Serttas, R.; Erdogan, Z., The natural flavonoid apigenin sensitizes human CD44(+) prostate cancer stem cells to cisplatin therapy. *Biomed Pharmacother* 2017**,** *88*, 210-217.

204. Scarlatti, F.; Sala, G.; Ricci, C.; Maioli, C.; Milani, F.; Minella, M.; Botturi, M.; Ghidoni, R., Resveratrol sensitization of DU145 prostate cancer cells to ionizing radiation is associated to ceramide increase. *Cancer Lett* 2007**,** *253* (1), 124-30.

205. Cakir, Z.; Saydam, G.; Sahin, F.; Baran, Y., The roles of bioactive sphingolipids in resveratrol-induced apoptosis in HL60: acute myeloid leukemia cells. *Journal of cancer research and clinical oncology* 2011**,** *137* (2), 279-86.

206. Tian, H.; Yu, Z., Resveratrol induces apoptosis of leukemia cell line K562 by modulation of sphingosine kinase-1 pathway. *International journal of clinical and experimental pathology* 2015**,** *8* (3), 2755-62.

207. Zhang, T.; Yan, T.; Du, J.; Wang, S.; Yang, H., Apigenin attenuates heart injury in lipopolysaccharide-induced endotoxemic model by suppressing sphingosine kinase 1/sphingosine 1-phosphate signaling pathway. *Chem Biol Interact* 2015**,** *233*, 46-55.